

A TORQUE TABLE DYNAMOMETER FOR  
QUALIFYING DC ELECTRIC MOTORS  
AND DETERMINING THE  
POWER REQUIREMENTS  
OF POWER TRAIN  
COMPONENTS

By

JOHN CHARLES BETHEA

Bachelor of Science

Oklahoma State University

Stillwater, Oklahoma

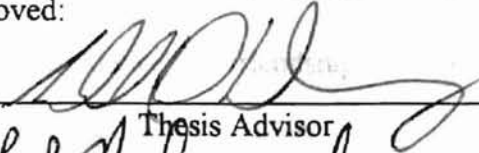
1995

Submitted to the Faculty of the  
Graduate College of  
Oklahoma State University  
in partial fulfillment of  
the requirements for  
the Degree of  
MASTER OF SCIENCE  
July 1997

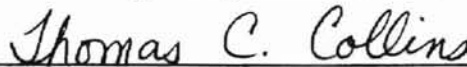
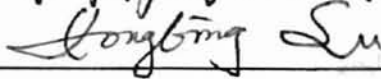
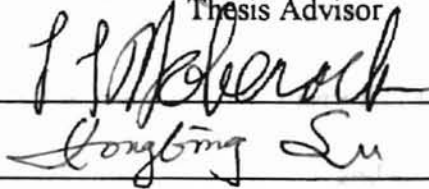
CONTENTS

A TORQUE TABLE DYNAMOMETER FOR  
QUALIFYING DC ELECTRIC MOTORS  
AND DETERMINING THE  
POWER REQUIREMENTS  
OF POWER TRAIN  
COMPONENTS

Thesis Approved:



Thesis Advisor



Dean of the Graduate College

Mr. Lee's contribution of parts—especially the  
... were both crucial to the completion of the

## ACKNOWLEDGMENTS

... workers at the MAE North Lab, among

I wish to express my deep gratitude to my advisor, Dr. Ron Delahoussaye. He is a man of strong character, deep wisdom, vast knowledge, wonderful humor, and great patience. He has graciously taught me, among many other things, that engineering is not a single man's endeavor. Rather, it is a community effort to enhance the world for the good of everyone. The word "help" has taken on new meaning. I have learned to use it often. It is one of the great honors of my life that I have had the opportunity to experience Dr. Delahoussaye's guidance and friendship, and to witness his performance as an engineer and teacher.

I also thank my committee members, Dr. Larry Hoberock, Dr. Dick Lowery, and Dr. Hong Bing Lu. They are, indeed, gentlemen and engineers. The value of their guidance and friendship has been immeasurable.

I wish to especially thank my wife, Joy Lynn. She has patiently, lovingly, and graciously sacrificed much more than I know, and has endured much more than I could ever write about. Without her, this project could not have been completed. I also thank my parents, from whom I have learned to be a parent. They not only gave me a first chance in school, but a second chance, as well. Without their support, guidance, and friendship, I could never have participated in this study. Dr. and Mrs. Ralph C. Bethea, and Mr. and Mrs. Sanford D. Lee have sacrificed much, and have

done so graciously and lovingly. Mr. Lee's contribution of parts--especially the battery, and advice on the electric circuitry were both crucial to the completion of the project.

Thanks also to James Davis and all of his workers at the MAE North Lab, among whom are Sanjay, Parag, and Sarath. Robert Taylor and Jack Nichols provided invaluable help in calibrating the tachometer. Their help and advice were crucial.

Thanks to Arounachalam Manickam for help with computers, to Chen Xin, and to Ojas. Thanks also to Reed Jackson, who unselfishly contributed many hours of electrical expertise toward the success of the project.

Special thanks to Greg Culp, Paul Padgett, Bob Baker, and Jim Braden of Halliburton Energy Services. They have each gone far beyond what I could have hoped for in providing much help and many resources.

Finally, thanks to the Mechanical and Aerospace Engineering Department faculty and staff for these years they have endured my being here.

## TABLE OF CONTENTS

Chapter	Page
I. INTRODUCTION .....	1
Background .....	1
The Problem .....	3
Objectives of the Study .....	3
Purpose of the Study .....	5
Outline of Work .....	6
Chapter Conclusion .....	7
II. REVIEW OF THE LITERATURE .....	8
Introduction .....	8
Various Types of Torque-Measuring Devices .....	8
The Torque Table Dynamometer .....	12
Analysis of Wheatstone Bridge Theory .....	15
Chapter Summary .....	18
III. METHODOLOGY .....	20
Chapter Overview .....	20
Overall Research Methodology .....	20
Particular Research Methodologies .....	23
Calculation of Deflection .....	25
Estimation of Natural Frequency .....	28
Calculation of Strain Gage Bridge Output Gain .....	33
Determination of the Sufficiency of Board Sampling Speed .....	34
Research Instruments .....	44
Data Collection Plan and Recording .....	45
Error Analysis .....	45
Error Reduction .....	45
Torque Table Stiffness .....	45
Torque Calibration .....	47
Data Acquisition Board Calibration .....	47

Tachometer Calibration	48
Resolution and Sensitivity	51
Repeatability	59
Accuracy	62
Final System Qualification -- Vehicle Simulation	63
Overview	63
Vehicle Selection and Speed Measurement	64
The Model of the Vehicle	66
Motor Torque/Speed Relationships	70
Simulation Results	76
Effect of Wheel Diameter on Predicted Vehicle Speed	78
Adaptability -- Model Rocket Motor Characterization	80
Description of Some Dynamometer Components	81
The Tachometer	81
Construction Material	85
 IV. RESULTS	 86
Costs	86
Motor Characterization	88
Conceptual Assumptions	88
Scope and Limitations	95
Conclusion	97
 V. SUMMARY, CONCLUSIONS, AND RECOMMENDATIONS	 98
Summary	98
Conclusions	98
Recommendations for Further Improvement	99
Concluding Comment	100
 SELECTED BIBLIOGRAPHY	 101
 APPENDICES	 103
APPENDIX A -- DYNAMOMETER DRAWINGS AND DIMENSIONS	104
APPENDIX B -- USER'S MANUAL AND HELPFUL SUGGESTIONS	142
APPENDIX C -- DATA ACQUISITION COMPUTER CODE	149
APPENDIX D -- MATLAB CODE	161

APPENDIX E -- BLACK BOX CIRCUIT DIAGRAM AND FILTERING.....	170
---	-----

APPENDIX F -- STRAIN GAGE LOCATION ON LEG.....	173
--	-----

LIST OF TABLES

	Page
Table 1.1.1.1. North-South Speed Sample Data - Determining the Peak Value	
Table 1.1.1.2. Comparison of Peak Value to Factor	
Table 1.1.1.3. Comparison of Peak Value to Factor	

## LIST OF TABLES

<b>Table</b>	<b>Page</b>
1. A Comparison of Test Runs Made With Speed Sampled Prior to Torque and Vice-Versa to Determine the Sufficiency of Board Sampling Speed .....	40
2. Strain Gage Output for Loading of the Calibration Bar Along Axes Perpendicular and Longitudinal to the Axis of the Motor Shaft .....	46
3. Observed Frequency and Tachometer Output Voltage .....	49
4. Dynamometer Microstrain Output vs. Torque .....	53
5. Real Time Torque Readout of Added Weights .....	55
6. Average Static Torque Over Many Data Readings For a Distance of Six Inches (Starting Actual Torque of 72 Oz-In).....	56
7. Maximum Power and Speed at Maximum Power for 17 Motor Trials .....	62
8. Actual Times for Loaded Vehicle Traverses of 48 Inches .....	66
9. Polynomial Coefficients for Three Motor Runs .....	70
10. Torque Requirements and Speeds for Various Loads At Constant Speed .....	73
11. A Comparison of Simulated and Measured Vehicle Speed .....	78
12. Approximate Out of Pocket and Rebuild Project Costs.....	87



10. Torque	48
11. Results	50
12. Torque Screen Readout Vs. Actual	57

### LIST OF FIGURES

Figure	Page
1. Photograph of a Typical Contest Vehicle	2
2. Photograph of the Dynamometer With Motor	13
3. Photograph of the Dynamometer Showing Calibration Bar and Track Drive Simulation Apparatus	14
4. Photograph of the Dynamometer Showing the Track Drive Simulation Apparatus and the inertial Disk	14
5. Schematics of the Wheatstone Bridge Circuit and Strain Gage Locations	16
6. Schematic of the Combined Bridge and Amplifier Circuit	19
7. Models of Leg Deflection	26
8. Force Distribution on a Leg Due to Motor Torque	29
9. A Leg Equivalently Modeled as a Clamped-Clamped Beam	30
10. Torque and Speed Sampling Vs. Time at a Slow Sampling Rate	35
11. The Erroneous Curve Shift Induced by the Slow Sampling Rate	36
12. Comparison of Erroneous and "Un-shifted" Torque-Speed Curves	38
13. Comparison of Erroneous and "Un-shifted" Power-Speed Curves	39
14. Interpolation of the Actual Speed-Time Curve	42
15. Alignment of Interpolated Points on the Speed Curve With Torque Data Points	43

16. Tachometer Calibration Circuit <small>for Run 'T711_8.M'</small> .....	48
17. Tachometer Calibration Results <small>for Run 'W171.M'</small> .....	50
18. Torque Resolution -- Real Time Screen Readout Vs. Actual for Static Measurement .....	43 57
19. Torque Resolution -- Average Measured Vs. Actual for Static Measurement <small>www.Added</small> .....	105 57
20. Superimposed Torque Vs. Speed Curves for 17 Motor Trials .....	60
21. Superimposed Power Vs. Speed Curves for 17 Motor Trials .....	61
22. Measured Time Vs. Load for Vehicle Traverses .....	65
23. The Model of a Vehicle .....	67
24. Schematic of Delt Drive Simulation Apparatus .....	71
25. Torque Required Vs. Added Load For Dynamometer Belt Drive Simulation.....	74
26. The Lower Left Corner of Figure 25 .....	75
27. Typical Simulated Vehicle Speed and Position Vs. Time Curves .....	77
28. The Effect of Wheel Diameter on Simulated Time to Complete a Vehicle Run .....	79
29. Vendor Thrust Curves for Model Rocket Engines .....	82
30. Dynamometer Thrust Curves for B6-5 Model Rocket Engines .....	83
31. Dynamometer Thrust Curves for B6-5 Model Rocket Engines .....	84
32. System Schematic .....	87
33. Adjusted Motor Torque and Speed Vs. Time Curves for Run 'T711_8.M' .....	89
34. Adjusted Motor Torque and Speed Vs. Time Curves for Run 'W171.M' .....	90

35. Motor Torque Vs. Speed Curve for Run 'T711_8.M'	91
36. Motor Torque Vs. Speed Curve for Run 'W171.M'	92
37. Motor Power Vs. Speed Curve for Run 'W171.M'	93
38. Isometric View -- Disk Added	105
39. Isometric View -- Shaft Housing Added	106
40. Isometric View -- Shaft Support Added	107
41. Isometric View -- Motor Mount Added	108
42. Isometric View -- Base and Platform	109
43. Front View	110
44. Side View	111
45. Top View	112
46. Inertial Disk	113
47. Inertial Disk Set Screw Plate	114
48. Motor Platform	115
49. Leg Clamp	116
50. Base	117
51. Shaft Bearing Retainer	118
52. Shaft Bearing Housing	119
53. Shaft Support	120
54. Motor Mount	121
55. Tachometer Mount	122
56. Shaft Pulley	123

57. Electrical Connector Mount .....	124
58. Support Leg .....	125
59. Calibration Bar Post .....	126
60. Calibration Bar .....	127
61. Base Support .....	128
62. Tachometer Pulley .....	129
63. Steel Shaft .....	130
64. Collar .....	131
65. Drive Train Plate .....	132
66. Bearing Block .....	133
67. Vertical Idler Arm .....	134
68. Horizontal Idler Arm .....	135
69. Drive Wheel .....	136
70. Idler Wheel .....	137
71. Outer Idler Bearing Retainer .....	138
72. Inner Idler Bearing Retainer .....	139
73. Driven Wheel .....	140
74. Driven Wheel Shaft .....	141
75. Black Box Layout .....	171
76. System Wiring Schematic .....	172
77. Strain Gage Location With Respect to the Motor Platform and the Base .....	173

## DEFINITION OF TERMS

RPM = revolutions per minute

oz = ounces (force)

lb = pounds (force)

in = inches

psi = pounds (force) per square inch

R = electrical resistance (ohms)

P = power (oz-in/s)

$\Omega$  = ohms

## Chapter I

### Introduction

#### Background

The design contest comprising about half the course content of MAE 3033 at Oklahoma State University has traditionally provided for OSU engineering students a stimulating insight into engineering design. In fact, perhaps the fundamental intent of the course is to teach mechanical design. As a major exercise, students are provided the opportunity to design and build, and finally, to operate a vehicle as it performs against other students' machines in a contest. The beneficial impact of the experience upon students in general, including the author, has been enormous.

The objective of the contest changes each semester. The rules do also, of course, but for each previous contest students have been allowed to use three small DC motors rated at 100 ounce-inches stall torque. Though rules have never encouraged a specific design, for every previous contest the vast majority of mechanisms designed by students have been wheeled, often track-driven, vehicles. A typical vehicle, which was used to collect data for this project, is shown in Figure 1. This tendency to produce vehicles like this is perhaps due to several factors such as the size of the playing field, the general objectives, the configuration of the motors for control via a joystick, and precedence. Wheeled vehicles are perceived as the simplest, most natural solution to the typical problems.

Cost constraints have led to the necessity of providing inexpensive motors for student use. In addition, motors are placed under extremely demanding conditions as enthusiastic

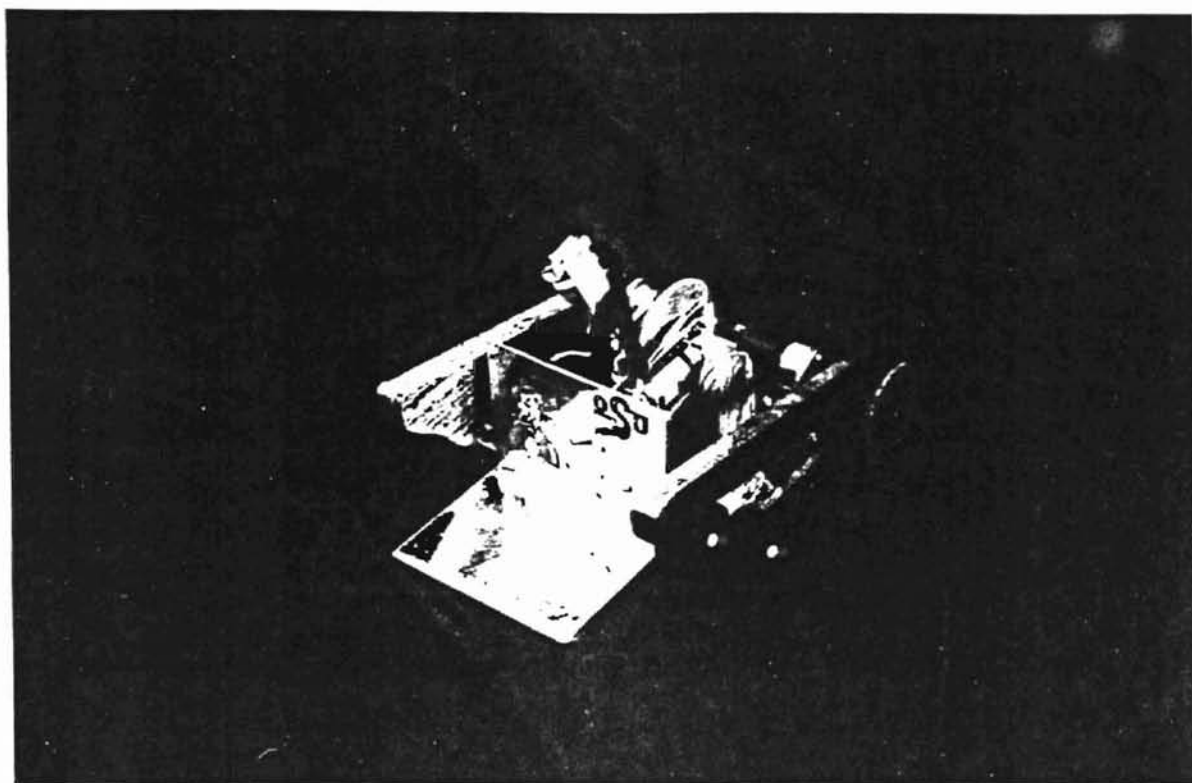


Figure 1. Photograph of a Typical Contest Vehicle

and often inexperienced students attempt to manipulate their design into a winning mechanism. As a result deterioration of motor characteristics can be rapid. Since the quality of a contestant's motors can be the deciding factor in the outcome of the contest, a method of characterizing particular motors accurately and efficiently was needed. In the course of meeting this need, it was possible to extend the project's objective to provide students with a general design tool with broad applicability.

### **The Problem**

The problem is to design and produce a system by which MAE 3033 students can better design, simulate, and evaluate their contest vehicles. The larger portion of this problem is addressed by producing a device to measure the power output of the motors used by students, and the power requirements of the devices they build. The goal sought by providing this capability is to make the evaluation of any particular motor convenient, accurate, precise, and quick. In addition, it is desired that a simulation program provide support in helping students to optimize characteristics of their vehicle through observing the effects of changes before they are physically made.

### **Objectives of the Study**

The primary objective of the study was to build a useable dynamometer which students can use as a design tool. In support of this goal, other objectives were to build the accessory circuitry, to collect and process torque and speed data by computer, to devise a system to simulate a track-driven vehicle in order to analyze the losses



typically occurring in student's designs, and to perform an error analysis on the entire power measuring system.

The dynamometer was then in turn developed with several important objectives in mind. For example, it was primarily desired that the device enhance and facilitate the students' exercise of design. It was to be relatively small and light-weight, and as mechanical in its operation as possible so that the device itself could be educational as well as easily repairable. It was to be rugged, simple, and have low building and maintenance costs in terms of time and money. Finally, the device was to be adaptable and applicable to a variety of potential uses and testing procedures. For example, it should be possible for future students to design and build interfacing accessory hardware to measure power train components peculiar to their machines. Students should then be able to investigate the characteristics of virtually any motor, drive train, or drive train component they suspect is performing poorly. Furthermore, once the actual power output of a particular motor and the speed at which that output occurs is known, then they can use these characteristics to design their vehicles. They can optimize vehicle weight, center of gravity, wheel radius, traction system, bearing selection, speed reduction, and any other parameters that may be important.

Finally, the entire project was constrained financially. Preliminary research indicated that it would be possible to produce a suitable dynamometer for no more than \$300. Final out-of-pocket expenses have totaled about \$150. This is lower than commercial packages which were investigated, which cost from \$500 to \$3000. However, the costs of commercially building the torque table dynamometer and its

associated circuitry, contained in the black box, total \$3665. This figure does not include the motor power supply, the computer, or the data acquisition hardware and software.

### **Purpose of the Study**

The purpose of the study is ultimately to increase the educational impact of the course, and thereby produce better engineers. Through the experience of designing a vehicle students are confronted often for the first time with a significant problem of thinking through a power delivery system in order to carry out a specified task wholly through mechanical means. They are driven not only by the pressure to achieve academically, or to win the contest. They are also stimulated by a desire to engineer a well-designed mechanism, and to guide their creation as it performs before their peers. While the design experience leading up to the contest has always been an extremely effective educational experience, avenues existed to enhance its impact even more. It is at this point that the student needs to start understanding basic engineering issues such as power, force, mechanical advantage, and efficiency. Students often are unaware even of what the design issues are which face them. For example, the availability of materials, decisions about wheel and other part dimensions, and weight distribution, can be issues which the student can not begin to address. Students have been in need of additional design tools to guide them in these design decisions.

In light of this need, the proposed methodology was twofold: to design measurement systems, devices, and strategies which will directly improve the quality of the actual

contest, and at the same time to make the design and building processes more meaningful for students.

The main approach to these objectives was to build the dynamometer. Its purpose was to test the torque produced by electric motors, and thereby permit, for the first time in the history of the course, an objective evaluation of powerplants. In addition, it is hoped that the dynamometer will help engineering students internalize the concept of power, since the device can be creatively adapted by them to help design and evaluate their own motors and drivetrain components.

MAE 3033 should now provide an even greater preparation of students as engineers by helping them internalize the basic engineering concepts of force, power, velocity, acceleration, and inertia. The students should also be provided with a basic instrument useable in several ways to help further develop decision making tools and skills. Hopefully, they will use the dynamometer creatively. The project has also provided a substantial exercise for the author, since considerable use of design, manufacturing, instrumentation, data acquisition, statistical, writing, organizational and other general engineering skills have been extensively required.

### **Outline of Work**

The remaining chapters of this paper will contain discussions of existing literature, theory, and devices, of the methodology used in approaching and solving the problem, of the results, and, finally, conclusions.

## Chapter Conclusion

The problem of building a useable dynamometer and vehicle simulation system has been formulated. The problem involves dynamic torque measurements and speed measurements of the motor. The purpose of the study is to enhance the educational impact of MAE 3033 at Oklahoma State University.

## **Chapter II**

### **Review of the Literature**

#### **Introduction**

This chapter contains a discussion of various methods and devices for measuring the power transmitted through shafts in general, and the power output of motors, in particular. A thorough evaluation of existing devices was particularly important because simply buying a device or system was a distinct possibility.

#### **Various Types of Torque-Measuring Devices**

The transmission of torque through a rotating shaft involves a power source and a power sink. Unfortunately, rotation of the shaft introduces several special problems in torque measurement. For example, it is not a simple matter to place a measuring device on a shaft which rotates, not to mention collect and receive information from that device. This consideration is significant to an extent that it defines the two categories of dynamic torque measurement devices [3, 316]. One category is devices which measure the strain or deflection of the shaft as torque is induced in it. The other category includes devices which involve mounting the shaft or source in bearings and then measuring the reaction force and moment arm.

A common approach to measuring the torque transmitted through a shaft is to mount strain gages directly on the rotating shaft at a 45-degree angle to its longitudinal axis, and then route the output signal through slip rings, or collect this data via

telemetry [3, 420]. A commercial example of this type of transducer which likely uses slip rings for signal transmission is the Lebow Torque Sensor, Model Number 1102-100 [9]. It is light weight and small. It features low rotor inertia, and a torque range and capacity of 100 oz-in, all of which was ideal for the purposes of the project. Unfortunately, its cost was \$499 for the transducer. Additionally, the device is no longer stocked by the vendor. Another slip ring device is GSE's Model 2220-1 Torque Transducer [5a]. It features acceptable characteristics, including a torque range of zero to 140 oz-in, but has a price of \$3095.

Another excellent commercial example of the principle of measuring torque in the transmission shaft is Torquemeters' GP series dynamometers [8]. These dynamometers feature a visual readout scale of transmitted torque. They have an impressive absolute accuracy at full torque of  $\pm 0.25$  percent. Importantly, calibration can be carried out easily and conveniently using a lever arm and weight. The principle of this static calibration feature was adopted into the dynamometer used in this project and was found to be very satisfactory. A very linear relationship between torque and readout is possible, with typical correlation coefficients of 0.999. Unfortunately, the lowest range offered by Torquemeters' devices is 5 to 300 ft-lb., which is much higher than was required for the project. Additionally, it was presumed that the cost of these particularly high-performance devices was far above that available for the project.

Another interesting application of the principle of determining torque through the transmitting shaft without the use of slip rings was put to use by Vibrac in their Optical Torque Transducer series [13]. These devices use an optical encoder disk attached to

the shaft to shutter light proportional to the angular displacement of the bar. The maximum angular deflection of the shaft is  $0.5^\circ$ . Other attractive features are a very low moment of inertia and high accuracy. The devices can also be used for static and dynamic measurements, which was attractive since it was desired to determine the stall torque of the MAE 3033 motors. This device provided a very attractive commercial option to building a dynamometer. Unfortunately, the cost of the basic device (Part No. TQ 100) is \$2400. Additionally, the necessary accessory circuitry ranges from \$470 to \$2475. This placed the device out of the cost range of the project.

The optical phase shift principle had been suggested [11]. This scheme involved routing the output of optical transducers through logic circuitry. The optical transducers were to be mounted on toothed disks located some distance apart on the torque-transmitting shaft. The width of the output pulse would be proportional to the torque. It was not considered a fully acceptable solution to the problem at hand primarily because it was incapable of performing static measurements.

A final rather fascinating method of measuring torque within the transmitting shaft is incorporated into GSE's Torkducer torque measuring devices [5b]. Following is an outline of the device's operation taken from GSE's catalog.

"This device uses a noncontact magnetoelastic design that eliminates the need for bonded materials, brushes, slip rings, and their need for maintenance. The ferromagnetic shaft does not have to be reduced, thereby retaining its full strength in the sensing area. Two knurled, annular bands are at 45 degrees to the shaft axis, and at

right angles to each other. The preferred magnetic direction formed by knurling overwhelms any inhomogeneities and residual stresses in the untreated shaft. A torque applied to the shaft creates a tensile stress in one knurled region, and a compressive stress in the second knurled region which results in an overall permeability change in each region. The permeability changes in each region are respectively transformed into voltages and detected by excitation and sensing coils. The voltage changes in the two regions are processed into an output voltage signal that is proportional to the applied torque. Dynamic and static torques can be measured in either direction of rotation [5b]."

The device is ideal for the project. The cost of the transducer, however, is \$1495. In addition, the accessory controller/monitor is \$795. These costs placed the device far outside the expense range of the project.

The second category of torque measuring devices includes those which involve mounting the shaft or source in bearings and then measuring the reaction force and moment arm. Doebelin states that the cradling concept is the most commonly used power dynamometer [3, 416]. However, these devices are mainly useful for measuring steady torque. Sources of error in the cradled configuration are bearing friction, static unbalance of the cradled member, fluid friction of air, and forces due to stretching and/or bending of the electric/hydraulic power lines. Doebelin recommends the torque table to eliminate these sources of error and to facilitate dynamic torque measurements [3, 417]. This was the configuration adopted for this project.



### The Torque Table Dynamometer

The torque table dynamometer is basically a platform suspended off the base by four uniform, slender legs, which are oriented at 45 degree angles. The motor is mounted on this platform. Figures 2, 3, and 4 show the actual device used for the project.

The intersection of the planes made by the two pairs of legs lies on the axis of rotation of the motor shaft. As the motor accelerates a heavy disk from rest to a steady velocity, the legs deflect an equal amount [4]. The strain in the legs may be measured by way of strain gages. The strain gages are located on each leg so that the backing material aligns with the edge of the motor platform. This facilitates accurate and uniform strain gage placement on each leg. The result is that deflection measurements are performed on each leg at the same location. Strain gages used were Vishay Measurements Group CEA-13-240UZ-120 120 ohm gages.

This strain is equivalent to that caused by a single force applied to the top of the leg, with a moment imposed so that the longitudinal axis of the ends of the leg are parallel. This corresponding "effective" force applied to the top of the legs may be determined. Then, knowing the distance from the axis of rotation to the top of the legs provides a measure of the torque transmitted through the shaft and into the legs.

Doebelin states that angular deflection of the platform is typically less than 1/2 of a degree. "This cross sprint flexure pivot configuration is very stiff in all directions except the rotational one desired, just as in an ordinary bearing" [3, 417].

Additionally, the strain gage bridge arrangement reduces the effect of all forces except

those related to the torque being measured. The next section contains an analysis of Wheatstone bridge theory and the canceling effect of both the bridge and the torque table configuration.

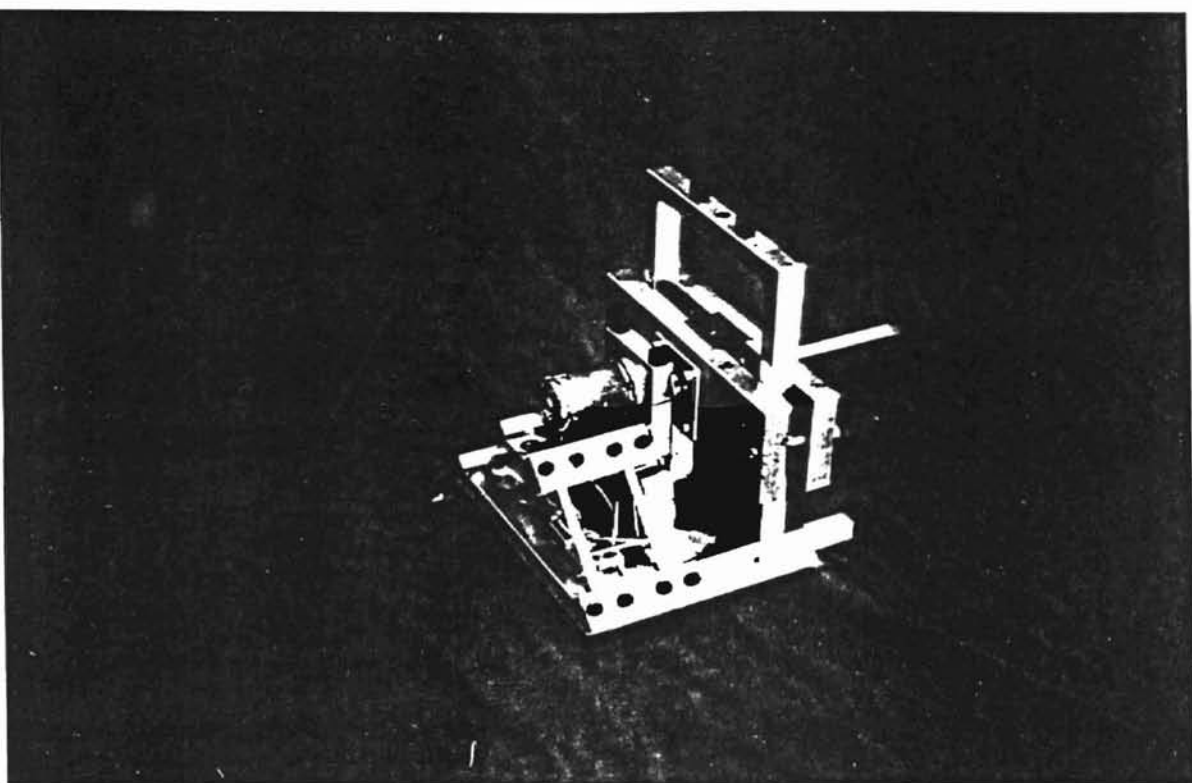


Figure 2. Photograph of the Dynamometer with Motor

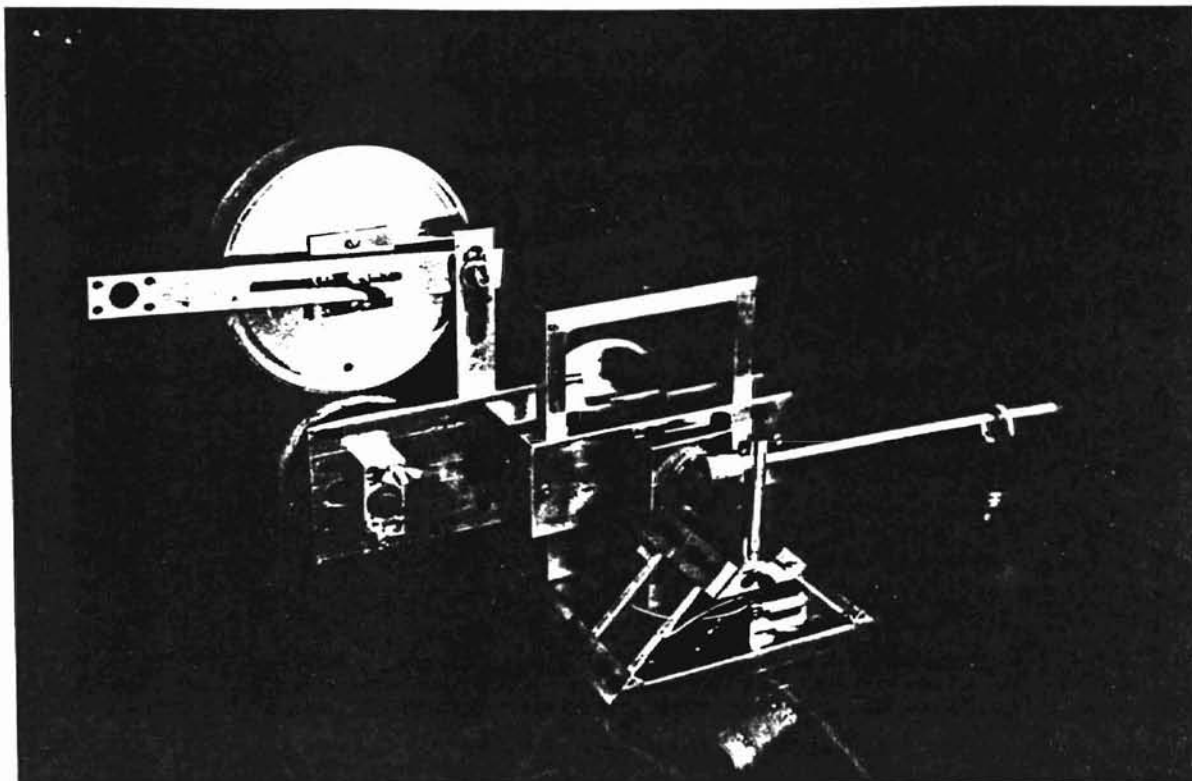


Figure 3. Photograph of the Dynamometer Showing Calibration Bar and Track Drive Simulation Apparatus

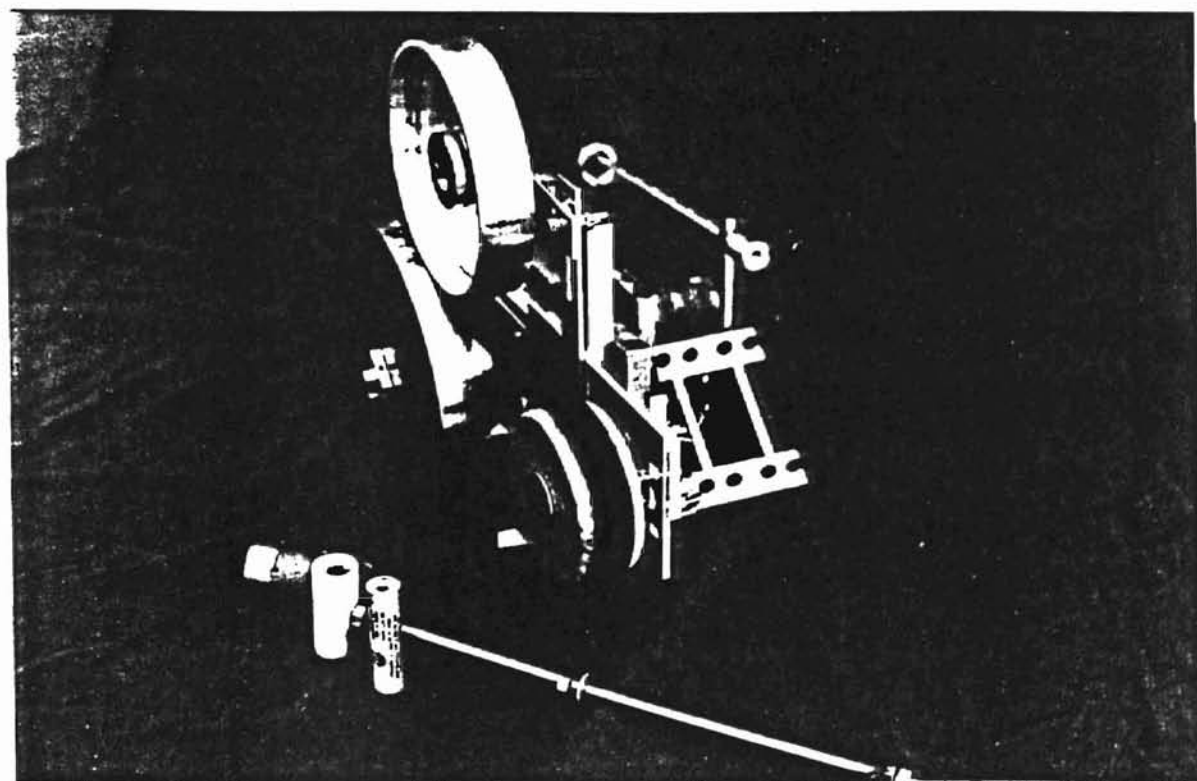


Figure 4. Photograph of the Dynamometer Showing the Track Drive Simulation Apparatus and the Inertial Disk

### Analysis of Wheatstone Bridge Theory.

Consider the schematic of the actual torque table dynamometer and the Wheatstone bridge shown in Figure 5. Initially, using variable shunt resistances as shown in the figure, set  $R_1 + R_2 = R_3 + R_4$ , where  $R_1$ ,  $R_2$ ,  $R_3$ , and  $R_4$  are the total resistances in each leg of the bridge. For example,  $R_1$  represents the resistance of the variable pot as well as the non-variable resistor shown in Figure 5. Then, the currents  $i_1 = i_2 = i_3 = i_4$ , and  $e_o = 0$ . Since  $e_o$  is zero, it must be true from Kirchoff's voltage law that  $R_1 i_1 = R_3 i_3$ , and  $R_2 i_2 = R_4 i_4$ . Rearranging terms and solving for resistances, it is shown that the product of  $R_1$  and  $R_4$  must equal the product of  $R_2$  and  $R_3$  in order to balance the bridge. It is therefore unnecessary to place four individual shunt resistances in the bridge in order to balance it. Rather, only two are necessary on opposite arms of the bridge so that the products of opposing resistors are equal. The next step is to show that the bridge arrangement helps to offset torques imposed in any orientation other than the rotational one desired.

In order to show that undesirable torques and forces are offset by the bridge arrangement, consider again that when the bridge is balanced,  $i_1 = i_2 = i_3 = i_4$  and  $e_o = 0$ . Furthermore,  $e_i = e_{AC} = i_1(R_1 + R_2)$ . Rearranging, then,  $i_1 = e_i / (R_1 + R_2)$ . It can be shown easily in a similar way that  $i_2 = e_i / (R_3 + R_4)$ . Now,  $e_o = e_b - e_d$ , which is to say that:

$$e_o = e_i [R_1 / (R_1 + R_2) - R_3 / (R_3 + R_4)]$$

Multiplying the right side by  $(R_1 + R_2)(R_3 + R_4) / (R_1 + R_2)(R_3 + R_4)$  gives:

$$e_o = e_i [(R_1 R_4 - R_2 R_3) / (R_1 + R_2)(R_3 + R_4)]$$

Clearly the bridge is balanced and the numerator is zero. Now  
 alternate  $R_1$  and  $R_2$  again to Figure 5, X and Y. Undesirable  
 current  $i_g$  is zero in both cases. First assume that the  
 $R_1 = R_3 = R_2 = R_4 = R$ , and observe  
 Also, starting with a balanced bridge  $e_o$

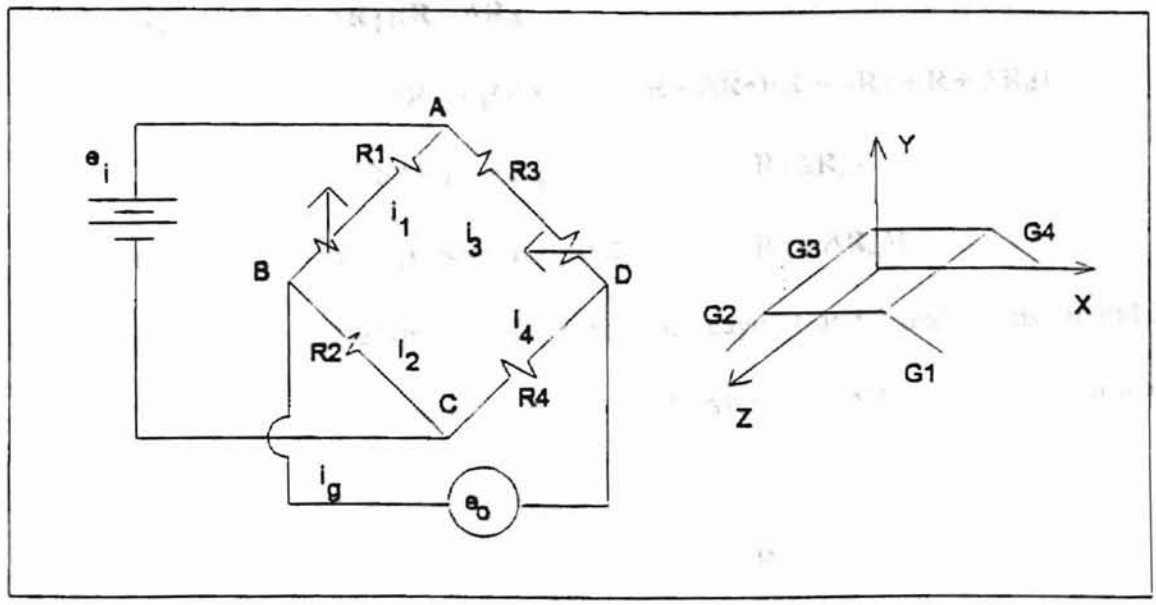


**Figure 5. Schematics of the Wheatstone Bridge Circuit and Strain Gage Locations**

Clearly then,  $e_0$  is zero when the bridge is balanced and the numerator is zero. Now, undesirable torque axes are, referring once again to Figure 5, X and Y. Undesirable forces are those in any direction. To consider these cases, first assume that the resistances are very close to equal so that  $R_1 = R_2 = R_3 = R_4 = R$ , and observe what happens when the resistances are varied. Also, starting with a balanced bridge  $e_0$  is zero, so that:

$$\begin{aligned} \Delta e_0 &= e_i [(R + \Delta R_1)(R + \Delta R_4) - \\ &\quad (R + \Delta R_2)(R + \Delta R_3)] / [(R + \Delta R_1 + R + \Delta R_2)(R + \Delta R_3 + R + \Delta R_4)] \\ &= e_i [R(\Delta R_1 + \Delta R_4 - \Delta R_3 - \Delta R_2) + \Delta R_1 \Delta R_4 - \\ &\quad \Delta R_2 \Delta R_3] / [(2R + \Delta R_1 + \Delta R_2)(2R + \Delta R_3 + \Delta R_4)] \end{aligned}$$

Now, a positive torque about the x axis places strain gages 1 and 2 under tension and 3 and 4 under compression, so that  $\Delta R_1 = \Delta R_2 = (-)\Delta R_3 = (-)\Delta R_4$ . The numerator to the above equation is then zero, and the adverse torque is offset. If a force is applied to the motor platform in the Y direction, then  $\Delta R_1 = \Delta R_2 = \Delta R_3 = \Delta R_4$ , and once again the numerator is zero. Similar analysis takes care of forces purely in the other two directions. The final adverse case is torque about the Y axis. The torque table configuration is extremely stiff in this direction relative to any other direction, so that offset by bridge circuitry is not necessary, even though it may be reasoned. Torque in this direction twists the strain gages making an analysis complex. However, the amount of twist in each gage is likely very nearly equal, and is likely negligible at any rate.

Figure 6 shows the complete circuit, with the amplifier in place to produce a measurable strain gage signal. In this case, resistances  $R_1$ ,  $R_2$ ,  $R_3$ , and  $R_4$  correspond to gages  $G_1$ ,  $G_2$ ,  $G_3$ , and  $G_4$ , respectively. The resistances are  $120 \Omega$  strain gages. The bridge is balanced by adjusting the variable  $20 \Omega$  pots shown in the figure. The output voltage from the bridge ( $e_o$  in Figure 5) is fed to the non-inverting amplifier to produce the new  $e_o$  shown in Figure 6, which has a gain of  $1 + (R_v/R_2)$ . Doebelin suggests that speed-torque curves may be generated quickly and automatically by accelerating an inertia from rest and measuring torque and speed. This was the approach adopted in the project.

Another quite common method of measuring torque in rotating shafts is the eddy current dynamometer. This method makes use of the interaction of eddy currents generated within a rotating metal disk and field coils. This type of dynamometer was not used because it cannot produce any torque at zero speed [3, 427].

### Chapter Summary

Various types of torque measuring devices were considered for the project. It was necessary to measure torque at speeds from zero up to about 250 RPM. The device had to be inexpensive, rugged, and fairly accurate. The torque table configuration was chosen because it featured these attributes. Importantly, it is also very easy to calibrate. Finally, the device offers the mechanical engineering student a wonderful array of mechanical elements -- spinning motors, bending beams, inertias and masses, and stresses and strains.

The circuit is a combined bridge and amplifier circuit. It consists of a 9V DC source connected to a Wheatstone bridge with resistors R1, R2, R3, and R4. The bridge nodes are labeled A, B, C, and D. The output of the bridge is connected to an operational amplifier (op-amp) configured as a differential amplifier. The op-amp has a non-inverting input (3) connected to node D and an inverting input (2) connected to node C. The op-amp is biased with a voltage divider consisting of resistors RZ and RV. The output of the op-amp is labeled e<sub>o</sub>. A schematic of a Wheatstone bridge is also shown with nodes G1, G2, G3, and G4.

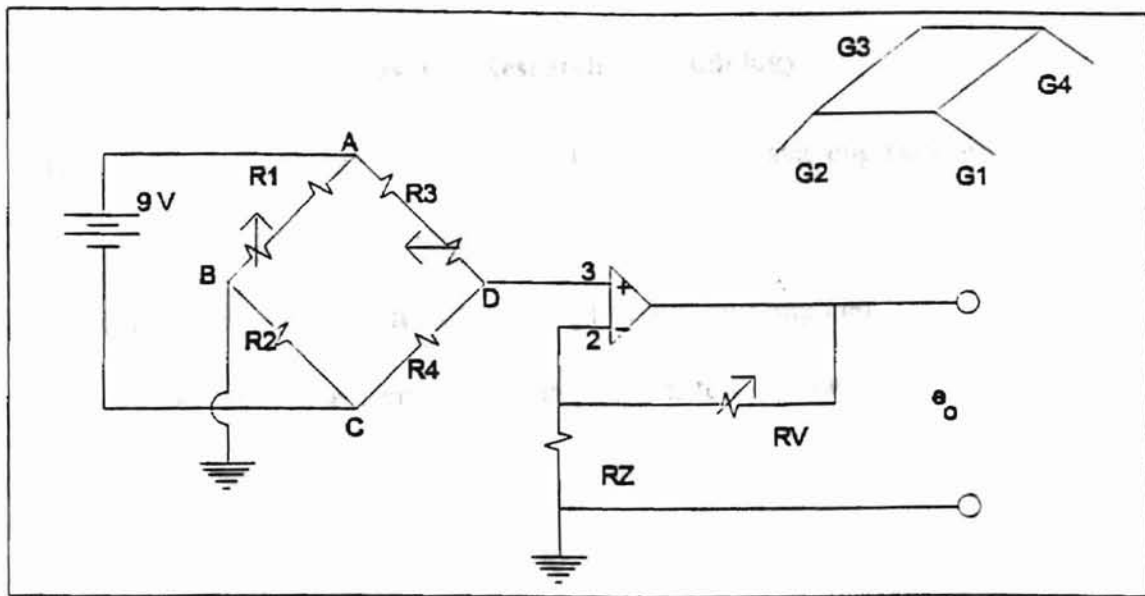


Figure 6. Schematic of the Combined Bridge and Amplifier Circuit



## **Chapter III**

### **Methodology**

#### **Chapter Overview**

This chapter contains discussions of the both the overall methodology used to solve the problem, and particular methodologies used to solve elements of it.

#### **Overall Research Methodology**

The overall research methodology roughly followed basic engineering design principles. As the decision to develop a torque table dynamometer eventually crystallized, the research methodology simplified to building and testing the device and its accessories. Thus, the approach to the problem fell into two general phases.

The first general stage was characterized by brainstorming, research, and preliminary decision making. At no time were stages definitively terminated, but were cycled through regular progressions. Even the initial step of analyzing and defining the problem was revisited in order to refine the scope of the project. Extensive and ongoing brainstorming followed, and was refined through library research. In addition other sources consulted such as periodicals, texts, commercial catalogs, professional technicians, and professors helped to refine the problem statement as well as to give shape to possible solutions. Finally, through consultation with the project advisor, a field of a few devices was selected, and eventually one particular device was chosen for preliminary trial runs. When it was determined that the torque table dynamometer

could fulfill the requirements of the project, then a second device was built with the improvements in sensitivity, durability, and other qualities. Several particular changes led to these improvements. For example, the second torque table's axis of rotation is easier to align with the planes of the legs. This is fairly critical in order to transmit the motor torque to the legs, where the strain gages are located. Another design improvement was moving the tachometer from its mount on the motor platform to the base underneath. This simplified the overall design greatly, improved access to the motor, and eliminated a troublesome direct linkage between the motor and tachometer. The second device has fewer parts than the first, and they are easier to machine. The two most important elements affected by the re-design, however, are the increased sensitivity and the change from a friction brake to the inertial disk now used. The increased sensitivity results from increasing the leg length and decreasing the arm from the axis of rotation of the motor to the point at which the leg is clamped into the platform.

Finally, the device was built, tested, refined, and evaluated. These steps mark the second general phase of the research effort.

The testing cycle of the dynamometer was progressive and covered almost the entire course of the project. The methodology perhaps resembled a spiral from very rough and cursory to fairly rigorous evaluation techniques. For example, very soon after the torque table design was considered seriously, the first dynamometer was built and tested using a Vishay Strain Indicator. These tests indicated that the torque table configuration was promising, that the method of braking would be an important design

consideration, and that various alterations would greatly enhance the operation of the dynamometer. For example, the second model features increased leg length and decreased distance from the axis of rotation of the motor shaft axis to the point of connection between the legs and the motor platform. Furthermore, the braking system was greatly altered and eventually abandoned in favor of having the motor accelerate an inertial disk.

The second dynamometer was also tested extensively using the Vishay Strain Indicator. These tests quantified the sensitivity of the device to torques induced in all planes, as well as indicated the quality of data collected under dynamic conditions.

The final qualifying stage for the dynamometer was to compare the performance of an actual vehicle with a model constructed from measurements made with the dynamometer. These tests established measures for the reliability, accuracy, precision, sensitivity, and resolution of the system. Basically, the test involved measuring the vehicle's speed. The dynamometer was then used to quantify its motor torque characteristics and to estimate the torque requirements of its power train. This information was used to simulate the vehicle, and the results were compared to the actual vehicle's performance.

This broadly characterizes the general experimental procedure. Within this framework, particular tests and procedures were developed in order to systematically arrive at a solution to the problem.

### Particular Research Methodologies

Early considerations in the design of the device involved estimating dimensions and configurations to maximize accuracy, precision, and sensitivity. The two most important components to size were the legs and the inertial disk. Leg length, width, and thickness impact deflection. Deflection is important because too small of a deflection would require excessive gains of the torque signal. On the other hand, too much flexibility in the legs could lead to vibrational problems. As for the disk, too low a value of inertia would result in an acceleration so high that too few data readings could be obtained for a torque-speed curve. If the inertia were too large, an unnecessarily large number of data points would be generated as the disk slowly accelerated. The sizing of the disk will be discussed first.

Motor runs consisted of applying a step voltage to the motor, which then accelerated the disk from rest. The torque applied to the disk decreased from a maximum value to near zero. The relationship,

$$T = I\alpha$$

where  $T$  = torque

$I$  = Moment of inertia of the disk

$\alpha$  = angular acceleration of the disk

was used to approximate the necessary disk dimensions. Since the motors were rated at 100 oz-in, an average torque of 40 oz-in was chosen, though it was understood that torque should decrease linearly throughout the test. It was desired that the run time be

about 2 seconds, so that about 15 data points for speed and 15 data points for torque could be obtained via the 16 Hz. data acquisition board. Therefore, a rough value of acceleration is

$$\begin{aligned}\alpha &= \omega_{\max}/t \\ &= (200\text{RPM})(\text{min}/60\text{s})(2\pi \text{ rad/rev})/(2 \text{ s}) \\ &= 10.5 \text{ rad/s}^2\end{aligned}$$

Choosing a disk diameter of about 8 inches, it is possible to solve for the necessary thickness of the disk, since

$$I = (W/g)r^2/2 = T/\alpha.$$

Solving for the weight,  $W$ , gives a necessary disk weight of 11.5 lb. The thickness is solved for by using the weight density of steel as .282 lb/in<sup>3</sup>.

$$\begin{aligned}\text{thickness} &= 11.5 \text{ lb}/(.282 \text{ lb/in}^3)(\pi 4^2 \text{ in}^2) \\ &= .81 \text{ inches}\end{aligned}$$

Therefore, a disk weighing approximately 11 lb, with a diameter of 8 inches and a thickness of about 3/4 inches was needed. A machined disk was found in a scrap-pile which had a diameter of 7.15 inches, a thickness of .60 inches, and weighed 9.5 lb. The disk was originally a part of a rotary shop machine, and was well-machined. It had been discarded accidentally, and was graciously made available for this project by the shop manager. The actual run times for motors accelerating this disk from rest were generally about 1.5 seconds.

The following sections outline the theory and calculations upon which leg dimensions were based.

## Calculation of Deflection

One of the first considerations was how to configure the leg attachment to the motor platform. Subsequently the legs could be dimensioned. It was desired that sensitivity and ease of manufacture be maximized. The two options considered were to pin one end of the legs and clamp the other, versus clamping both ends. For the following discussion please refer to Figure 7. The clamped-pinned configuration is modeled by the upper figure as a simple cantilevered beam, and the next lower figure shows the clamped-clamped condition as a cantilevered beam with a force and moment acting as shown. It is known that

$$\delta_1 = \frac{FL^3}{3EI}$$

and

$$\delta_2 = \frac{Fl^3}{12EI},$$

so that  $\delta_1 = 4\delta_2$ . The question is whether the clamped-pinned configuration experiences more or less strain at the joint than the clamped-clamped configuration. Referring to the shear and moment diagrams for the clamped-clamped condition, and observing that the middle figure is symmetric, it is clear that the moment at  $L/2$  is zero, and that sectioning the middle figure at this point results in the lowest figure, which is equivalent. For the lowest figure, the deflection is

$$\delta_3 = \frac{1}{2}\delta_2 = \frac{1}{8}\delta_1.$$

Finally, the deflection of a beam at the joint of a cantilevered beam is

$$\delta_0$$

the beam that know

$$\eta = \frac{1}{10} \frac{1}{10}$$

at the end

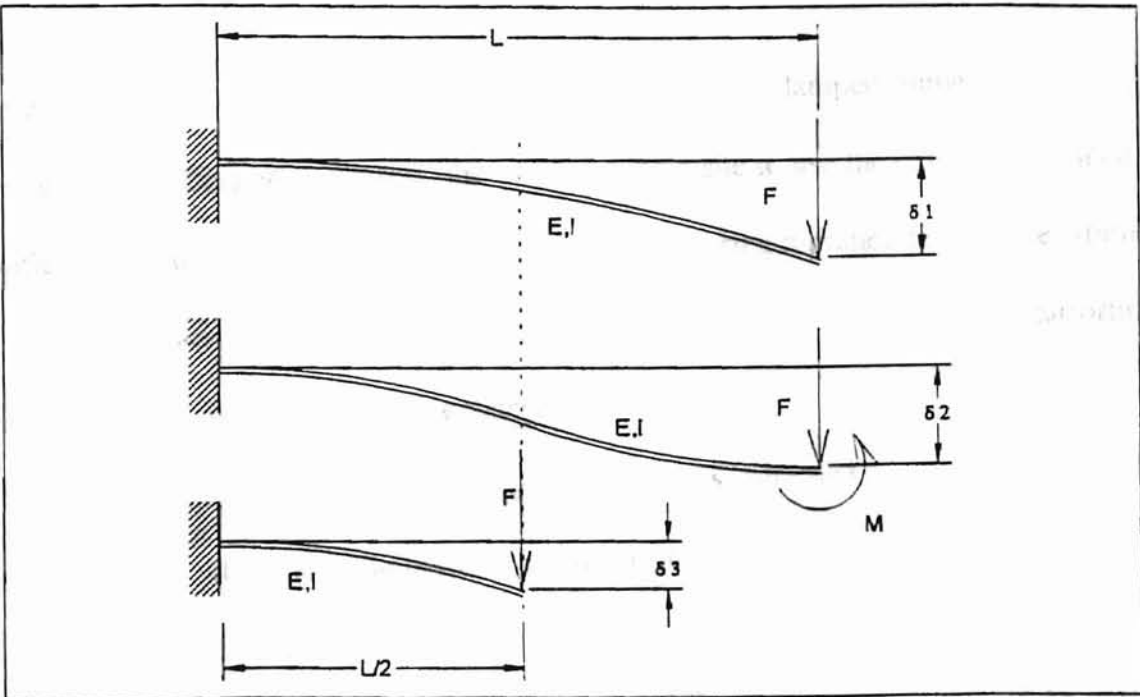


Figure 7. Models of Leg Deflection

Finally, it is known that the strain at the joint of a cantilevered beam is used for the

$$\varepsilon = \frac{3t\delta}{2L^2},$$

where  $t$  is the beam thickness.

Then,  $\varepsilon_1 = \frac{3t\delta_1}{2L^2}$  and  $\varepsilon_3 = \frac{3t\left(\frac{1}{8}\delta_1\right)}{2\left(\frac{L}{2}\right)^2} = \frac{1}{2} \frac{3t\delta_1}{2L^2} = \frac{1}{2} \varepsilon_1$ . This indicates that the clamped-

clamped condition should feature half the sensitivity of the clamped-pinned configuration. Despite this result, the decision was made to use the clamped-clamped configuration to reduce the complications of manufacturing a pinned joint. The strain gages were located at the base of the leg where the leg was clamped into the platform, because this is where the strain is greatest.

The next decision was to size the legs. Constraints were that deflection be around  $1/2$  of a degree, that the angle between the planes of the legs be  $45^\circ$ , and that the device be around 7 inches wide. From geometrical scaled drawings, it was decided that a leg flexing length of 2.5 inches be practical, with a moment arm from the axis of rotation of the motor shaft to the leg joint of 1.5 inches. A leg width of  $1/4$  inch was also decided upon. The leg width is not as critical in determining flexure as the thickness, since the cross sectional moment of inertia for a beam is  $\frac{1}{12}wt^3$ , where  $w$  is the width and  $t$  is the thickness. Then, the  $1/2$  degree deflection of the motor platform recommended by Doebelin results in a relative displacement  $\delta_2$  of 0.0131 inches. The thickness needed for this deflection may be solved for from the deflection equation



above, and is 0.078 inches. Therefore, 3/32 inch aluminum sheet was used for the legs.

The next design consideration was vibrations induced by the DC motor. The next section contains a discussion of natural frequency.

### **Estimation of Natural Frequency**

It was important to calculate the natural frequency of the dynamometer platform on which the test motor is mounted because of the possibility of noisy strain gage signals introduced through excessive vibration. A classical approach is used, in which the dynamometer legs are modeled as beams. Referring to Figure 8, the reaction of the motor as it accelerates the inertial disk is transferred to the legs of the dynamometer. The force due to the torque decreases proportionally to an increase in the distance  $y$  along the length of the leg. This is shown in Figure 8, and is evident from the definition of torque:

$$T = Fd,$$

where  $F$  = force, and  
 $d$  = moment arm from the force to  
the reference axis

The dynamometer platform is constrained to rotate about the longitudinal axis of rotation of the motor shaft. Because the angle of deflection is very small and the legs are clamped, the legs may be modeled as beams supporting a mass constrained to move in the  $X$  direction as shown in Figure 9. The force  $P$  is due to the torque acting at  $Y = d$  in Figure 8. The moment  $M_0$  in Figure 9 is imposed by clamping the leg to the

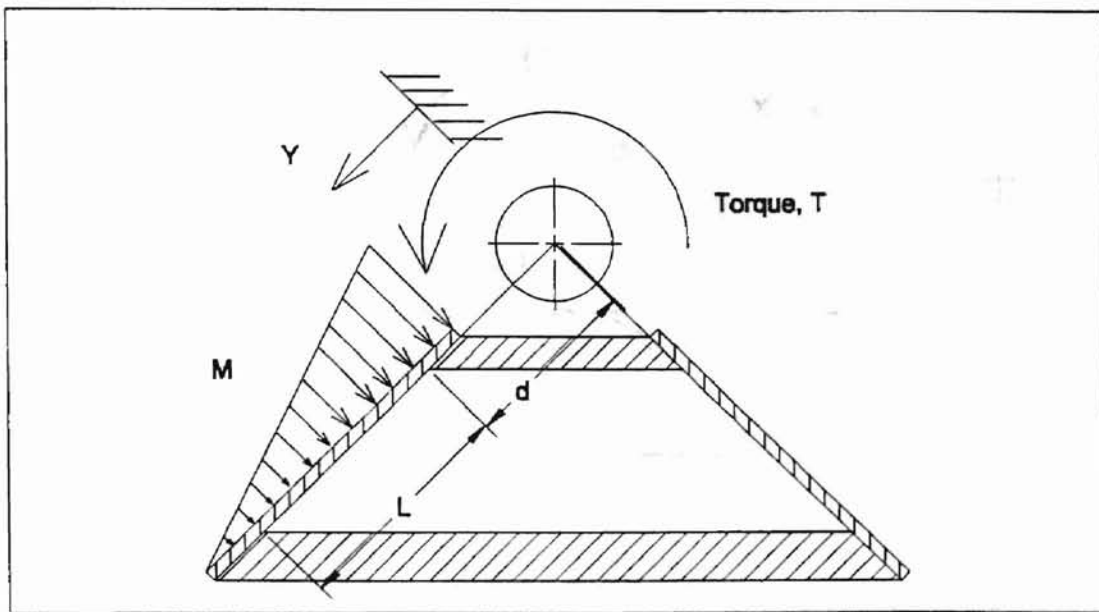
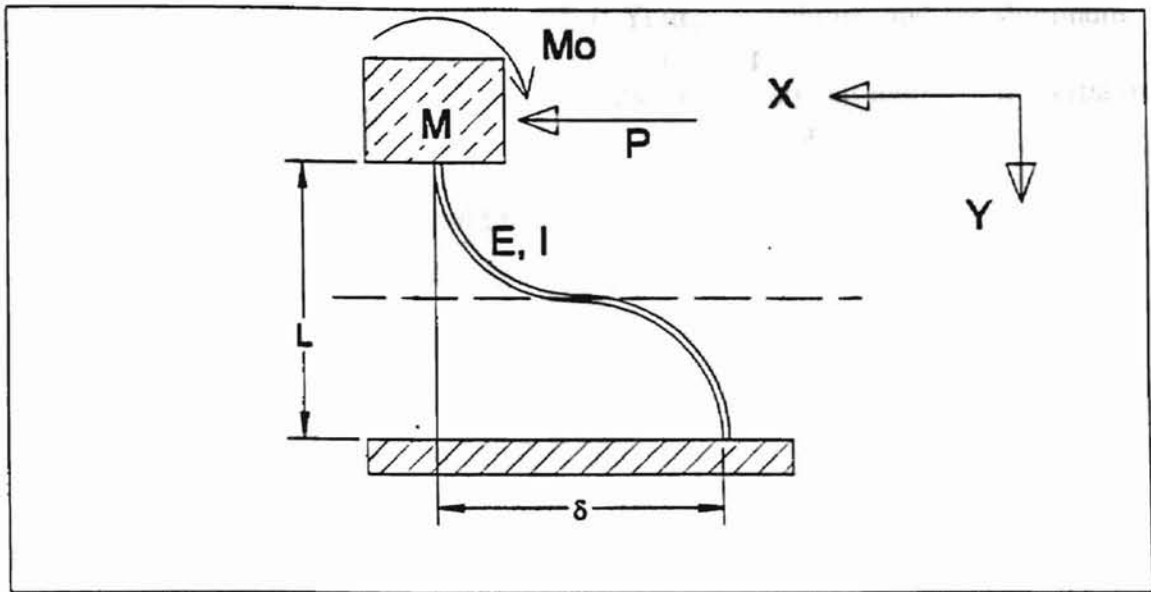


Figure 8. Force Distribution on a Leg Due to Motor Torque

rise and fall of the platform, motor leg clamps, bolts, motor  
 are lumped together to make the total mass  $M$ .  
 The equivalent system shown in Figure 9 is  
 as



**Figure 9. A Leg Equivalently Modeled as a Clamped-Clamped Beam**

base and motor platform. The masses of the platform, motor, leg clamps, bolts, motor mount, and calibration bar and post are lumped together to make the total mass  $M$ , shown in Figure 9. As was stated previously, from statics it can be shown for the system that the static deflection,  $\delta_{st}$ , is,

$$\delta_{st} = \frac{PL^3}{12EI}$$

where  $P$  is the applied force  
 $L$  is the length of the beam  
 $E$  is Young's Modulus, and for aluminum is  $10^7$  psi  
 $I$  is the cross sectional moment of inertia of the beam and is

$$\frac{\text{width} \times \text{thickness}^3}{12}$$

Now, the spring constant is:

$$K = \frac{P}{\delta_{st}}$$

and

$$P = T \times d$$

where  $T$  = the applied torque of the motor, and  
 $d$  = the distance from the axis of rotation of the motor shaft to the attachment of the leg to the platform.

Finally, the natural frequency is:

$$\omega_n = \sqrt{\frac{K_{eff}}{M_{eff}}}$$

where  $K_{eff}$  is the total spring constant for all four legs, and  $M_{eff}$  is the total mass stated above.

The parts comprising the mass  $M$  were weighed separately on a Petite model P-1 postal scale which was calibrated using a 1/2 pound weight. The 12-oz weight which had been designed for calibration of the dynamometer was weighed at 11-3/4 oz. using this scale. A typical motor (Barber-Colman model FYQM-63410-2-2) was weighed at 6.6 oz, and the platform, bolts, clamps, motor mount, and calibration bar and post were all weighed together at 15.2 oz. One 4-in leg was weighed at 1/4 oz., and about 1 inch of each leg is embedded in the platform assembly during operation. Therefore, the embedded portions of the legs add about 0.2 oz. to the total weight of the platform assembly. The motor, platform assembly, and embedded leg portions weigh together 22.0 oz. This was the weight used in natural frequency calculations.

Substituting the terms for  $P$  and  $\delta_{st}$  into the spring constant equation, and counting the four legs gives:

$$K = \frac{4\text{legs} \times P}{PL^3/12EI}$$
$$= \frac{48EI}{L^3}$$

For the legs, the length in flexure is 2.50 inches, the thickness is .090 inches, and the width is .235 inches, so that the cross sectional moment of inertia is  $1.43 \times 10^{-5} \text{ in}^4$ . Finally, then, the natural frequency of the platform expressed in cycles per second is:

$$f_n = \frac{\sqrt{\frac{K_{eff}}{M_{eff}}}}{2\pi}$$

= 55.8 cycles per second.

Since the gear reduction of the motor's gearbox is 30:1, the corresponding shaft speed is:

$$\begin{aligned} \text{RPM}_{\text{shaft}} &= (55.8 \text{ Rev}_{\text{armature}}/\text{s})(60 \text{ s}/\text{min})(\text{Rev}_{\text{shaft}}/30 \text{ Rev}_{\text{armature}}) \\ &= 111.6 \text{ RPM.} \end{aligned}$$

Because this value is about the middle of the operating range of the motor, this value of natural frequency would seem to signal trouble with vibration at this speed. It is possible that some of the scatter of the data is due to this fact.

A design consideration related to sizing the legs involved the calculation of the strain gage bridge output gain. Additionally, the rather slow sampling rate of the 16 Hz. data acquisition board caused concern. These two considerations are discussed next.

### Calculation of Strain Gage Bridge Output Gain

The output gain was calculated after the first dynamometer was produced. The gain was calculated from the following relationship for A/D boards.

$$e_{out} = \frac{e_{in} FK\varepsilon}{4 + 2F\varepsilon}$$

where  $e_{out}$  = output voltage  
 $e_{in}$  = input voltage  
 $F$  = gage factor  
 $K$  = bridge constant  
 $\varepsilon$  = strain

The first device was tested with a 4 in-lb static torque induced on the legs. The circuit was a 1/2-bridge, with a bridge constant of 2.06 and a gage factor of 2.11. The observed strain using a Vishay Strain Indicator was  $200 \mu\epsilon$ , so that the output voltage was 1.1 mV. Therefore, for the 16-bit Keithley-Metrabyte ADC-16, with a range of +/- 5 volts, the gain needed to be around 5000. A potentiometer was used in the circuit to control the gain.

### **Determination of the Sufficiency of Board Sampling Speed**

It was desired to determine the effect on data of sampling the motor shaft speed first, followed by a sampling of the torque, versus sampling the two signals in the reverse order. This determination was important because it was suspected that the top sampling rate of 16 Hz of the ADC-16 board was too slow to gather useable data during the dynamic test. The data acquisition board was used despite its slow sampling rate because it was available. The purchase of a faster apparatus was avoided because of the cost.

The disk accelerates fairly smoothly from zero up to approximately 250 revolutions per minute in about 3 seconds during the span of the dynamic test, while the torque decreases fairly linearly from a maximum value at low RPM to nearly zero. This behavior is shown in Figure 10. The arrows show the locations on the actual torque and speed curves at which samples are made for motor run 'T161.M'. Figure 11 shows the erroneous shift that the data acquisition system performs on the samples. In the case where torque is sampled first, speed reading 1,  $S_1$ , for example, is assigned by the computer code to correspond in time with torque reading 1,  $T_1$ , even though 1/16

seconds have passed between the measurements. As a result, the speed curve is erroneously shifted to the left, as is shown in Figure 11. The effect is that  $S_1$  assigned to  $T_1$  is greater than the actual speed at the time  $T_1$  was made by an amount  $\delta_1$ . From

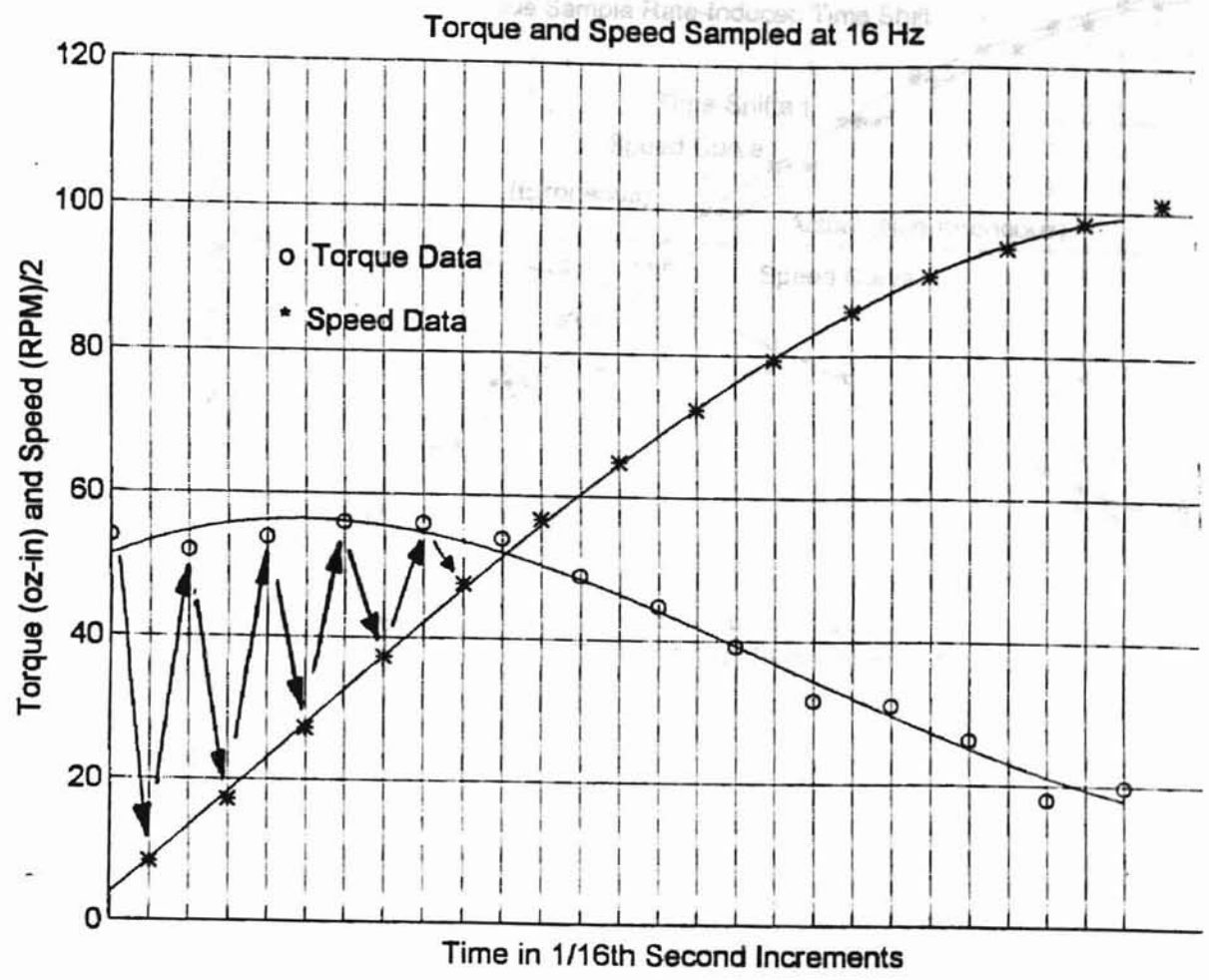
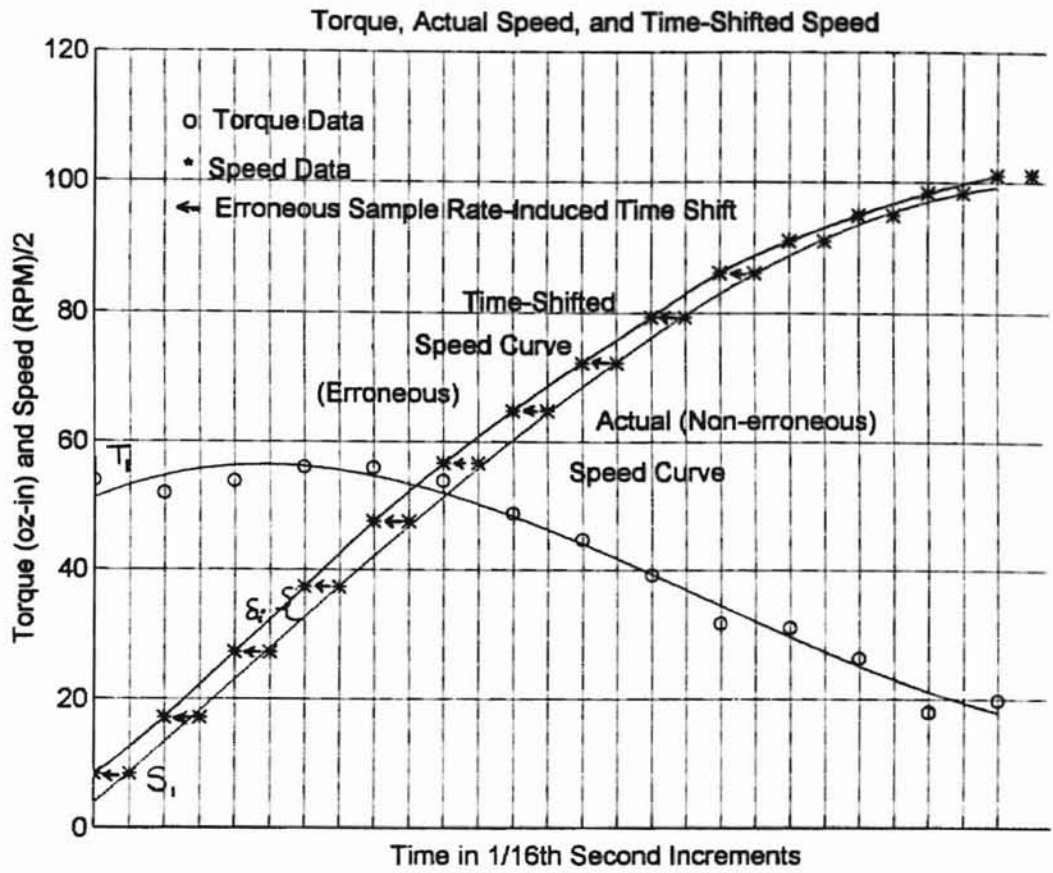


Figure 10. Torque and Speed Sampling Vs. Time at a Slow Sampling Rate





**Fig 11. The Erroneous Curve Shift Induced by the Slow Sampling Rate**

Figures 10 and 11,  $\delta_1$  appears to be about 5 RPM. Since power is the product of speed and torque, the effect of this condition is that the power curve generated will be higher than the actual power output by an amount equal to the product of  $T_i$  and  $\delta_1$ . This is shown in Figures 12 and 13. Conversely, if speed is sampled first then each torque reading will be assigned to a speed reading made 1/16 seconds prior. The torque reading  $T_i$  assigned to  $S_i$  is lower than the actual torque at the time  $S_i$  was made by an amount  $\delta_2$ . In this case the generated power curve is lower than the actual power by an amount equal to the product of  $S_i$  and  $\delta_1$ .

A simple test was designed and carried out to examine the effects of the order of sampling motor speed and torque output. First, ten motor runs were made sampling speed prior to torque. For each run, a polynomial second degree curve fit of calculated power versus speed was used to evaluate the maximum fitted power and the speed at which this point occurred. The program "DCMOTR33.C" was used to generate the data and to build the MATLAB M-file, which then performed the plotting, the polynomial curve fit, and the evaluation routines. Then, ten runs were made sampling torque prior to speed, and the same data treatment was carried out as was done for the first ten runs. These data sets, with the computed averages and standard deviations, are included in Table 1. It is evident from comparing the two power averages that the order of sampling does, indeed, significantly impact the fitted curves in the manner which was expected. Furthermore, the effect of the order was correctly anticipated. The maximum power from the fitted curves is 39 oz-in/s higher for torque sampled first than for speed sampled first. Not surprisingly, there is only 0.3 percent difference

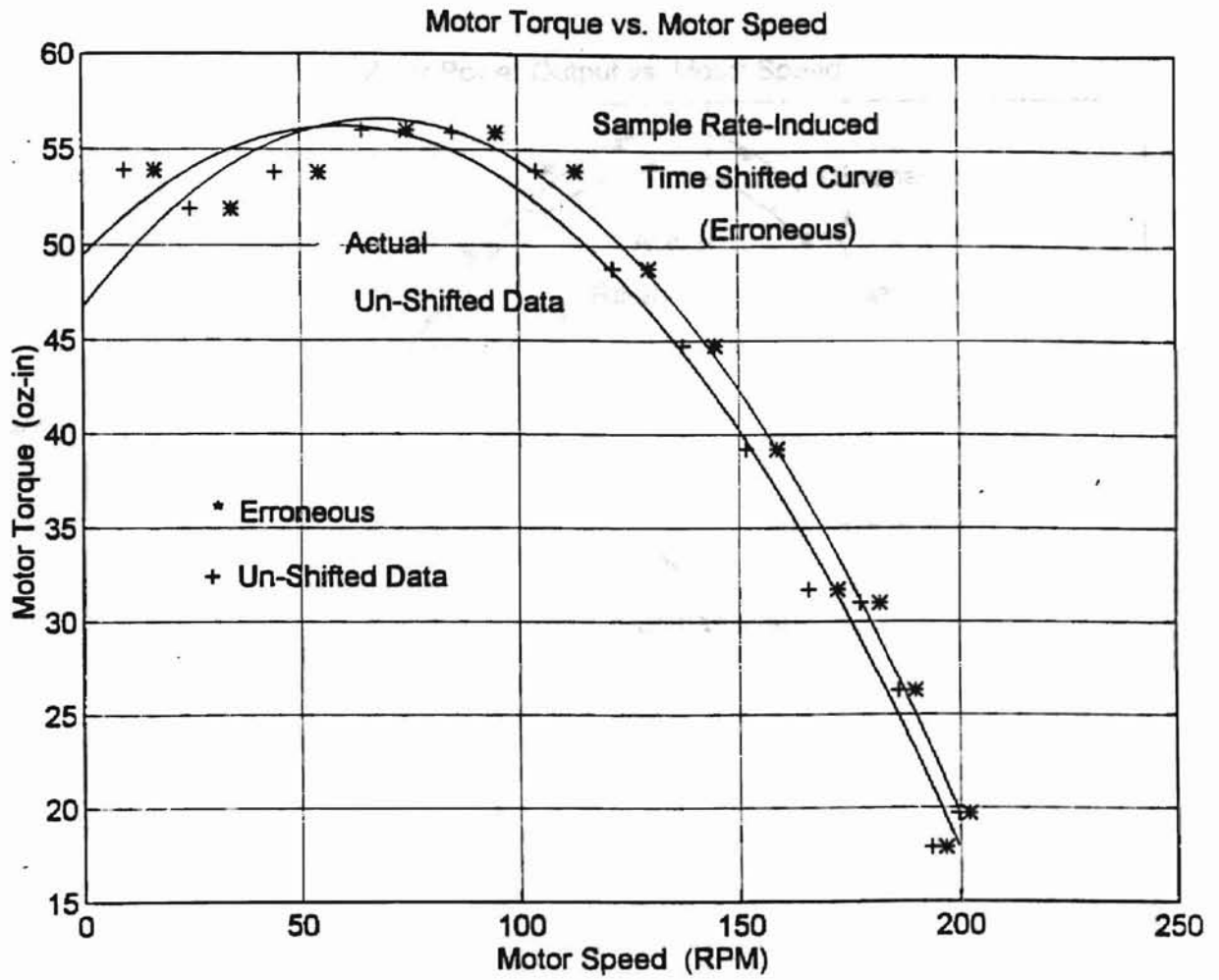


Figure 12. Comparison of Erroneous and “Un-shifted” Torque-Speed Curves

occurs for the two conditions

be speed for both cases. I

be char + 200 rpm and

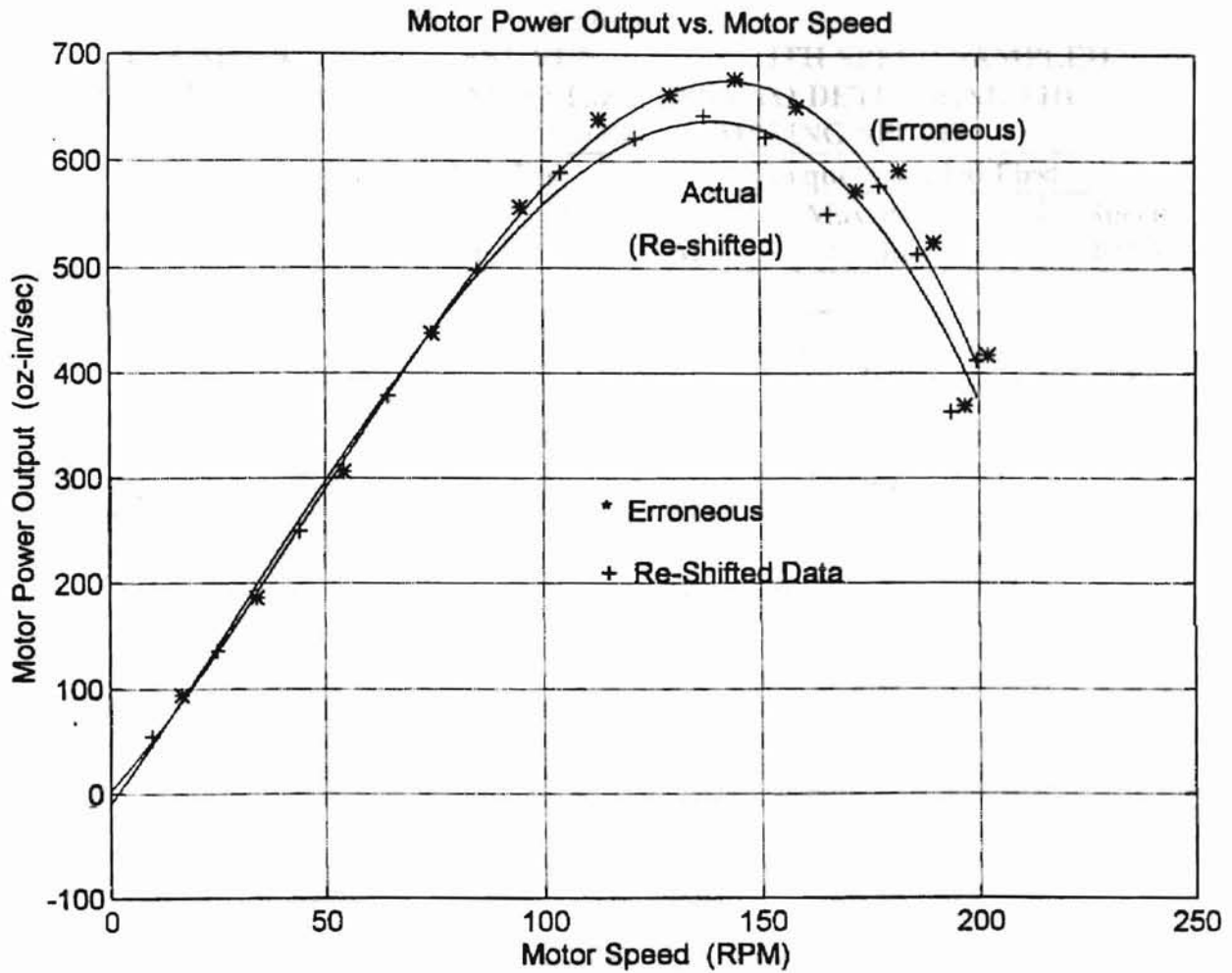


Figure 13. Comparison of Erroneous and "Un-shifted" Power-Speed Curves

STATE UNIVERSITY

between the average speeds at which maximum power occurs for the two conditions. This is because the calculated power values are fitted to the speed for both cases. It may be argued that the average power outputs shown in the chart provide an upper and a lower bound on the actual power output of the motor. Therefore, a student could

**TABLE 1**  
**A COMPARISON OF TEST RUNS MADE WITH SPEED SAMPLED**  
**PRIOR TO TORQUE AND VICE-VERSA TO DETERMINE THE**  
**SUFFICIENCY OF BOARD SAMPLING SPEED**

Run Number	Speed Sampled First	Torque Sampled First		
	Max Power (oz-in/s)	Speed (RPM)	Max Power (oz-in/s)	Speed (RPM)
1	613	143	671	136
2	617	147	685	138
3	633	131	628	139
4	636	135	588	144
5	579	147	687	143
6	668	136	708	137
7	669	133	698	137
8	620	136	739	132
9	617	145	699	147
10	704	135	642	140
<b>Average</b>	<b>635.6</b>	<b>138.8</b>	<b>674.5</b>	<b>139.3</b>
<b>Standard Dev.</b>	<b>33.9</b>	<b>5.7</b>	<b>41.7</b>	<b>4.1</b>

conservatively use the lower bound as a design parameter. However, it was felt that the range of about 40 oz-in/s was too broad. Since it was known that the actual power curve fell between the upper and lower curves, and that the upper and lower curves were established simply by swapping the order of sampling, it seemed reasonable that the generated curve most closely approximating the actual behavior of the motor would be obtained simply by artificially adjusting one of the variables to accommodate for the

1/8 of a second elapsing between the torque and the speed measurements. This was accomplished in the following way using a methodology encapsulated in the sample Matlab 'M' file 'T161.M' included in Appendix D. First, time arrays for speed and torque data are created. The speed and torque array values are incremented by 1/8 seconds, with the initial times staggered so that the speed array begins at zero plus 1/16 seconds. This accounts for the fact that torque is sampled first (at time zero) in the computer code, followed by an alternate sample of speed and torque every 1/16 seconds. It was then necessary to create a large array with fine increments in order for Matlab to plot a smooth, continuous curve of torque vs. speed. An initial array size of 300 was tuned down to 270, with increments of 0.0065 seconds. This arrangement conveniently spans a total time of 1.7485 seconds, which is greater than the total duration of the torque test. Matlab commands were then used to fit a spline curve relating the computer speed data points to the speed time array. The expression for the resulting curve was evaluated at time elements from the torque time array. This artificially shifted the speed data to correspond with respective torque readings. This is shown with the arrows in Figure 14. In effect, speed data points were chosen off the spline which correspond in time to the torque data points, and the measured speed data points could then be 'discarded'. This is shown by the "+" marks in Figure 15. The arrows show alignment of the sampled speed data points with the sampled torque data points. The next step was to fit a curve relating the corrected speed values to the torque time array elements. A final evaluation of the fit at the 'absolute' time elements yielded an array of 270 speed data points which had been corrected to account for the

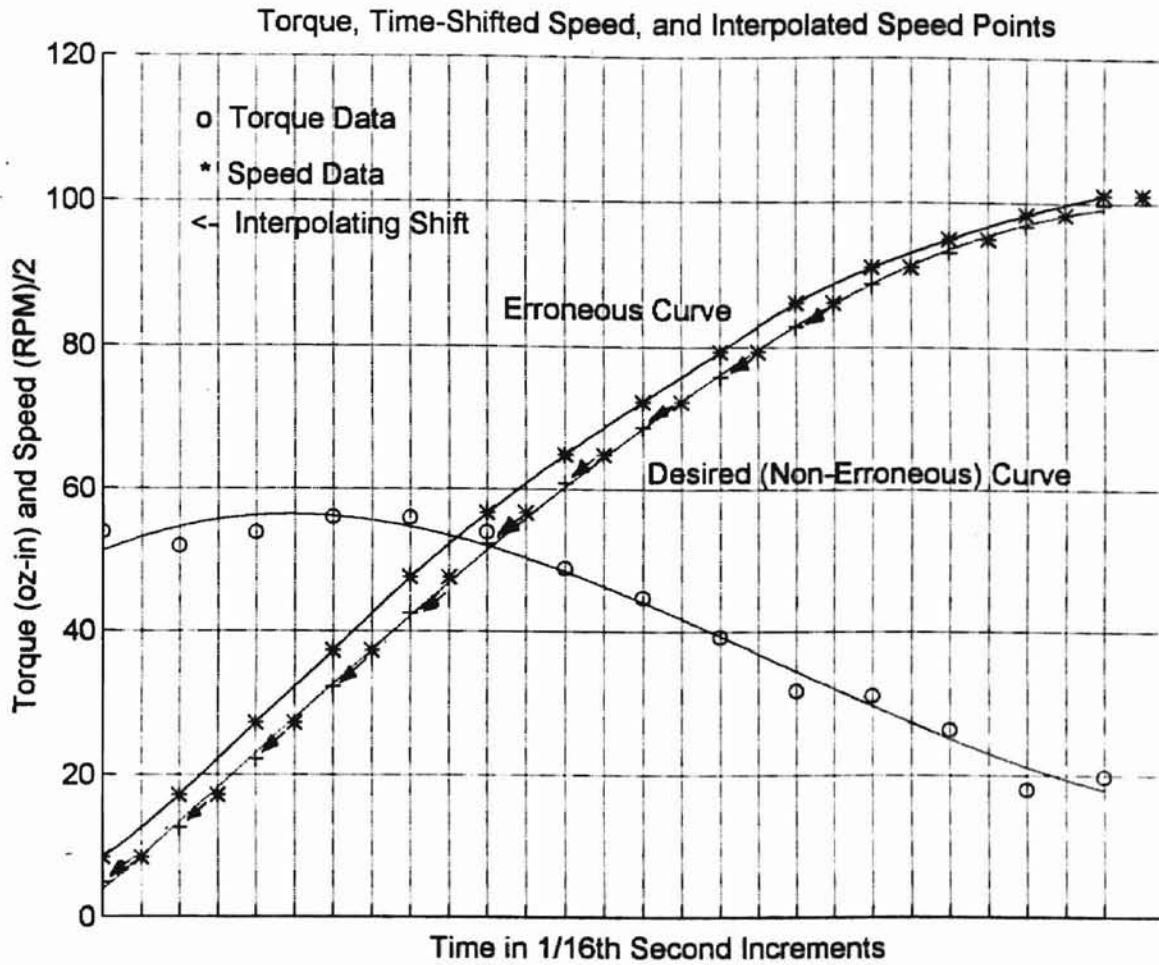


**Figure 14. Interpolation of the Actual Speed-Time Curve**

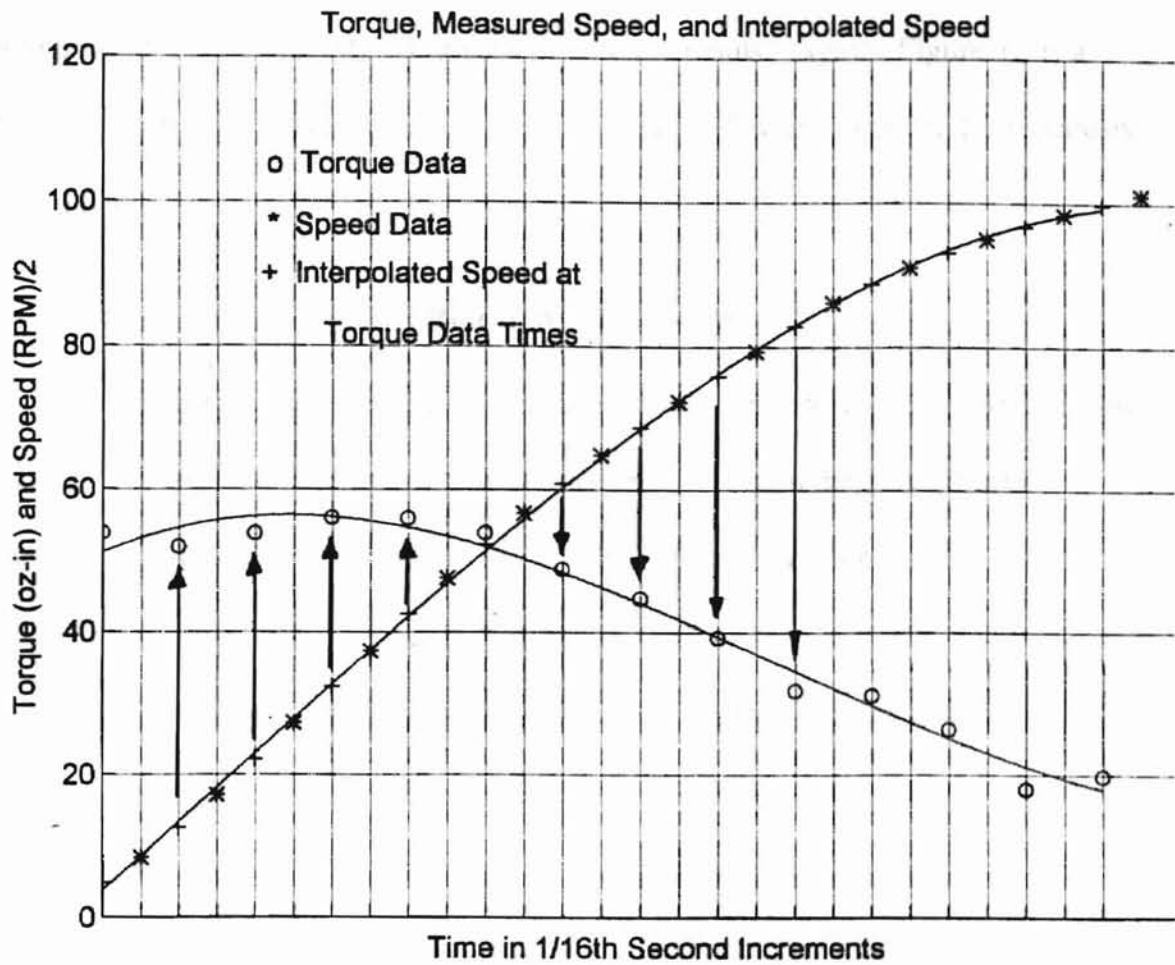


**Figure 15. Alignment of Interpolated Points on the Speed Curve With Torque Data Points.**



speed and order of data acquisition. Torque data was plotted in the same way, except that it was not necessary to shift the curve. A polynomial curve fit was generated relating the torque to the corrected speed values. This fit was evaluated at 'absolute' times to give 270 points which could be plotted. These torque and speed data points were used to produce the Matlab graphs of computer runs. Again, Figure 13 is a typical comparison between computer data "un-shifted" in this way, and erroneously shifted data.

### **Research Instruments**

Research instruments used may be broadly categorized according to phases of the project. For example, the dynamometer was built largely in the MAE North Laboratory at OSU. Instruments included standard machine shop articles such as industrial lathes and mills, grinders, band saws, drill presses, calipers, and many other tools and instruments. During the laboratory phase instruments included an analog Tektronix oscilloscope and a Hewlett-Packard 54501A digitizing oscilloscope, three different brands of digital multimeters, soldering irons, drills, a 486 computer (OSU # 171128), a Keithly-Metrabyte ADC-16 Analog to Digital data acquisition board, calculators, and miscellaneous tools.

Strain gages used were Vishay Measurements Group CEA-13-240UZ-120 120 ohm gages. These gages feature  $\pm 0.3\%$  error at  $24^{\circ}\text{C}$ . Lot number R-A48AF84 was used.

## **Data Collection Plan and Recording**

Data was recorded in two 150-page lab notebooks dedicated to the project. These notebooks also were used to record experimental procedures, hypotheses, brainstorming sessions, interviews, photocopies, and other pertinent information. The notebooks contain records of all data files used in the project. Generally, the data collection plan for raw data generated by the dynamometer was simply the construction of Matlab files within the C program, with Matlab code and raw data.

## **Error Analysis**

### **Error Reduction**

Considerable effort was expended in reducing various types of error. Main sources of error which were anticipated were in the inherent design and construction of the dynamometer, and in speed measurements, torque measurements, and data acquisition board measurement of voltage.

It is important to note that the accuracy of the device is based upon torque readings, that the reported value of precision is based upon power measurements, and that the estimated value of resolution is based on strain measurements made with a Vishay Strain Indicator. It would be more desirable if accuracy, resolution, and precision were based on one output -- power, for instance.

### **Torque Table Stiffness**

The inherent stiffness of the torque table configuration is an extremely important factor in the quality of measurements made by the device. The following experiment

was intended to demonstrate that the configuration does, indeed, possess high degrees of stiffness in every direction except the rotational one. The experiment consisted of simply recording strain gage output while loading the calibration bar as it was oriented off the back of the platform, so that the torque imposed on the platform was along an axis perpendicular to the axis of rotation of the platform. Table 2 shows the data recorded for this test.

Table 2

**Strain Gage Output for Loading of the Calibration Bar  
along Axes Perpendicular and Longitudinal  
to the Axis of the Motor Shaft**

<b>Torque (oz-in)</b>	<b>Perpendicular to motor shaft axis</b>	<b>Longitudinal to motor shaft axis</b>
0	0.05	0.08
24	1.03	0.10
36	1.53	0.10
48	2.04	0.11
60	2.54	0.12
72	3.03	0.12
84	3.51	0.15
96	4.02	0.13
0	0.07	0.07
<b>Range</b>	<b>3.97</b>	<b>0.05</b>

Quite significantly, the range of voltage change induced by torque non-coincident with the axis of rotation of the platform is less than 1.8% of the range of voltage induced by torque acting about the axis of rotation of the platform. When a line is fit to the data generated by loading off the back of the platform, it is seen that the slope is very small, on the order of magnitude of  $10^{-4}$ . Additionally, the intercept is 0.08, which is the value of the initial data point. Perhaps most importantly, the value of  $(1-r^2)^{1/2}$  is 0.274.

This value is roughly the ratio of the vertical standard deviation of the data about the line to the total vertical variation of the data [1, 112]. In other words, not only is the line nearly flat, but the majority of the data points vary vertically about the line by almost 30 percent of the total vertical movement of the line. This means essentially that there is a poor relationship between undesirable torque and strain gage output. The effect of undesirable torque is statistically insignificant.

### **Torque Calibration**

Torque calibration of the dynamometer is simple. A calibrating bar is oriented horizontally off the platform, so that a vertical force acting on it imparts a torque to the platform to which it is attached. This torque is transferred to the legs, where the strain gages are located. The calibrating bar is notched every inch so that a weight may be located fairly precisely. The weight is moved and strain gage output is noted so that a relationship between actual torque and strain gage output may be established. As has been discussed, these relationships were very linear. Typical correlation coefficient values were on the order of 0.999.

### **Data Acquisition Board Calibration**

The Keithley-Metrabyte ADC-16 data acquisition board is basically a voltmeter. The manual for the device included instructions for calibrating it. Though the specified calibrating power supply was not available, calibration was performed using a military spec power supply. The A/D board was accurate within about 0.5 percent.

### Tachometer Calibration

It was necessary to calibrate the tachometer, especially since it was obtained in the used condition, with little recorded information about its age or prior conditions of use. The circuit used to perform the calibration is shown in Figure 16. The calibration procedure was to tape a tab onto the shaft of the dynamometer and run the motor, so that the tab triggered an optical interrupter once per revolution. The transducer was an Optek 880 Opto Interrupter. The output signal from the transducer was seen on an

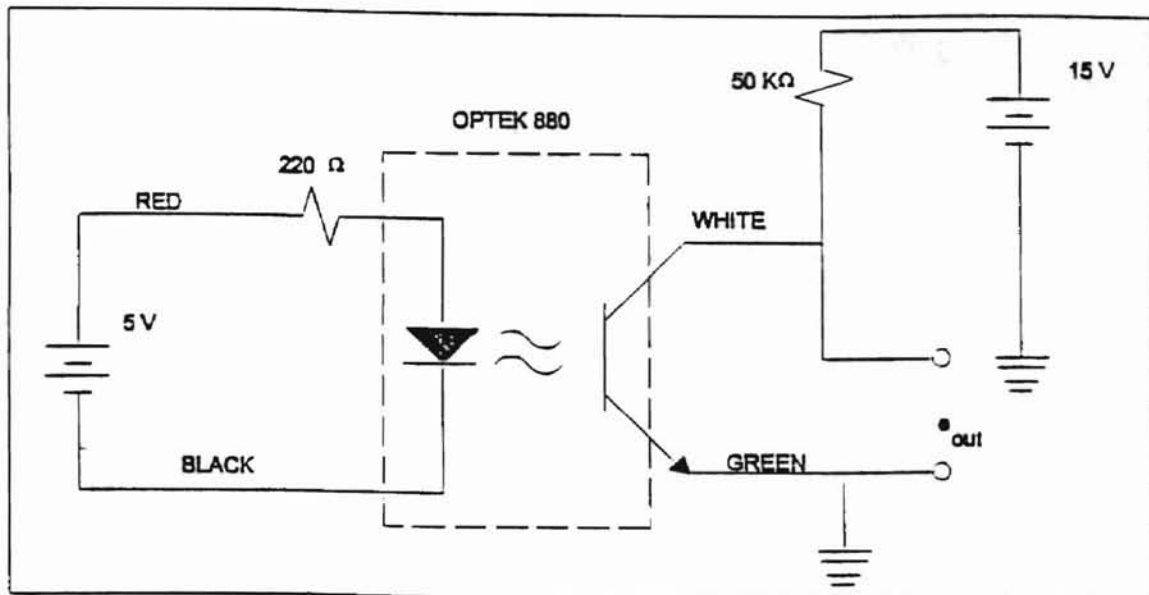


Figure 16. Tachometer Calibration Circuit

HP54501 Digitizing oscilloscope as a series of pulses representing the frequency of interruption, and therefore the speed of the motor. The frequency was displayed directly using the frequency readout feature of the oscilloscope. The tachometer voltage at each frequency data point was read off a digitizing multimeter. The speed of the motor was controlled with a laboratory power supply. Table 3 shows the observed frequencies and corresponding tachometer output voltage values. In addition, a line fitted through the data points yields a slope of 53.78 RPM per volt, with an intercept of -1.2. This is shown graphically in Figure 17. Table 3 shows calculated values of RPM

**Table 3**  
**Observed Frequency and Tachometer Output Voltage**

Voltage	Frequency (Hz)	Frequency (RPM)	Line Fit of Calculated Frequency (RPM)	Error
3.70	3.27	196	197.8	-1.8
3.25	2.89	173	173.6	-0.6
2.79	2.48	149	148.9	0.1
2.40	2.10	126	127.8	-1.8
2.10	1.85	111	111.7	-0.7
1.55	1.37	82	82.1	-0.1
1.07	0.95	57	56.3	0.7
0.55	0.49	30	28.4	1.6
2.15	1.90	114	114.4	-0.4
2.60	2.32	139	138.6	0.4
3.01	2.66	160	160.7	-0.7
3.47	3.13	188	185.4	2.6
3.85	3.45	207	205.8	1.2
4.28	3.80	228	229.0	-1.0
4.75	4.25	255	254.2	0.8
5.15	4.60	276	275.7	0.3

... least squares fit, and also the error between the  
... average for absolute values of error is  
... error is 1.1 RPM, which is about  
... This indicates a strong linear

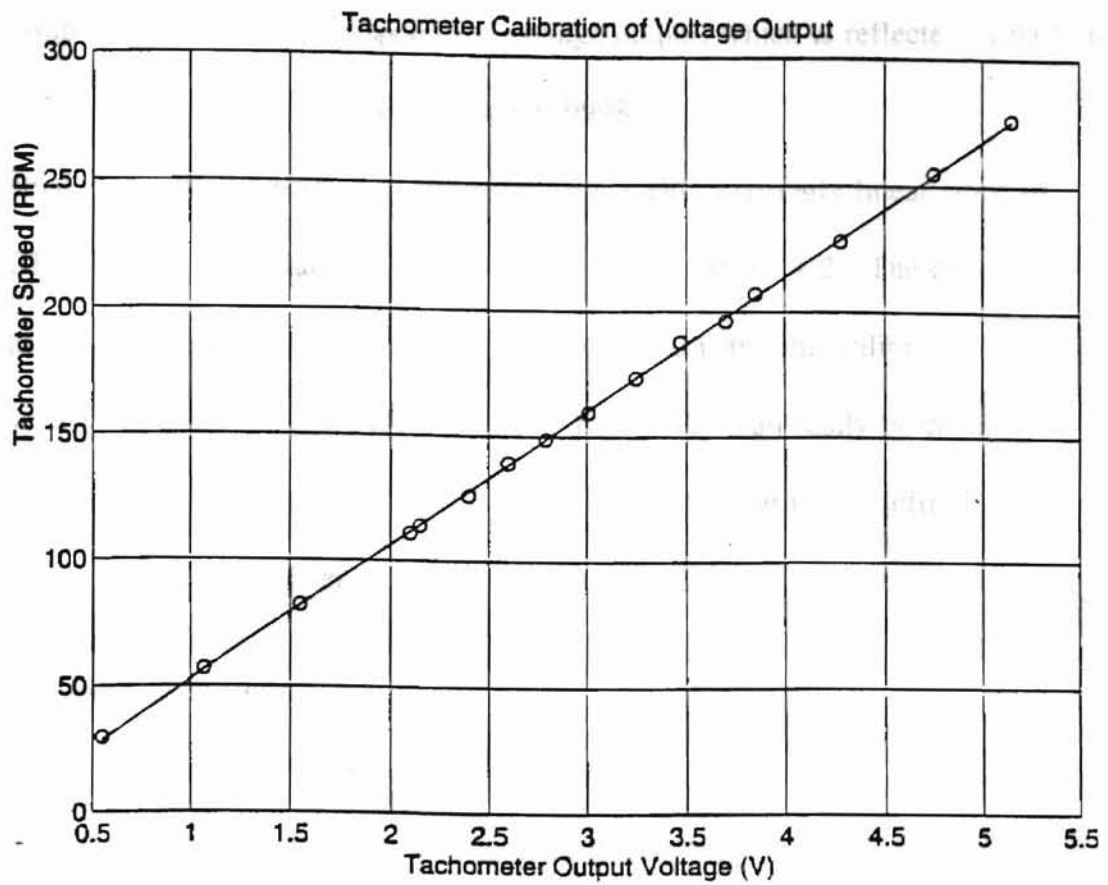


**Figure 17. Tachometer Calibration Results**

at measured voltages using the least squares line fit, and also the error between the measured and calculated values of RPM. The average for absolute values of error is 0.9. The standard deviation of the signed values of error is 1.1 RPM, which is about 0.4 percent of the full range of 250 RPM of the motors. This indicates a strong linear relationship between tachometer speed and voltage output, which is reflected visually in Figure 17, and in a correlation coefficient of 0.99987.

In conclusion, the calibration of the tachometer yields a strongly linear slope of 53.78 RPM/volt, with a relatively small offset at zero RPM of -1.2. The data acquisition system performs calculations involving speed using this calibrated tachometer factor and intercept value. Both of these values can easily be changed throughout the computer program by entering any new value at the "#define" statement near the beginning of the program code.

### **Resolution and Sensitivity**

The resolution and sensitivity of the system are of great interest because they can be indications of the quality of the measurement system [1, 53]. This section contains a discussion of the methodology employed in quantifying the system's resolution and sensitivity. It is shown that the resolution of the system is less than 0.5 oz-in of torque, which is about 0.5% of the expected range of torque measurement.

Resolution is "the smallest increment of change in the measured value that can be determined from the instrument's readout scale [1, 53]." Sensitivity, on the other hand, is "the change of a transducer's output per unit change in the measured quantity



[1,53]." In other words, resolution is the smallest increment reliably discernible from the readout scale. Sensitivity refers to the smallest increment of change in the measured quantity which the transducer is capable of transmitting. For example, a high-quality transducer with exceptional sensitivity should feature a readout device -- a dial, indicator, screen, or whatever -- with equally good resolution. Conversely, fine readout device resolution is wasted on a transducer which has comparatively low sensitivity. The sensitivity and resolution of the dynamometer and its readout system were found to be of the same order.

The sensitivity of the dynamometer is about that of the overall system resolution. Table 4 contains data recorded using a Vishay Strain Indicator. At the time the test was made, the dynamometer legs were 0.05 inches thick, and were slightly wider than those currently supporting the platform. As a result, that configuration was more sensitive than is the current configuration. However, the stiffnesses of the two configurations may be compared using the strain equation.

$$\varepsilon = \frac{6Fx}{Ebt^2},$$

where F = force  
x = strain gage location  
E = Young's Modulus  
b = width of beam  
t = thickness of beam

Therefore, the data in Table 4 has some use in indicating the sensitivity of the dynamometer itself. In Table 4, the relationship between torque and microstrain output is quite linear ( $r = 0.99928$ ), with 6.08 microstrain per ounce-inch. The strain

**Table 4**  
**Dynamometer Microstrain Output vs. Torque**

Weight Radius (in)	Torque (oz-in)	Microstrain ( $\mu\epsilon$ )
0	0	-1
1	16	127
2	32	225
3	48	319
4	64	416
5	80	510
6	96	605
7	112	700
8	128	790
0	0	4
8	128	792
7	112	700
6	96	606
5	80	514
4	64	420
3	48	323
2	32	230
1	16	132
0	0	5

equation above shows that doubling the thickness reduces the microstrain output by four times, so that an expected relationship between microstrain and torque for the new, thicker legs used on the second device which was built is about 1.5 microstrain per ounce inch of torque. One microstrain, then, should result in about 0.67 ounce-inches of torque. Since the Vishay readout unit increment is one microstrain, and furthermore, since the Vishay readout was quite stable especially at the lower radiuses in Table 4, the sensitivity of the dynamometer may be estimated at about 0.7 ounce-inches.

Regarding the overall system resolution, two situations exist, corresponding to the two modes available while the data acquisition program is running. The first mode involves either single analog-to-digital conversions or a relatively quick averaging of a few conversions. The data points used in the torque-speed and power-speed graphs are single conversions. Real time readouts of torque provided by the data acquisition program are actually averages of a few samples of torque. While real time readout is potentially of some use to the student, it is anticipated that greater benefit from a design standpoint can be obtained from both the dynamic torque tests, and the second general mode of operation. This mode features the capability of the system to average a relatively large number (say, 25) of data points to measure a supposedly static value of torque. For example, it is useful to know the power consumption of a drive belt, of various bearings and bushings, and of different configurations of bearing arrangements (cantilevered vs. simply supported). These measurements can be made at a steady state speed by averaging many conversions as the belt drive simulation runs. It became evident that two different methodologies were needed to estimate the system resolution of the two modes of utilizing the torque measuring capability of the system.

The methodology used to estimate the resolution of torque in the real time mode is as follows. The program was begun and calibrated, and placed in the real time read out mode. The 12-ounce weight was placed on the calibration bar at a distance of 6 inches. Small uniform aluminum tabs, 12 of which weighed 1.0 ounces, were placed on the weight one at a time while observations of the real time torque read out were recorded. Each incremental addition of a tab resulted in an increase in torque of about

0.5 ounce inches. The real time readout fluctuated generally by about one ounce inch of torque, due to the increase of gain of the noise generated by the bridge circuit. Table 5 contains the data generated by this test, while Figure 18 shows the general fluctuation ranges, and shows a line fit through the averages of the ranges. It can be seen from the graph that the readout resolution is more closely 1 oz-in of torque than 0.5 oz-in.

However, the resolution determined for the second mode of data acquisition operation is finer than that of the real time read out mode. The methodology for obtaining the resolution of the second mode of data acquisition operation is as follows. The program was run and calibrated. However, rather than using the real time readout

**Table 5**  
**Real Time Torque Readout of Added Weights**

<b>Weight (oz)</b>	<b>Actual Torque (oz-in)</b>	<b>Measured Torque Range (oz-in)</b>	<b>Average Measured Torque (oz-in)</b>
12	72	71/72	71.5
12.083	72.5	72/73	72.5
12.167	73	72/73	72.5
12.25	73.5	73/74	73.5
12.333	74	73/74	73.5
12.417	74.5	74/75	74.5
12.5	75	74/75	74.5
12.583	75.5	74/76	75
12.667	76	75/76	75.5
12.75	76.5	76/77	76.5
12.833	77	76/77	76.5
12.917	77.5	76/78	77
13	78	77/78	77.5

mode, the dynamic testing mode of the program was entered. Rather than running the motor, however, a static torque test comprising 25 torque data was performed. As each aluminum tab was added to the weight (once again placed at 6 inches radius), another test was run. Average values and standard deviations were then obtained on

the torque measurement data sets using Matlab. The radius selected was 6 inches, so that the addition of each tab incremented the torque by 0.5 ounce inches. The data for this test are included in Table 6 and are plotted in Figure 19. It can be seen that the resolution of the system in this mode is at least 0.5 ounce inches of torque.

The percent error in Table 6 provides a measure of the accuracy of the system. The average percent error is 1.8, with a standard deviation of 0.1. It is important to

**Table 6**  
**Average Static Torque Over Many Data Readings**  
**For A Distance of Six Inches (Starting Actual Torque of 72 Oz-In)**

Weight (oz)	Actual Torque (oz-in)	Average Measured Torque(oz-in)	Standard Deviation of Measured Torque (oz-in)	Difference Between Actual and Average Torque	Percent Error Between Actual and Measured
12.0	72.0	70.84	0.45	1.16	1.6
12.0	72.0	70.94	0.43	1.06	1.5
12.0	72.0	70.73	0.44	1.27	1.8
12.08	72.5	71.32	0.48	1.18	1.6
12.17	73.0	71.77	0.44	1.23	1.7
12.25	73.5	71.99	0.42	1.51	2.1
12.33	74.0	72.74	0.44	1.26	1.7
12.42	74.5	73.12	0.45	1.38	1.9
12.50	75.0	73.63	0.45	1.37	1.8
12.58	75.5	74.19	0.47	1.31	1.7
12.67	76.0	74.70	0.49	1.30	1.7
12.75	76.5	75.02	0.49	1.48	1.9
12.83	77.0	75.52	0.41	1.48	1.9
12.92	77.5	76.07	0.44	1.43	1.8
13.0	78.0	76.68	0.49	1.32	1.7

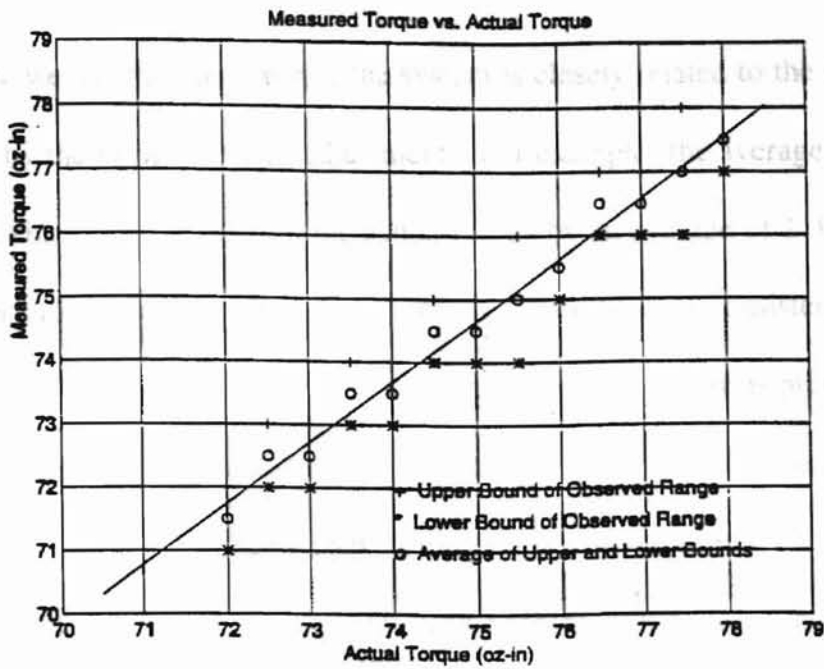


Figure 18. Torque Resolution -- Real Time Screen Readout Vs. Actual for Static Measurement

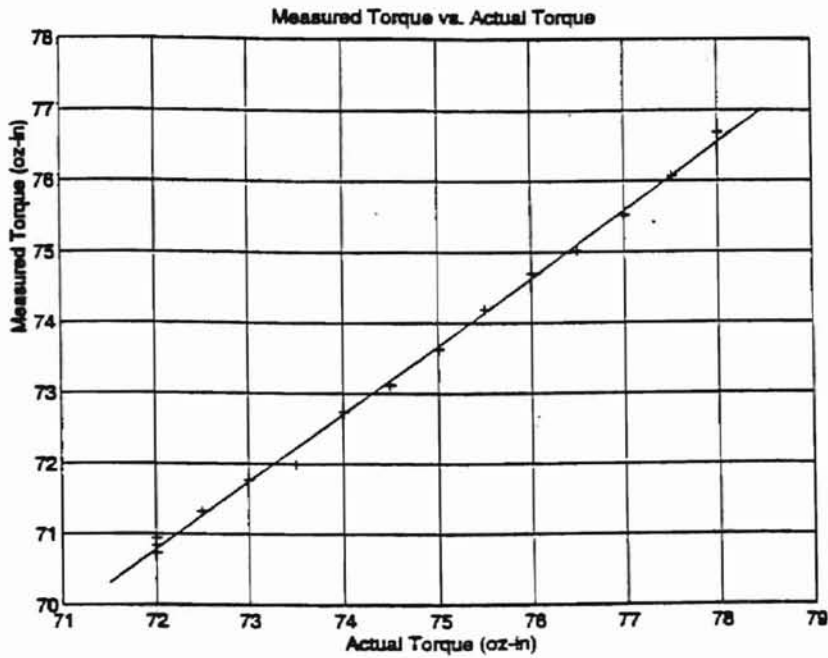


Figure 19. Torque Resolution -- Average Measured Vs. Actual For Static Measurements

consider, however, that the error of the system is closely related to the offset, which is controlled by the bridge balance adjustment. For example, the average measured data values in Table 6 are offset from the actual torque by an average of 1.32 ounce inches, with a standard deviation of 0.12 ounce inches. This offset is consistently lower than the actual torque, which suggests that the accuracy of the system is presently greatly improved by eliminating the offset in the measurements. The argument that the system resolution is at least 0.5 ounce inches of torque rests on the nearly 1-to-1 relationship between actual and measured torque for each addition of 0.5 ounce inches of torque. A line fit through the measured torque values produces the following relationship.

$$T_{\text{meas}} = 0.9596 T_{\text{act}} + 1.70$$

where

$$T_{\text{meas}} = \text{Average measured torque (oz-in)}$$

$$T_{\text{act}} = \text{Actual torque (oz-in)}$$

The line fit has a correlation coefficient of 0.998, which is quite linear.

In conclusion, it has been suggested that the sensitivity of the system is about that of the resolution of the system, where sensitivity is defined as the smallest increment of change in the measured quantity which the dynamometer itself is capable of detecting, and resolution is the smallest increment of change discernible by the system's data acquisition system. The resolution of the system is at least 0.5 ounce inches of torque when an averaging procedure of static torque is used. The resolution of computer screen real time torque readouts of static torque is about +/- 0.5 ounce inches, so that a fluctuation of about 1 ounce inch is typical. Though improvements in both the

system resolution and accuracy are possible, the existing levels are adequate for the design purposes of MAE 3033 students.

### **Repeatability**

An important criteria for evaluating the dynamometer was precision. Precision is basically how well the device repeatedly measures the same quantity. The procedure for evaluating the precision of the dynamometer was simply to obtain torque vs. speed and power vs. speed curves for a particular motor over a period of time. From these curves values for maximum power and the speed at which maximum power occurs can be compared. Table 7 contains this data. In addition, the curves are superimposed in Figures 20 and 21. The conservative assumption, of course, is that the variation of the actual motor characteristics was insignificant. In other words, it is unknown how much of the scatter in Figures 20 and 21 is due only to motor variation.

From Table 7 it can be seen that the standard deviation of maximum power of 21.6 is 4.0 percent of the average value of 543.1 oz-in/sec. This means that for one standard deviation, the precision of the device is 8.0 percent of the 'full-scale' reading. The two-sigma precision is 15.6 percent of full-scale reading. However, perhaps as important from a design standpoint, the standard deviation of the speed at which maximum power occurs is only 2.2 percent of the average value. The two-sigma precision of the speed at which the maximum power occurs is 6.8 percent of the full-scale value. Finally, from observing the superimposed torque vs. speed and power vs.



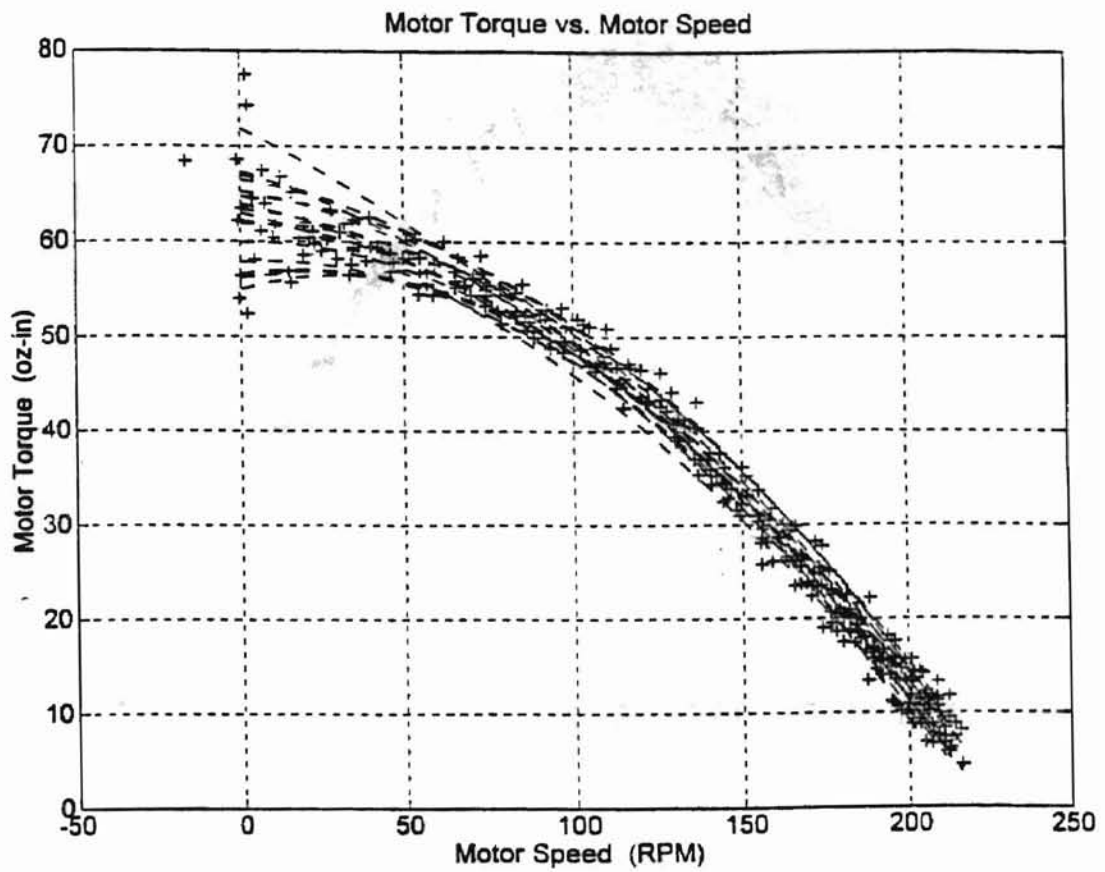


Figure 20. Superimposed Torque Vs. Speed Curves for 17 Motor Trials

...dynamometer was just sufficient

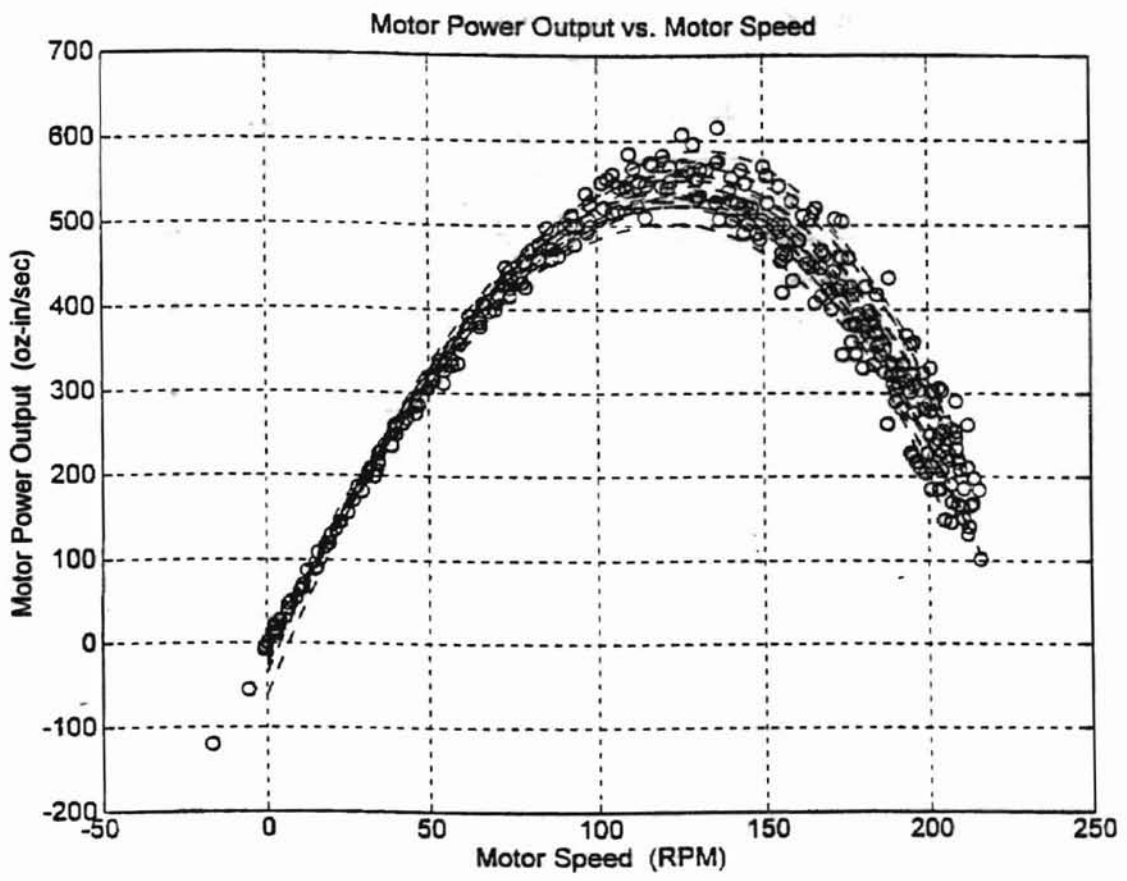


Figure 21. Superimposed Power Vs. Speed Curves for 17 Motor Trials

speed curves for the 17 runs, the precision of the dynamometer was judged sufficient for the design purposes of MAE 3033 students.

**Table 7**  
**Maximum Power and Speed at Maximum Power**  
**for 17 Motor Trials**

Run File Name	Maximum Power (oz-in/sec)	Speed at Max Power (RPM)
s713 1	502.1	121.6
s713 2	523.5	124.8
s713 3	523.5	130.4
s713 4	522.2	122.0
s713 5	539.2	121.3
s713 6	533.7	125.0
s713 37	553.6	127.2
s713 38	561.8	125.1
s713 39	538.9	126.3
s713 40	546.6	126.3
s713 41	559.0	128.1
s713 42	528.7	125.0
s713 43	531.2	126.5
s713 44	536.3	125.6
f712 9	588.5	131.0
f712 11	568.6	128.6
f712 12	575.8	129.5
Average	543.1	126.1
Standard Deviation	21.6	2.8

### Accuracy

Perhaps one of the single most attractive features of the dynamometer is that it can be calibrated conveniently using physical weights. The high value of linearity of the relationship between induced torque and strain gage output has already been remarked upon. The ramification of this feature is that the accuracy of the system is verified

physically before measurements are made. To observe the effect of this, note in Table 6 the values of the percent error between torque readings and the product of weight added and radius. The average percent error is 1.76. Also, note in Table 10 (p.73) that after running the data acquisition mode of the program 12 times, the dynamometer was tested with weights for torques of 96 and 48 oz-in. The percent errors are 0.8 and 1.9, respectively. These observations are typical. It may be conservative to say that the dynamometer features an error of less than 2 percent.

### **Final System Qualification--Vehicle Simulation**

#### **Overview**

It seemed reasonable that the best indication of the quality of the entire system, including the dynamometer, circuitry, data acquisition system, and data treatment in Matlab, was simply to simulate an existing vehicle and compare the model with an actual vehicle. A close approximation of an actual vehicle should qualify the dynamometer as a useful design tool for MAE 3033 students.

The experimental outline was to select an existing vehicle and determine its time to traverse some distance. A distance of 48 inches was chosen, since this is typical of a contest requirement. Next, a simple model of the vehicle was designed using Newton's laws and kinematics. This model requires an expression for torque. This expression was provided by using the dynamometer to obtain a torque-speed relationship for one of the vehicle's motors. Additionally, the torque requirements of a belt drive and a loaded driven wheel supported by cantilevered ball bearings were obtained at constant

speed. This torque requirement was subtracted from the value of the motor output torque found by solving the motor's torque-speed relationship. The solution of the model using the Runge-Kutta method provided a comparison between actual vehicle performance and a simulated run using vehicle characteristics obtained with the dynamometer.

### **Vehicle Selection and Speed Measurement**

The experimental procedure began with selecting an existing vehicle with a drive system and bearings comparable to what could be tested on the dynamometer. A vehicle was selected which weighed 7 lb., 14 oz and featured a belt drive. The rear wheels, which were the powered wheels, were supported by cantilevered ball bearings. The front wheels rotated on simply supported ball bearings. New belts were made for this vehicle which were the same width and of the same material as was used on the dynamometer for simulation. This was done to reduce torque differences due to the belt. This vehicle was timed using a stopwatch as it traversed 48 inches of flat surface starting from a standstill. Weight was added to the vehicle for subsequent runs so that the behavior of the simulation could be compared. The final run was made with the vehicle transporting 33.4 pounds of payload. The total weight driven by the motors was 41.3 pounds. The time data is included in Table 8.

The relationship between added weight and measured average run time is somewhat linear with a correlation coefficient of 0.99404. Figure 22 shows the relationship

and Figure 22 include the total vehicle loads.

The graph shows that the total time of

Table 4

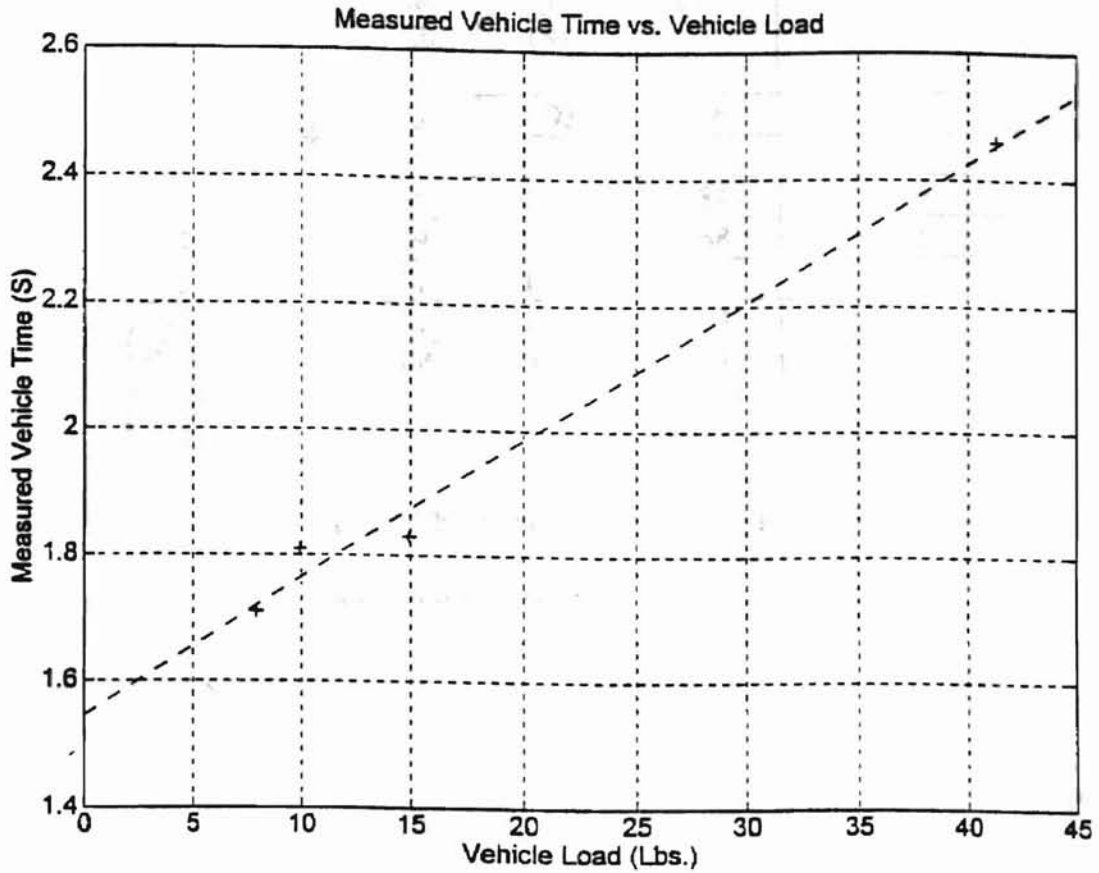


Figure 22. Measured Time Vs. Load For Vehicle Traverses

graphically. The vehicle loads shown in Figure 22 include the total vehicle loads, including the weight of the vehicle itself. The graph shows that the total time of

**Table 8**  
**Actual Times for Loaded Vehicle Traverses of 48 Inches**

Run No.	Car Alone 7.9 Lb. (S)	9.9 Lb.. (S)	14.9 Lb.. (S)	41.3 Lb.. (S)
1	1.73	1.93	2.06	2.41
2	1.65	1.80	1.84	2.53
3	1.65	1.78	1.84	2.46
4	1.79	1.71	1.68	2.41
5	1.71	1.84	1.74	2.50
Average	1.71	1.81	1.83	2.46
Standard Deviation	0.005	0.07	0.13	0.05

traversal is fairly linear with load. This means that the vehicle spends a small portion of its run time accelerating, with the majority of the time spent at full speed. The model supports this observation. The speed is effected mainly by the additional torque requirement of the drive train.

### **The Model of the Vehicle**

The vehicle is modeled as a mass with one wheel, as shown in Figure 23. Assumptions are no slipping of the wheel, rigidity of the mass and wheel, and that the mass is a point mass  $M$  located at the center of gravity of the wheel. The problem is to find the acceleration of the mass.

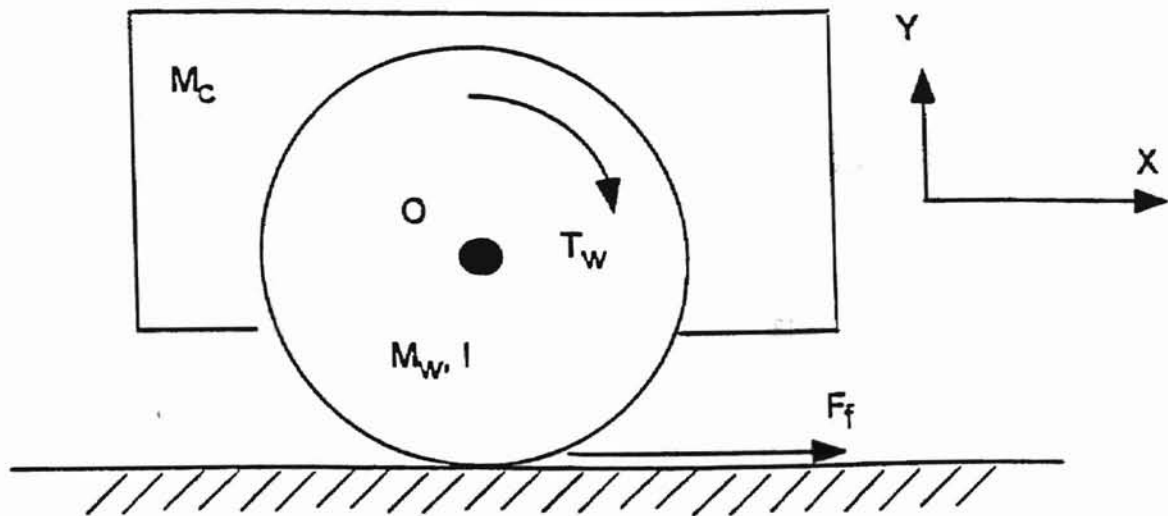


Figure 23. The Model of a Vehicle



The summation of forces in the x-direction yields:

$$\Sigma F_x = (M_c + M_w)a = F_f$$

where:  $M_c$  = Mass of the vehicle

$M_w$  = Mass of the wheel

$a$  = Acceleration in the x-direction

$F_f$  = The force of static friction between  
the wheel and the ground

The summation of moments about the point O yields:

$$\Sigma M_o = I\alpha = T_w - F_f r$$

where:  $I$  = Inertia of the wheel

$$= \frac{1}{2} M_w r^2$$

$\alpha$  = Angular acceleration of the wheel

$T_w$  = Torque supplied to the wheel

$r$  = radius of the wheel

Solving the two equations for  $F_f$  and equating the result gives:

$$(M_c + M_w)a = \frac{T_w - I\alpha}{r}$$

Since  $a = r\alpha$ , the expression for inertia can be substituted into the above equation to give:

$$a = \frac{T_w}{r \left( M_c + \frac{3}{2} M_w \right)} \quad \text{Eq. A}$$

where  $T_w$  is a function of motor speed. The relationship for torque as a function of motor speed was a second order polynomial created by performing a least squares curve fit on torque vs. speed data. The data was obtained by the data acquisition system, and

treated as described elsewhere. Equation A was broken into 2 first order differential equations for use in Matlab's Runge-Kutta function "ODE23". This was done in the following way.

Equation A can be written as

$$a = C_1 \times (a_0 C_2^2 X_1^2 + a_1 C_2 X_1 + a_2)$$

where

$$C_1 = \frac{1}{r \left( M_c + \frac{3}{2} M_w \right)}$$

and the remainder of the equation is torque expressed as a second order polynomial function of motor speed with coefficients  $a_0$ ,  $a_1$ , and  $a_2$ .  $C_2$  is a conversion factor to convert the linear velocity  $X_1$  to angular velocity. The coefficients are returned from Matlab's polyfit routine, which performs a least squares fit of the data. Then,

$$\dot{X}_1 = \text{acceleration} = C_1 \times (a_0 C_2^2 X_1^2 + a_1 C_2 X_1 + a_2)$$

and

$$\dot{X}_2 = X_1$$

These are the two first order differential equations passed to Matlab's Runge-Kutta routine.

The next step in the procedure was to use the dynamometer to obtain the motor output torque/speed relationship.

## Motor Torque/Speed Relationships

Torque-speed curves for the motor were obtained using the procedure described in Appendix B, Section 3. Torque data was also obtained for the shaft bearings, belt, and loaded idler wheel using the procedure described in the same section. A schematic of the setup for obtaining this data is shown in Figure 24. The shaft bearing torque requirement was subtracted from the value of the torque obtained by evaluating the torque function at each speed in the Runge-Kutta routine. The data are shown in Table 9. Three motor runs were made, with the data saved to files "M221.M", "M222.M", and "M223.M". The motor runs were made by holding the inertial disk as stationary as possible for about 1/2 seconds after the relay was triggered. This allowed the torque to develop to its stall value before the disk was allowed to accelerate. However, the data files had to be specially treated to obtain the polynomials shown in Table 9. The torque data points at zero RPM weighted the polynomial so that eliminating them

**Table 9**  
**Polynomial Coefficients for Three Motor Runs**

File Name of Run	Polynomial Coefficients		
	$a_0$	$a_1$	$a_2$
M221	-0.0004	-0.1491	67.1674
M222	-0.0003	-0.177	68.4822
M223	-0.0005	-0.1119	62.9176

produces a curve which more closely shows the behavior of nonzero RPM torque data points. The varying values for  $a_2$  in Table 9 reflect the sensitivity of the intercept to the torque values which become the initial ones after the zero RPM torque values are

Experimental Test

and the selection of the initial value is also

subject of F

power vs. speed curves, however

equipment of a belt and

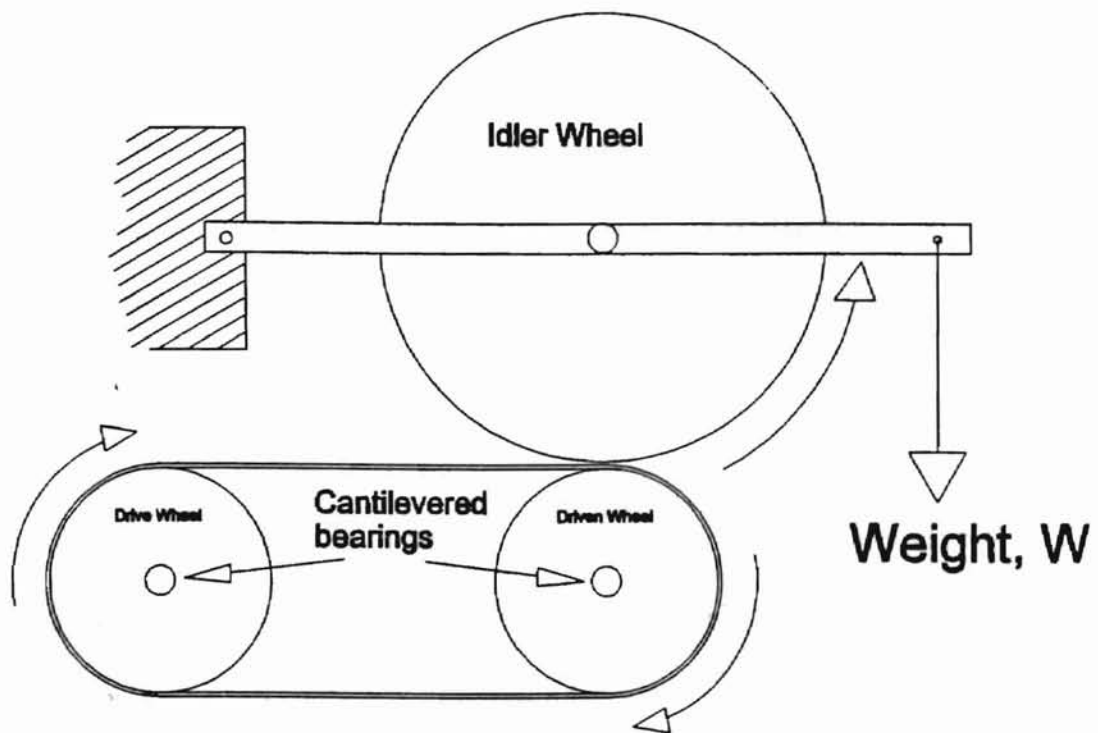


**Figure 24. Schematic of Belt Drive Simulation Apparatus**

eliminated. The effect of the torque curves to the selection of the initial value is also evident in Figure 20. This effect has no bearing on power vs. speed curves, however, since they occur at zero speed. Table 10 lists the torque requirements of a belt and loaded cantilevered ball-bearing driven wheel at various loads. The average torque requirement of the shaft bearings was calculated as 3.3 oz-in. This value was subtracted from the torque deducted from the torque generated by the polynomial, since this torque was due to the function of the dynamometer itself. The torque data in Table 10 was used to generate a linear relationship between the load placed on the idler wheel and the torque requirement of the cantilevered bearings. The relationship is not dependent on speed because when one part rolls on another without sliding there is little variation of rolling friction with velocity [7]. The correlation coefficient of 0.98854 supports this. The relationship is:

$$\text{Torque required (oz-in)} = 1.34964 \times \text{Load (lb.)} + 5.12$$

Eq. B

The data is graphed in Figure 25, with the extrapolated point at a load of 20.6 pounds. This is 1/2 the combined total load of the vehicle and the 33.4 pounds added to the machine in the timing run. One-half the combined load was used since the dynamometer simulates only one of the vehicle's two belt drives. The extrapolated point had to be extrapolated since the dynamometer's idler arm was not capable of supporting this much actual weight. Please note that Figure 26 is the lower left corner of Figure 25. These are the actual weights added to the vehicle.

Equation B was used to interpolate torque requirements at loads corresponding to the actual loads placed on the vehicle during the measured time trials. From these interpolated values the shaft torque requirement was deducted. Then, this adjusted

**Table 10**  
**Torque Requirements and Speeds for Various Loads At Constant Speed**

Condition	File Name of Run	Load (lb.)	Speed (RPM)	Std Deviation	Torque Req (oz-in)	Std Deviation
No Belt	m224	NA	258.6	1.8	3.6	1.28
	m225	NA	258.9	1.9	3	0.92
Belt Only	m226	NA	251.5	1.3	5.5	1
	m227	NA	250.4	1.6	4.8	1.4
Idler Only on Driven Wheel	m228	1.8	244.5	0.9	7.7	1.3
	m229	1.8	244.7	1.1	7.1	1.1
Idler + 1.22 lb	m2210	4.3	236.4	1.2	10.5	1.1
	m2211	4.3	236.3	0.8	10.3	1.6
Idler + 2.22 lb	m2212	6.5	218	4.8	15.7	1.6
	m2213	6.5	219.4	2.8	14.5	1.5
idler + 3.22 lb	m2214	8.8	210.6	7	15.9	2.4
	m2215	8.8	207	4.8	16.8	2
Calibration						
96 Oz-in	m2216	NA	NA	NA	95.2	0.4
48 Oz-in	m2217	NA	NA	NA	47.1	0.4

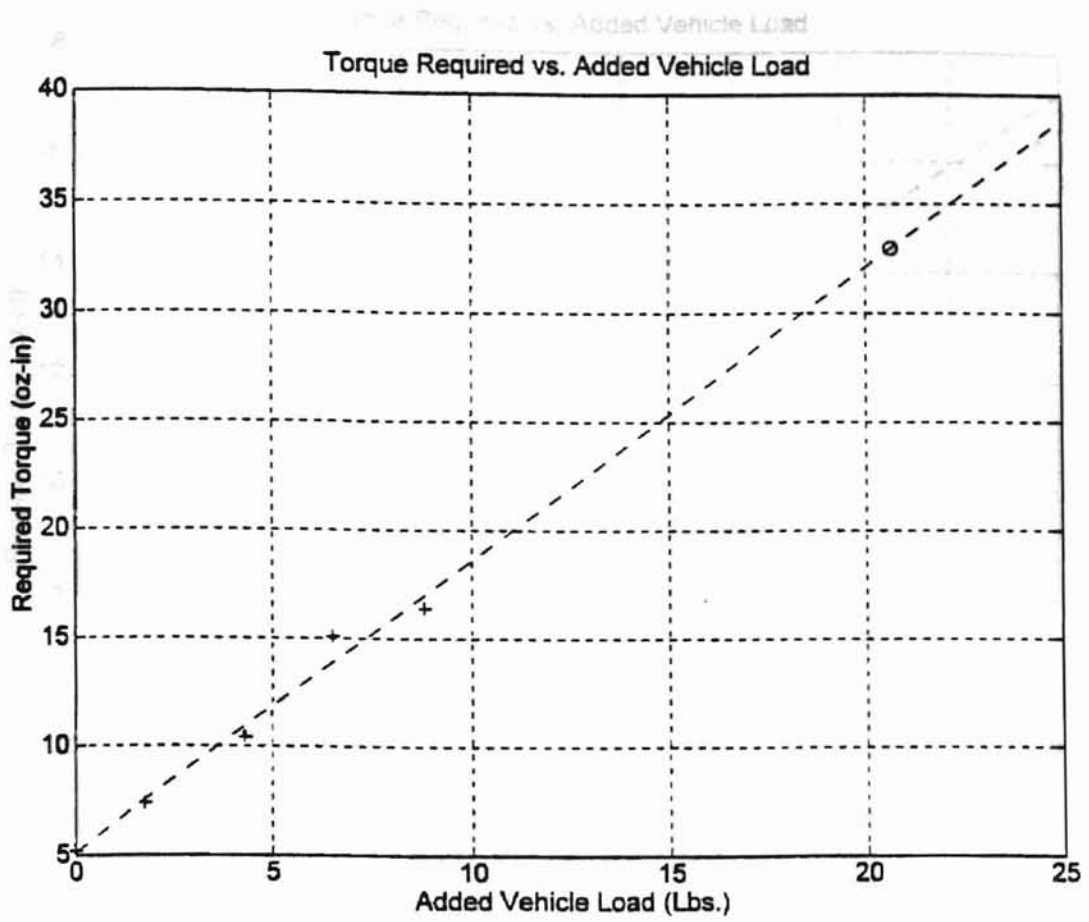


**Figure 25. Torque Required Vs. Added Load For Dynamometer Belt Drive Simulation**

value was calculated from the torque output of the motor calculated from the torque speed characteristics of the motor. In this way, simulated values were compared with the actual values.

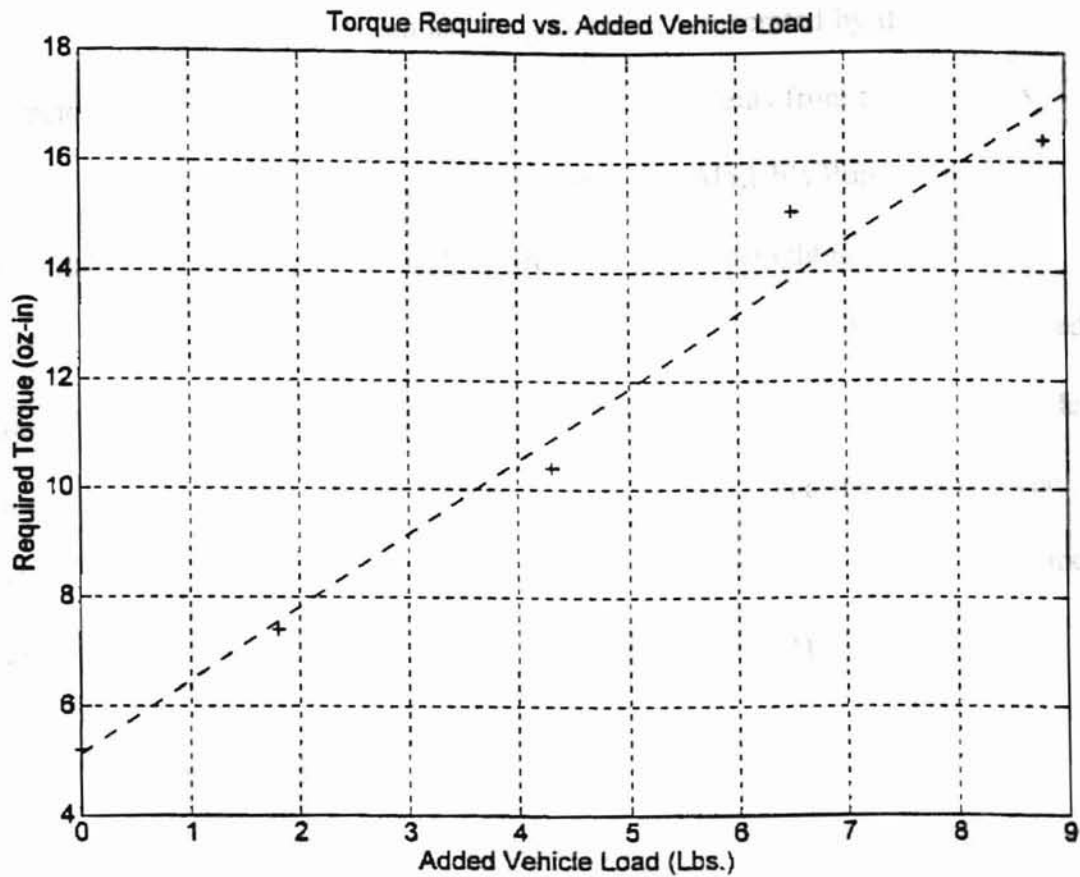


Figure 26. The Lower Left Corner of Figure 25



value was in turn deducted from the torque output of the motor calculated from the torque-speed relationship within Matlab's Runge-Kutta routine. In this way, simulated vehicle run times were generated which could be compared with the actual times.

Figure 27 shows how students can use the information generated by the dynamometer to simulate vehicle performance. The coefficients from the torque vs. speed curve obtained with the dynamometer are passed to Matlab's Runge-Kutta routine, with the wheel diameter, wheel weight, and vehicle weight entered into Equation A. At least one item of interest can be seen in Figure 27. The vehicle spends only about the first 1/4 second accelerating. This supports a similar observation made when loading a vehicle with successive weights, described in an earlier section. The code which generates Figure 27 is found in the Matlab script files 'MYSIM17.M' and 'TESTWO3B.M', which calls the former. These codes are in Appendix D.

### **Simulation Results**

Table 11 shows the results of the comparison between measured vehicle run times and simulated times for traversing 48 inches. It is evident from the data that the predicted torque for this test is lower than the actual drive train torque requirements for payloads up to 7 pounds, but higher than the actual values for the 33.4 pound payload. In other words, the line fitted through the data in Figure 24 would better approximate the measured vehicle performance if the line were flatter. However, the data demonstrates that the model approximates the observed behavior of the vehicle. The percent error between the estimated and actual vehicle speed times ranges between 5 and 15 percent.

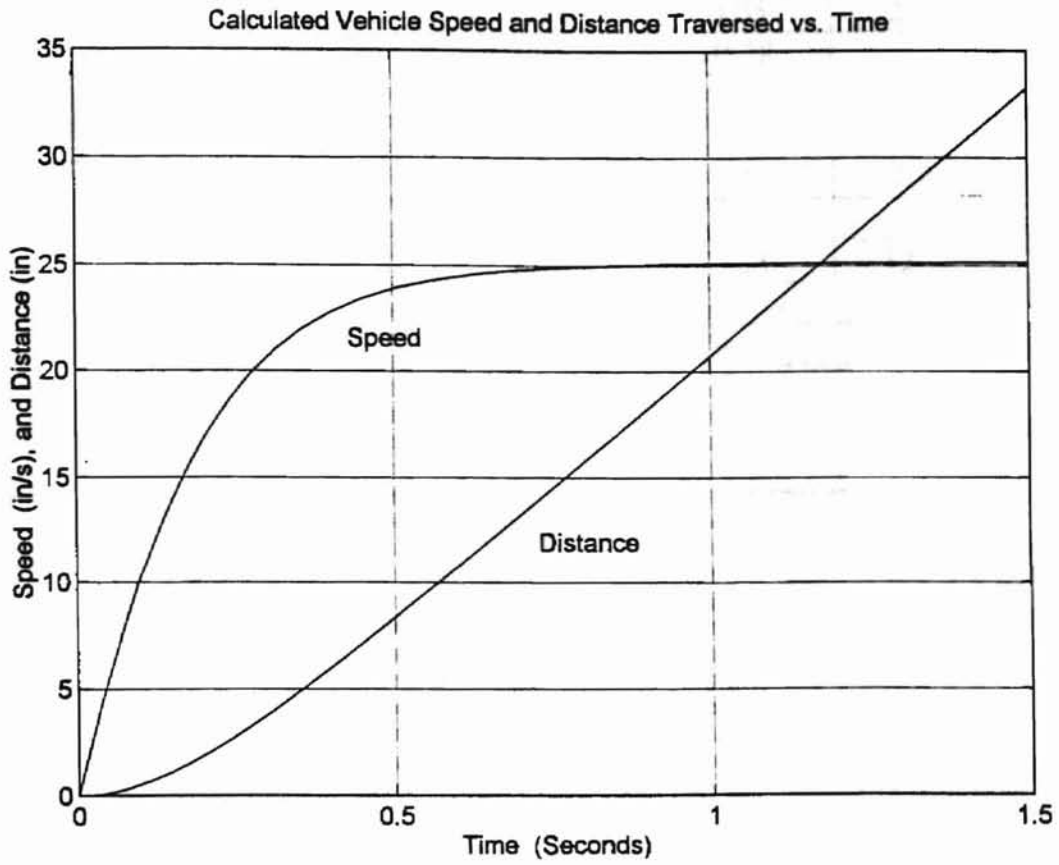


Figure 27. Typical Simulated Vehicle Speed and Position Vs. Time Curves

**Table 11**  
**A Comparison of Simulated and Measured Vehicle Speed**

File Name	Load Condition	Simulated Time (S)	Measured Time (S)	Error (S)	Percent Error
m221	Vehicle only	1.6	1.71	0.11	6.4
	+2 lb..	1.64	1.81	0.17	9.4
	+7 lb..	1.78	1.83	0.05	2.7
	+33.4 lb..	2.74	2.46	-0.28	11.4
m222	Vehicle only	1.59	1.71	0.12	7
	+2 lb..	1.63	1.81	0.18	9.9
	+7 lb..	1.78	1.83	0.05	2.7
	+33.4 lb..	2.76	2.46	-0.3	12.2
m223	Vehicle only	1.62	1.71	0.09	5.3
	+2 lb..	1.66	1.81	0.15	8.3
	+7 lb..	1.8	1.83	0.03	1.6
	+33.4 lb..	2.82	2.46	-0.36	14.6

### Effect of Wheel Diameter on Predicted Vehicle Speed

Having performed a vehicle simulation, it is interesting to now observe the effect of wheel diameter on the model's predicted vehicle speed. Figure 25 shows that simulated speed is very sensitive to changes in wheel diameter in the range of up to about four inches. This is the range in which students typically design their wheel diameters.

The data for Figure 28 was generated by the model for an unloaded vehicle, and is found in the Matlab file "M221.M". The wheel diameter was incremented by one inch from one to 15 inches, and the resulting simulated speeds were recorded. Assumptions made were no slipping of the wheel and no increase in vehicle or wheel weight with

increasing wheel diameter. The time to complete a run resulting at the fastest traverse is from about 11.5 seconds at 0 inches to about 1.5 seconds at 15 inches. In this region,

however, wheel diameter has a significant effect on the time to complete a run. At 0 inches, the time to complete a run is about 11.5 seconds. At 15 inches, the time to complete a run is about 1.5 seconds.

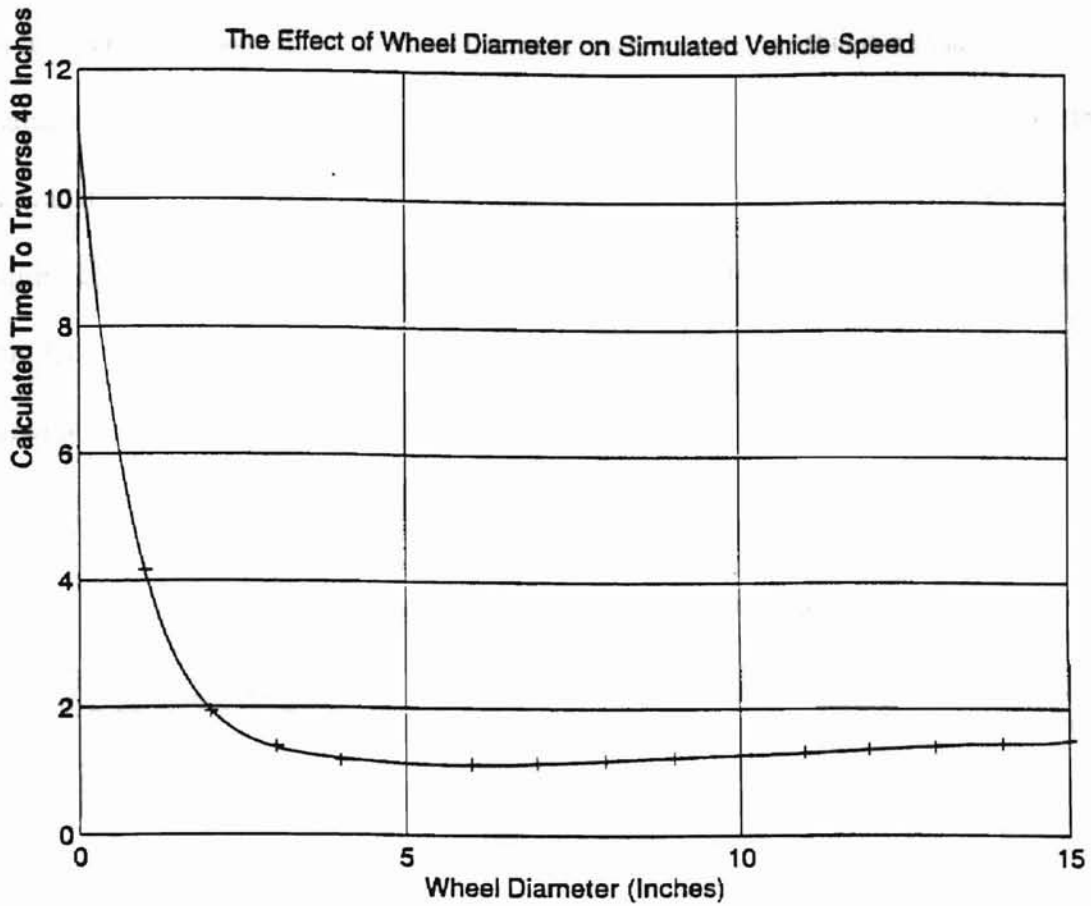


**Figure 28. The Effect of Wheel Diameter on Simulated Time to Complete a Vehicle Run**

increasing wheel diameter. The range of diameters resulting in the fastest traverse is from about 3.5 up to 7 inches. Because the curve flattens out somewhat in this region, however, lower values may be better design choices for various reasons. Interestingly, a wheel diameter of about 3.5 to 4 inches has come to be the ongoing buzzword passed down from class to class. It is interesting to speculate on whether this is a result of some mechanical natural selection, or if it is simply the easiest, simplest wheel to build given the tools available to the student.

Figure 28 illustrates the capability of the system to aid students in making significant design decisions. Not only does using the dynamometer help to highlight which elements of the vehicle constitute important design considerations, but it can also be used to optimize these elements and understand them better.

#### **Adaptability--Model Rocket Motor Characterization**

There is an interesting side note on the success of the dynamometer in characterizing motors. One of the original objectives for the dynamometer was that it be adaptable to a variety of situations. The dynamometer was very successful in characterizing solid propellant model rocket engines. The engines were rated at 4 to 6 Newtons (14.4 to 21.5 oz) of thrust, with distinctive thrust/time plots. Several motors were tested on the dynamometer using an adaptation which consumed less than an hour of shop time to manufacture. The adaptation consisted of a Delrin tube in which the cylindrical rocket motors were held. The tube was screwed onto a six-inch bar of screw stock, which was inserted and fixed to the calibration post. The rocket motor

and tube were oriented vertically so that the thrust imposed a torque on the dynamometer platform, which could be detected by the strain gages. The dynamometer was then calibrated by placing a 1-Kg. mass on the Delrin cylinder, and observing a voltage change on the oscilloscope screen of 4.0 volts. The motor was then fired, and its thrust-time plot was recorded on the oscilloscope. Oscilloscope printouts of the experimental thrust/time plots are shown in Figures 30 and 31. A close correspondence in plot shape may be observed between the experimental data and vendor information provided with the rocket engines, which is shown in Figure 29. However, a peak thrust of 2.5 pounds was recorded by the dynamometer, while the rated peak thrust of the motor is 3.0 pounds. Furthermore, vendor information provided with the rocket motors reports a "shelf" value of about 1 pound. The measured shelf value is slightly less than 1/2 pounds. Repeated tests indicate substantial variation in rocket motor performance.

### **Description of Some Dynamometer Components**

#### **The Tachometer**

The tachometer is a Servo-Tek Model Number SD-740B DC tachometer generator (catalog number TG-234). Its catalog rated output is 20 VDC/1000 RPM. Linearity is 0.1%, and ripple is 3% RMS. The body is 1-1/16 inches in diameter by 2-3/16 inches long. The shaft is 0.120 inches in diameter by 1/2 inches long. Its retail price was \$65.00 at the time it was incorporated into the project. (1995-96 Servo Systems catalog Montville, NJ (800-922-1103))

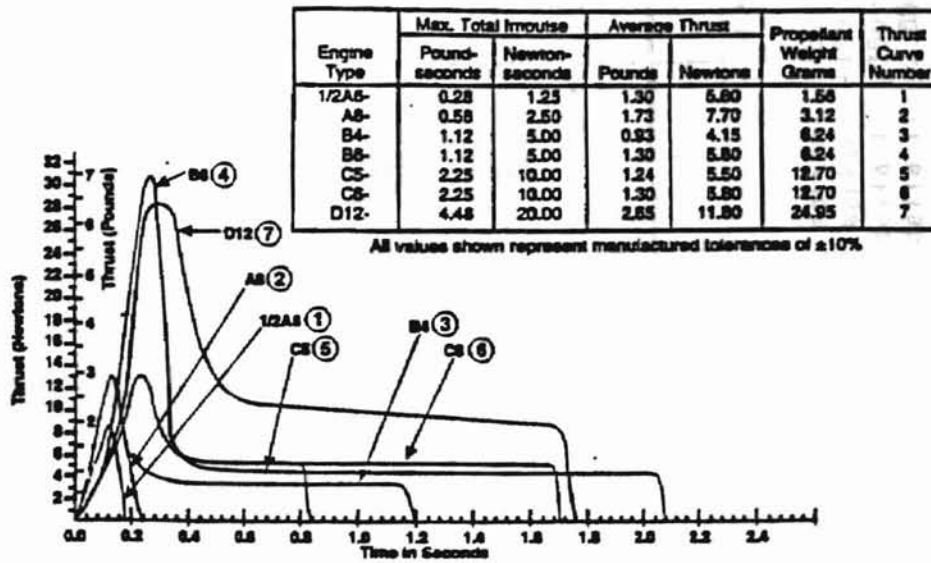


Figure 29. Vendor Thrust Curves for Model Rocket Engines

hp stopped

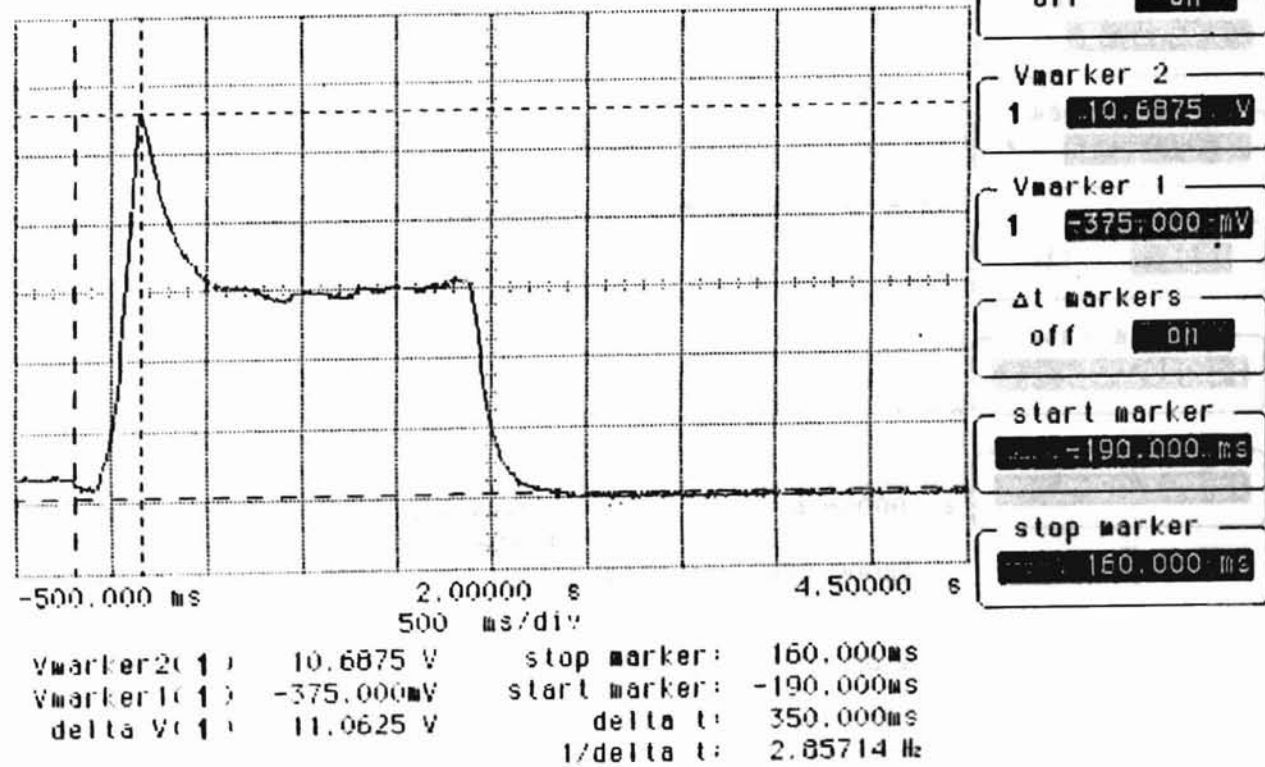
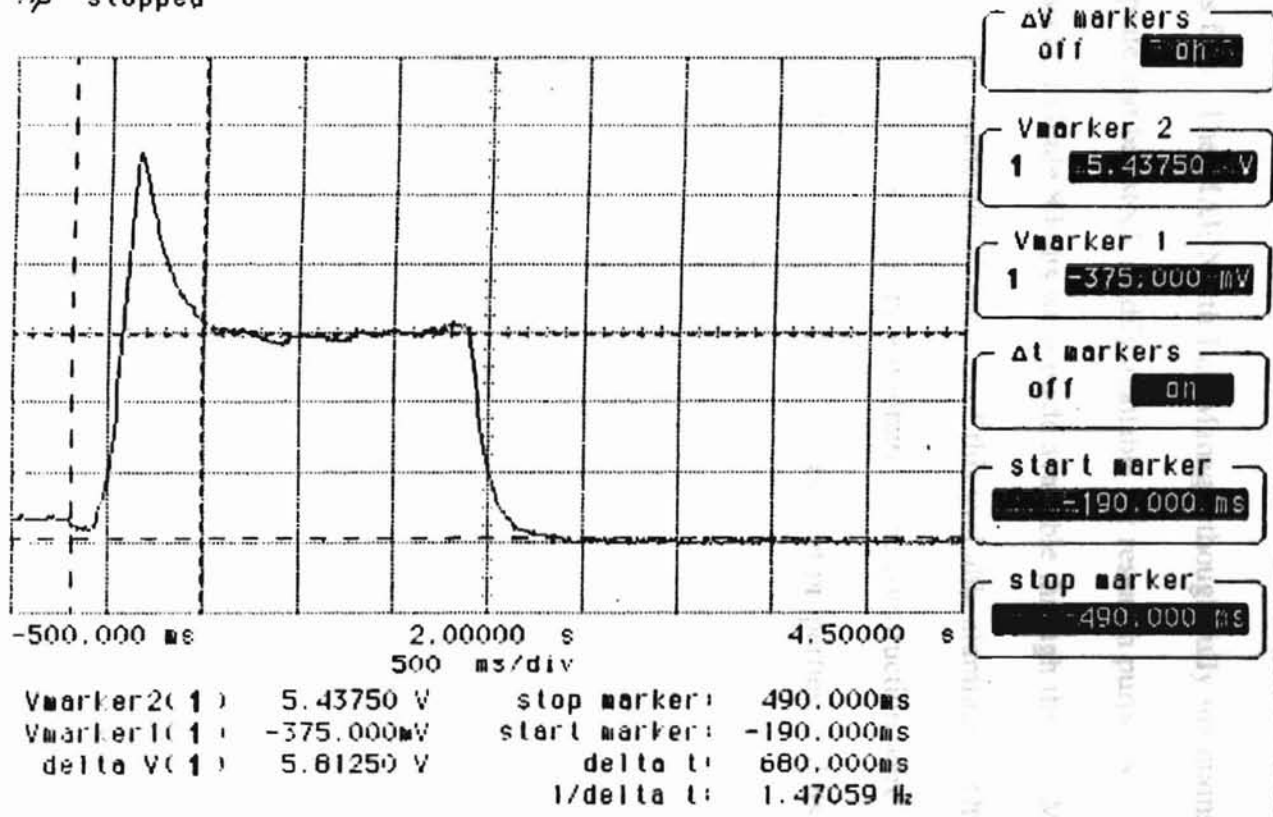


Figure 30. Dynamometer Thrust Curves for B6-5 Model Rocket Engines



hp stopped



B6S  
10/2

Figure 31. Dynamometer Thrust Curves for B6-5 Model Rocket Engines

## Construction Material

## Chapter IV

The dynamometer is made primarily of aluminum. This decision was made because the material was free. The MAE North Lab Manager thoughtfully maintains a scrap pile of various plate and bar stock readily available for research purposes.

Additionally, assorted Grade 8 bolts were made available through the Lab Manager.

The dynamometer was made almost entirely of this available aluminum. Other less compelling but strong reasons for using aluminum in the construction were its excellent machinability, its aesthetic quality, its corrosion-resistant properties, and its light weight.

## Chapter IV

### Results

This chapter contains a discussion of the results of the project in terms of the design objectives and the financial constraints. Additionally, some assumptions underlying the operation and testing of the device, as well as the scope and limitations of the system are discussed.

The result of the project is a system represented by the schematic in Figure 32. The black box containing the circuitry is the central routing component of the system. Through it, the computer collects speed and torque signals from the tachometer and the strain gages, both of which are located on the dynamometer. The dashed line between the motor and the torque table represents the interaction between the motor and the dynamometer as the motor transfers torque through the motor platform and legs.

### Costs

The approximate out of pocket costs and estimated rebuild costs for the project are shown in Table 12. The rebuild cost is the cost of commercially rebuilding the torque table and the black box. This price does not include the power supply for the motor, the computer, or the data acquisition hardware and software.

**Table 12**  
**Approximate Out of Pocket and Rebuild Project Costs**

	<b>Costs (\$)</b>	
	<b>Out of Pocket</b>	<b>Rebuild</b>
Machinist (\$60/hr. for 50 hrs.)	0	3000
Aluminum		20
Screws and Bolts	25	40
Circuitry	25	150
Instrument Assembly (\$60/hr. x 4 hr.)	0	240
Tachometer	0	65
Strain Gages	90	90
Miscellaneous	10	50
<b>Totals</b>	<b>150</b>	<b>3655</b>

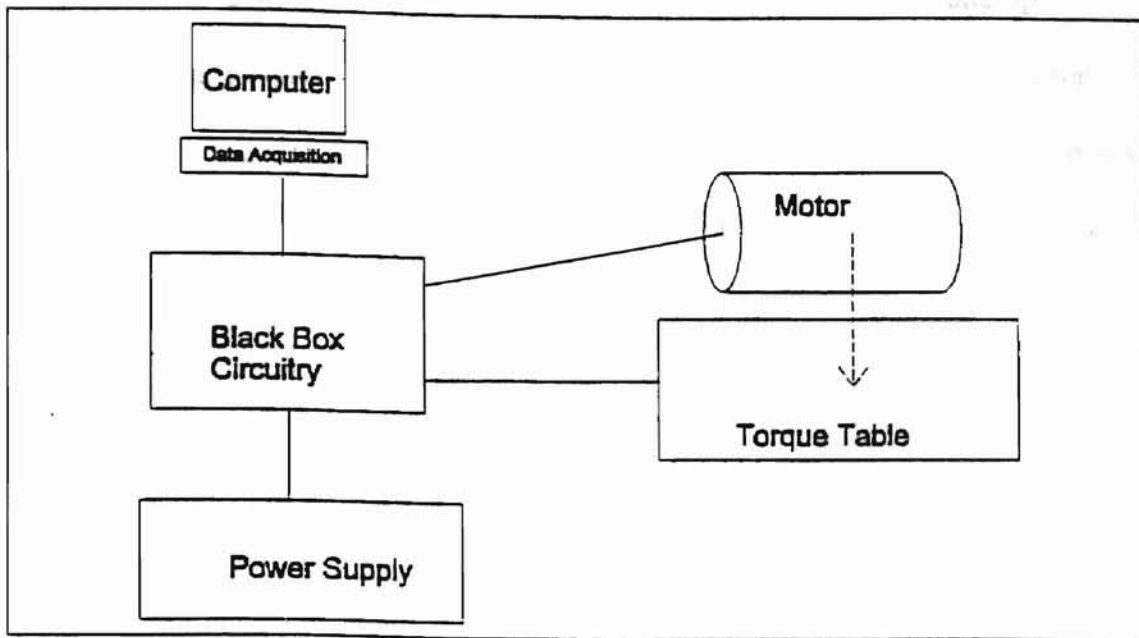


**Figure 32. System Schematic**

## Motor Characterization

Figures 26 and 27 show values for torque and speed derived directly from voltage values collected by the computer for two typical runs. The data has been processed by shifting speed values, as discussed previously. It can be seen that the speed, represented by the '+' marks, remains at zero while the torque climbs to a maximum. The torque falls off as the speed increases. For these runs the disk was held stationary for about 1 second after power was relayed to the motor. This was an attempt to capture true stall torque. Figures 28 and 29 show second order curve fits relating torque to motor speed. Figure 30 then shows a second order curve fit relating motor power to motor speed. The relatively small amount of scatter about the torque/speed and power/speed curves indicates the success of the design.

## Conceptual Assumptions

Several assumptions have been made. Technically, it is assumed that dynamometer components other than the legs and shaft are perfectly stiff, particularly the inertial disk and the platform. These assumptions are reasonable considering the thickness of these components, and, indeed, the robustness of the entire mechanism. The effect upon the operation of the dynamometer if, for example, the disk behaved with significant elasticity is that this component would perform as an energy-absorbing spring. As the motor accelerated the disk, it would initially absorb energy, which would be released at a time dependent upon the spring constant of the disk and the torque of the motor. The

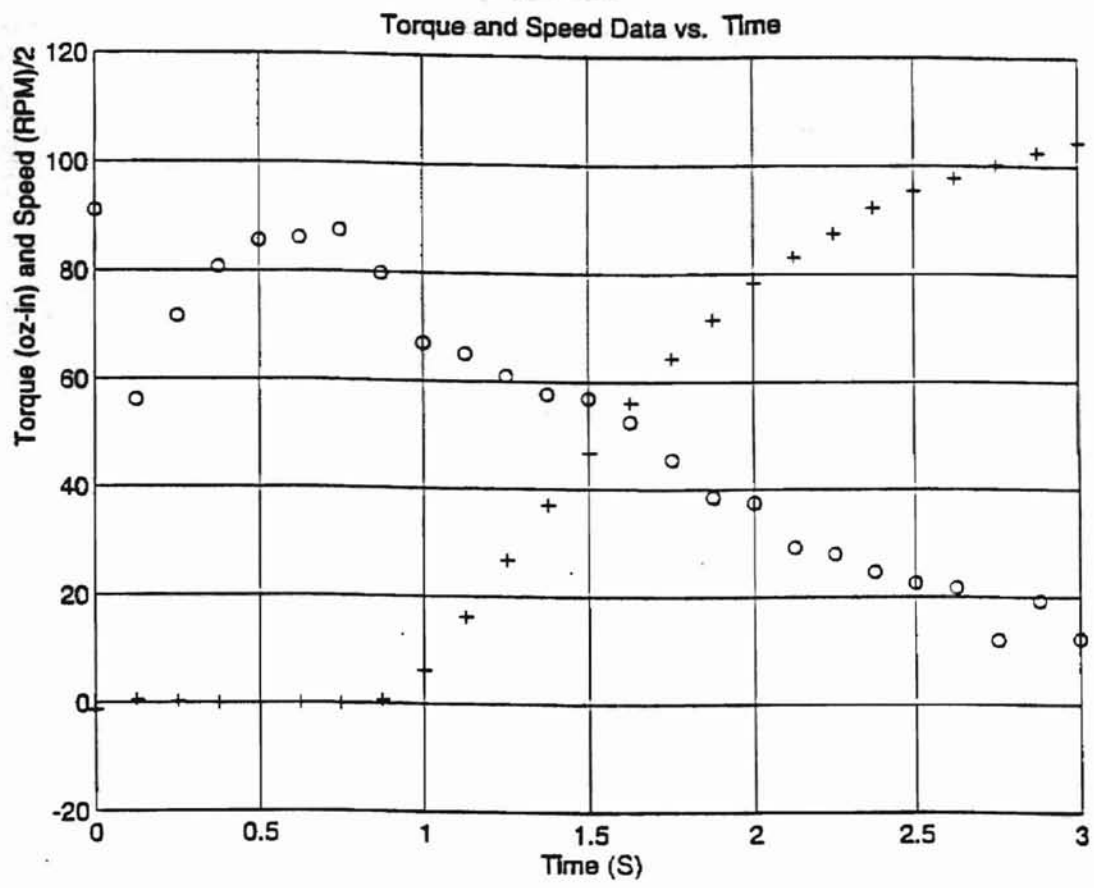
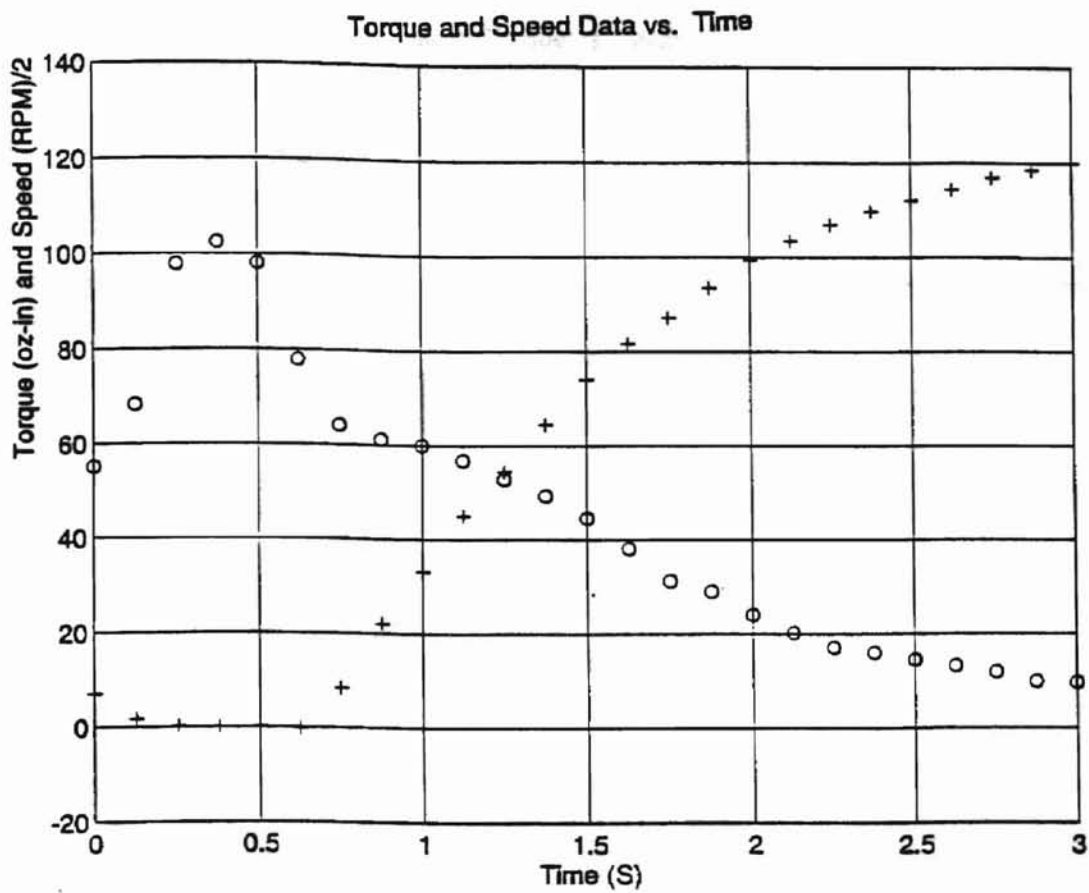
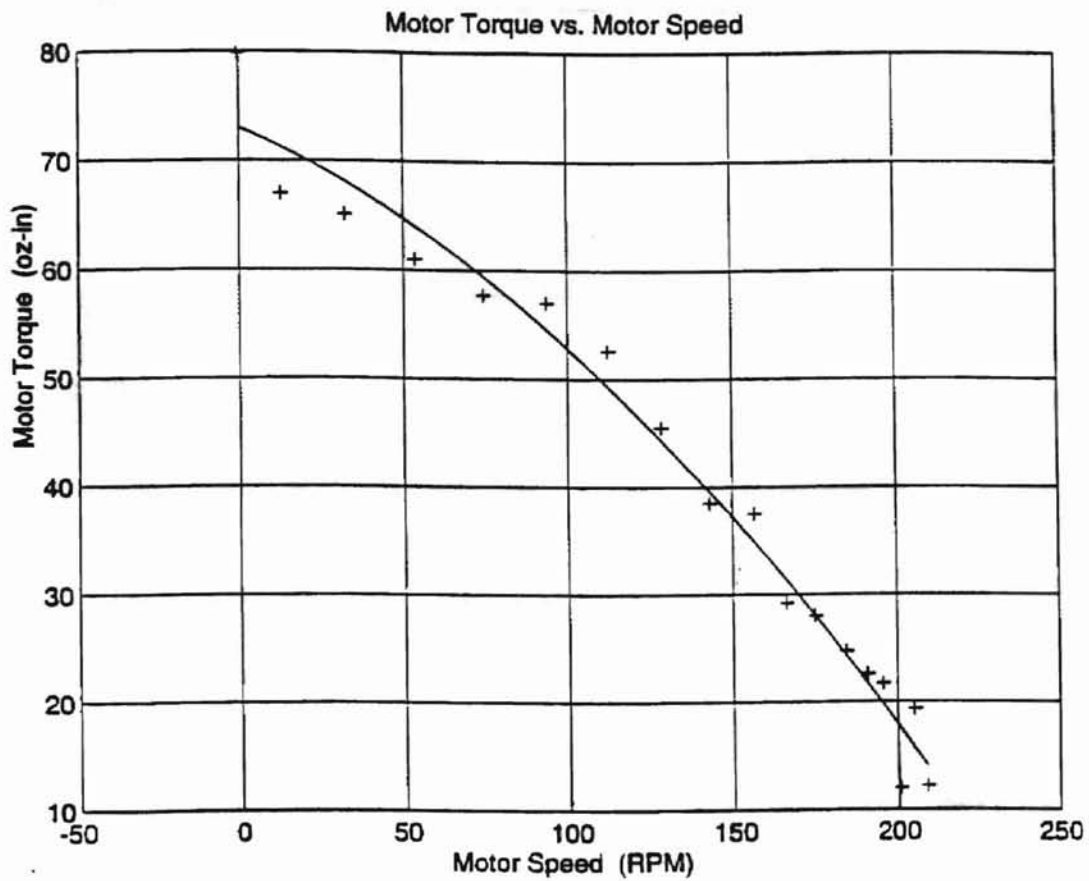


Figure 33. Adjusted Motor Torque and Speed Vs. Time Curves for Run 'T711\_8.M'



**Figure 34. Adjusted Motor Torque and Speed Vs. Time Curves for Run 'W171.M'**



**Figure 35. Motor Torque Vs. Speed Curve for Run 'T711\_8.M'**



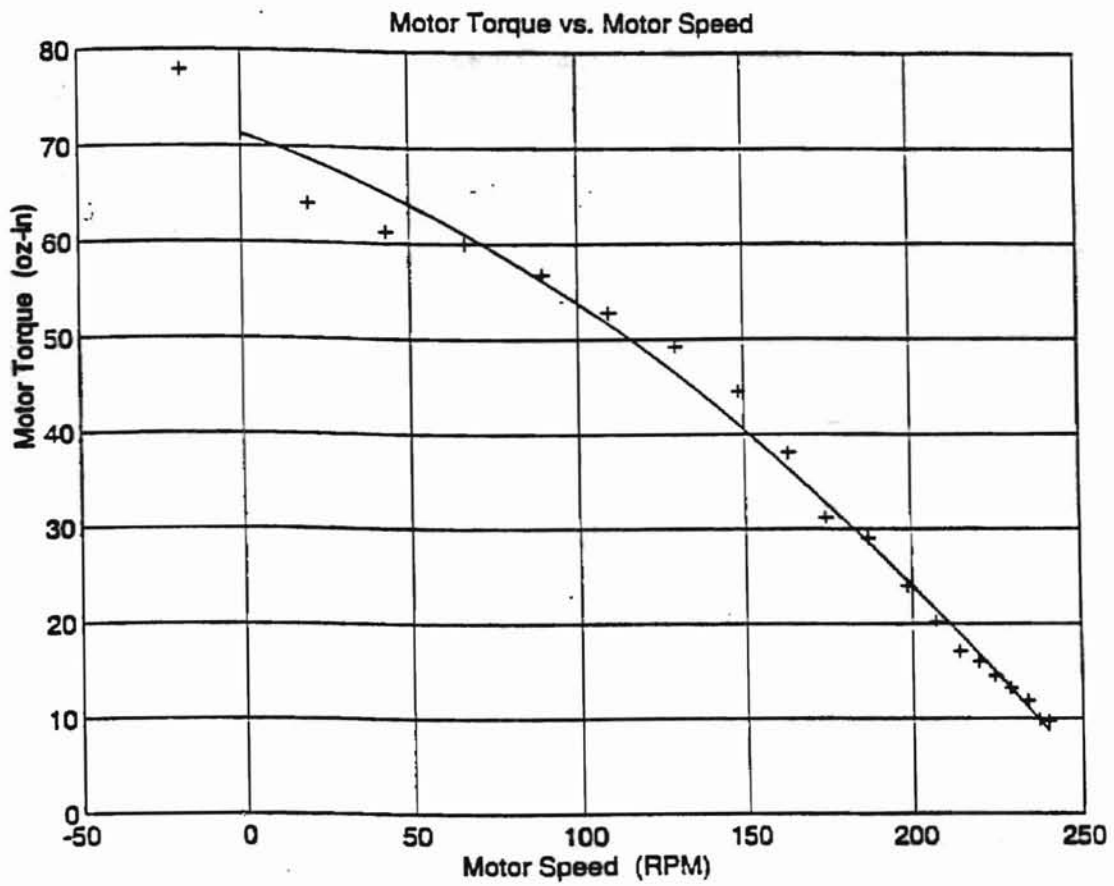


**Figure 36. Motor Torque Vs. Speed Curve for Run 'W171.M'**

adjusted, and the power/speed curve

the platform behaved

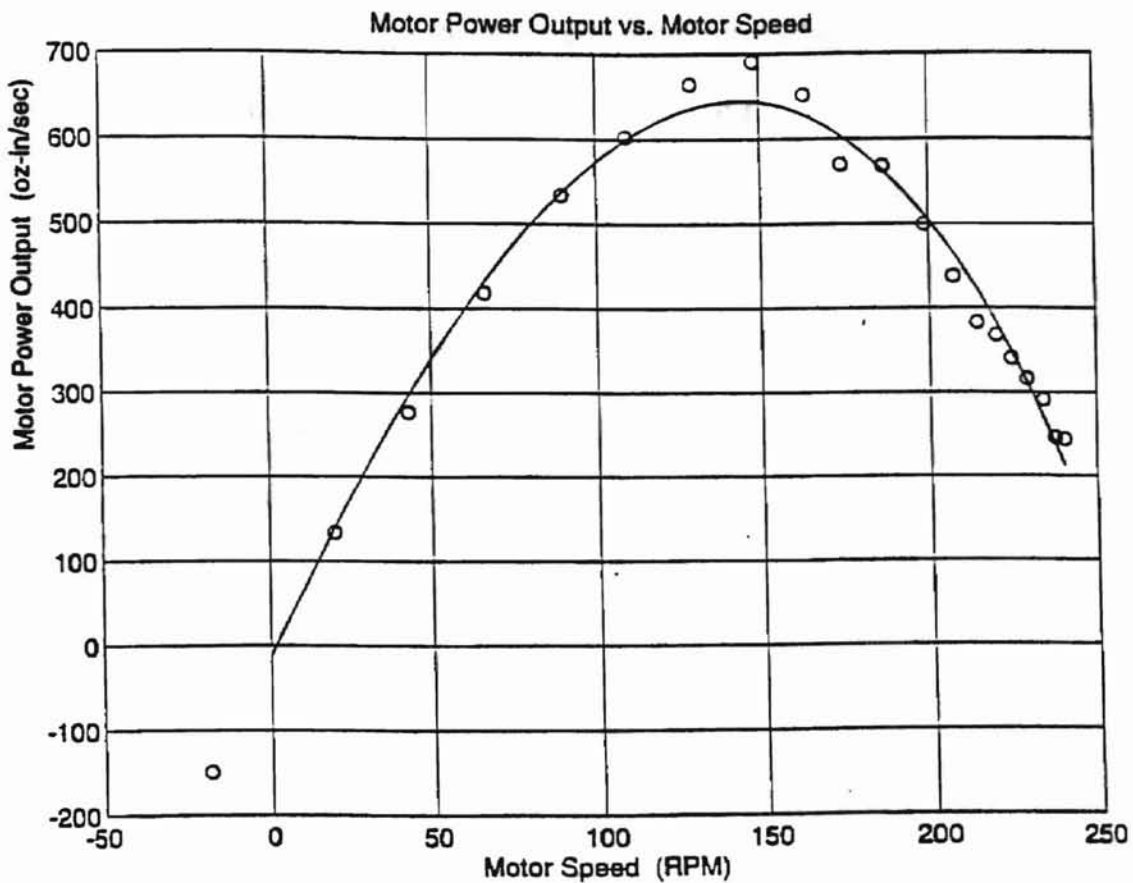


Figure 37. Motor Power Vs. Speed Curve for Run 'W171.M'

early part of the torque/speed curve should be flattened, and the power/speed curve should perhaps be shifted to the right and flattened as well. If the platform behaved elastically, then the most significant effect would be that the legs would not deflect equally. Bridge output would be effected and torque readings would be in error. Once again, the thickness of the platform and the motor mount bracket, and the tight joint made possible because of the grade 8 bolts makes the assumption of stiffness reasonable. Another assumption is that the legs are built-in to the platform and the base plate. The built-in condition for beams is normally difficult to achieve in practice. In this case, the 3/8-inch leg clamps, the strength and number of leg clamp bolts, and the relative flexibility of the legs makes an assumption of the built-in condition reasonable. If the legs in fact performed as if there were pinned connections with the platform and the base, then the effect of the rotation of the platform under induced torque would not be accurately reflected by the strain gages located on the legs. Once again, the torque and power curves would be flattened if the legs behaved as pinned beams.

It is assumed that the legs, which are machined to the same dimensions with small tolerances, will deflect equally. This assumption is based on other assumptions of similarity of leg material properties. To reduce the possibility of unequal leg deflection, legs were cut adjacently from the same sheet of aluminum stock, and with the same orientation with regard to the direction of rolling.

Other assumptions made are that the O-ring tachometer drive belt behaves inelastically, that electro-magnetic interference between the motor, strain gages, lead

wires, and circuitry is negligible, and that the oscilloscope data reflects the actual behavior of the dynamic test. This last assumption appears reasonable, since the Hewlett-Packard 54501A samples at 10 MHz, which is quite fast.

### **Scope and Limitations**

The scope of the project is quite broad. Since the project involves designing a system by which students can both design and evaluate their own mechanisms from start to finish, successful completion required that at least five major components of the project be brought together. The dynamometer is the main component of the project, and its operation is integrated with a data acquisition system by way of the appropriate circuitry. The data then must to be processed into a meaningful form of plots, charts, and tables using the appropriate software. Finally, a simulation software system provides a method of using the data meaningfully, so that better contest machines can be designed. The five main components of the project, then, are:

- 1) the dynamometer
- 2) data acquisition hardware and software
- 3) circuitry
- 4) data generation, treatment, and analysis
- 5) simulation.

As a result of the broad scope of the project, several limitations are imposed upon the study. For example, suggestions on how students can fully utilize the entire system are not exhaustive. The dynamometer has been made a general design tool basically to provide a measure of the maximum power of a motor, the shaft speed at which maximum power is available, and power requirements of various bearings, belts, and

loadings. Physically, the dynamometer is limited to the power measurement of motors with dimensions similar to those used in the MAE 3033 contests, though modifications may easily be made to accommodate motors of different dimensions and power ranges. As a side note, about one hour of time was required in a machine shop to adapt the dynamometer so that home-kit rocket motors could be characterized. These tests are discussed more fully in another section.

The dynamometer itself is limited to providing a measure of power output. Though circuitry is in place to measure power input, this aspect of the project has not been fully developed.

Another limitation of the project is that an exhaustive consideration has not been given to the dynamics of the motor, shaft, bearings, and disk during the dynamic test. On occasion when the relay actuates the motor, initially high torque and speed measurements were observed. These are believed to be due to the 'slop' which can exist between the motor shaft roll-pin slot in the shaft, and between the motor armature and the motor housing. When a motor is activated it is often possible to see the armature kick against the motor housing as the motor starts. This initial kick-in may result in very high initial torque and speed readings. Shaft deflection and natural frequency calculations are based upon these high torque values.

## **Conclusion**

The result of the project is a fairly rugged, suitably accurate dynamometer. The device features adjustable gain, a manual coarse offset adjustment, automatic fine offset adjustment, excellent calibration capability, and fairly consistent, accurate measurement of motor power under dynamic conditions.

## **Chapter V**

### **Summary, Conclusions, and Recommendations**

#### **Summary**

The objective of the project was to develop a system which would assist students in designing MAE 3033 contest vehicles. The system includes a torque table dynamometer suitable for measuring not only motor characteristics, but power train components, as well. Procedures were carried out to determine the accuracy, sensitivity, resolution, and precision of the system. The system is fairly convenient to calibrate and use. It has been demonstrated that simulation of contest vehicles is worthwhile, with percent errors between actual and simulated results ranging between 5 and 15 percent. The accuracy of the device under dynamic conditions is about 1.8% of full-scale. Furthermore, under dynamic conditions the precision of the system is about 4% of full-scale, and the system resolution is about 1.4% of full scale. Data acquisition software and circuitry were developed to support the collection of data.

#### **Conclusions**

The project was successful in several areas. First, a system was developed by which students can obtain empirical data upon which they can base decisions affecting the design of their contest vehicles. Second, the system should enhance the educational impact of the course by making engineering concepts such as power, torque, and speed

more visceral for students. Third, the project provided a substantial challenge to the author, and a tremendous learning experience.

### **Recommendations for Further Improvement**

A number of significant improvements may be considered to enhance the dynamometer as a design tool. First, a number of accessory exercises could be devised to develop students' skills in experimental methodology, statistics, numerical analysis, mechanics of mechanisms, instrumentation, and data acquisition. A short report in which students defend their chosen configuration and dimensions could provide practice in report writing, as well.

An interesting project evaluation could be provided in the design, administration, evaluation, and interpretation of pre- and post tests to determine the development of students' general comprehension of quantities of speed, acceleration, force, inertia, and power.

Additionally, several improvements could be made in the design of the dynamometer.

- 1) Heavy duty bearings, so the disk need not be removed for storage.
- 2) Refinement of the precision of the device, so that finer elements of the drivetrain could be evaluated.
- 3) Extension of applicability to real-time readout of actual power consumption while the student is operating his device.
- 4) Development of Capability to read power in and thereby find efficiency of the motor.
- 5) Refinement of the software.



### **Concluding Comment**

The effort of the many individuals responsible for the success of this project has had one focus: better engineers for the future. It is the author's hope and desire that students use the dynamometer creatively.

## SELECTED BIBLIOGRAPHY

- [1] Beckwith, T. G., Marangoni, R. D., & Lienhard, J. H. (1993). Mechanical Measurements (5th ed.). Reading, MA: Addison-Wesley.
- [2] "Digital/Optical Torquemeter," (1983), Electronic Engineering. Vol. 44, No. 683, (Nov.) p. 138.
- [3] Doebelin, E. O. (1990). Measurement Systems: Application and Design (4th ed.). New York, N. Y., McGraw-Hill.
- [4] Emmerling, A. A., (1958). Dynamometer (Patent Description Number 2,845,795).
- [5a] GSE, Inc. (1994). Catalog No. SKY94/6113. 23642 Research Dr., Farmington Hills MI 48335-2621 Phone no. (810) 476-7875.
- [5b] GSE, Inc. (1994). Catalog No. SKY95/6139. 23642 Research Dr., Farmington Hills MI 48335-2621 Phone no. (810) 476-7875.
- [6] Krepchin, I. P., (1986). "How To Calculate Rolling Resistance", Modern Materials Handling, Vol. 41 Number 6, May 1986, p. 72.
- [7] Norton, Robert L., (1996). Machine Design. Upper Saddle River, N.J., Prentice-Hall, p. 478.
- [8] "Overseas Survey," Mechanical Engineering. February, 1971, p. 62.
- [9] Servo Systems Co. (1995-1996). Catalog. 115 Main Rd., Montville, NJ, 07045-0097 (800) 922-1103.
- [10] Shigley, J. E., & Mischke, C. R. (1989). Mechanical Engineering Design. New York, N. Y., McGraw-Hill.

- [11] Taylor, R. M., Personal Interview, Oklahoma State University, June 13, 1995.
- [12] Thompson, W. T., (1993). Theory of Vibration With Applications. Englewood Cliffs, N. J., Prentice Hall.
- [13] Vibrac Corp (1995). Brochures for Torque-Measuring Tranducers (Series I and II). P.O. Box 840, Amherst, NH 03031. Phone no. (603) 882-6777.

## Appendices

## **Appendix A -- Dynamometer Drawings and Dimensions**

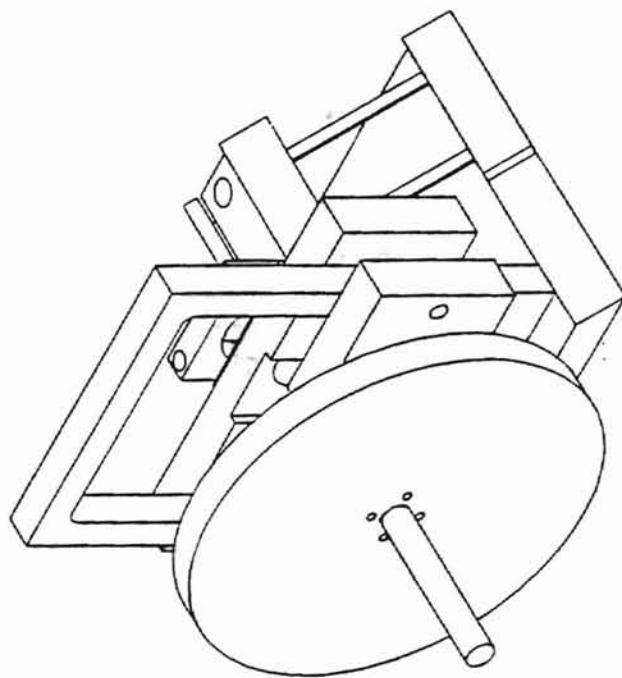


**Figure 38. Isometric View -- Disk Added**

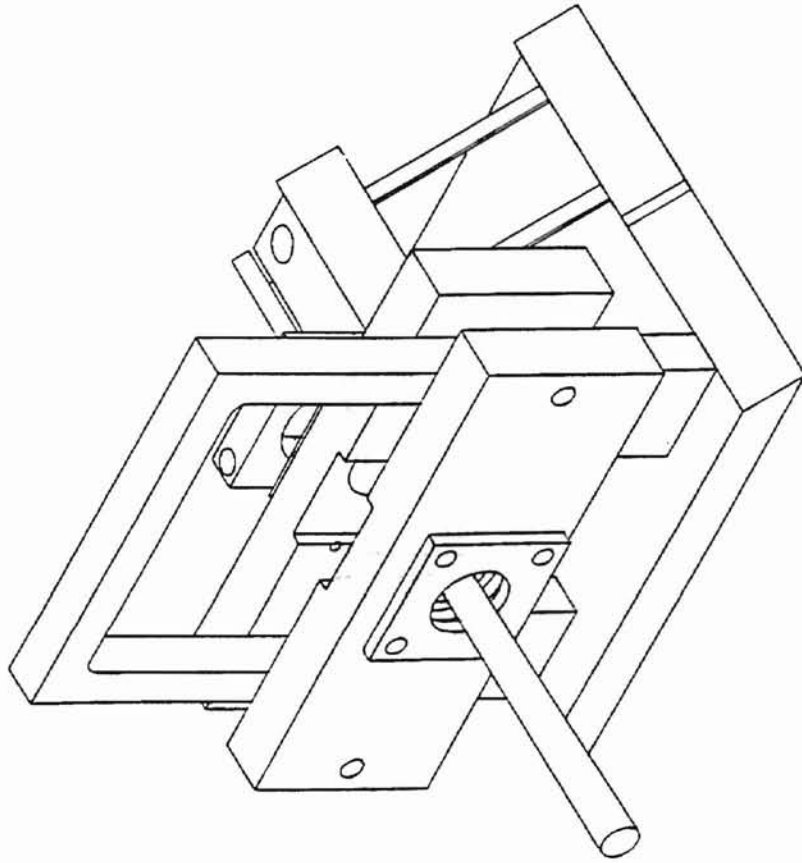


**Figure 39. Isometric View -- Shaft Housing Added**

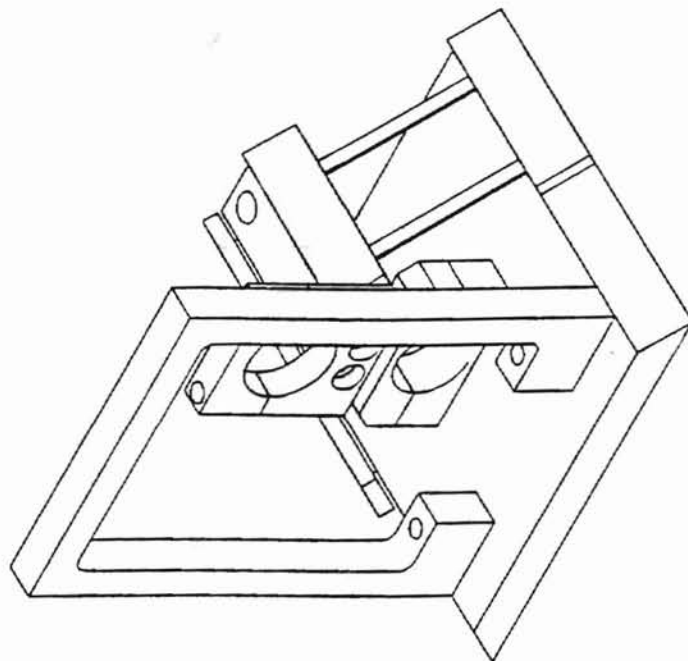


**Figure 40. Isometric View -- Shaft Support Added**



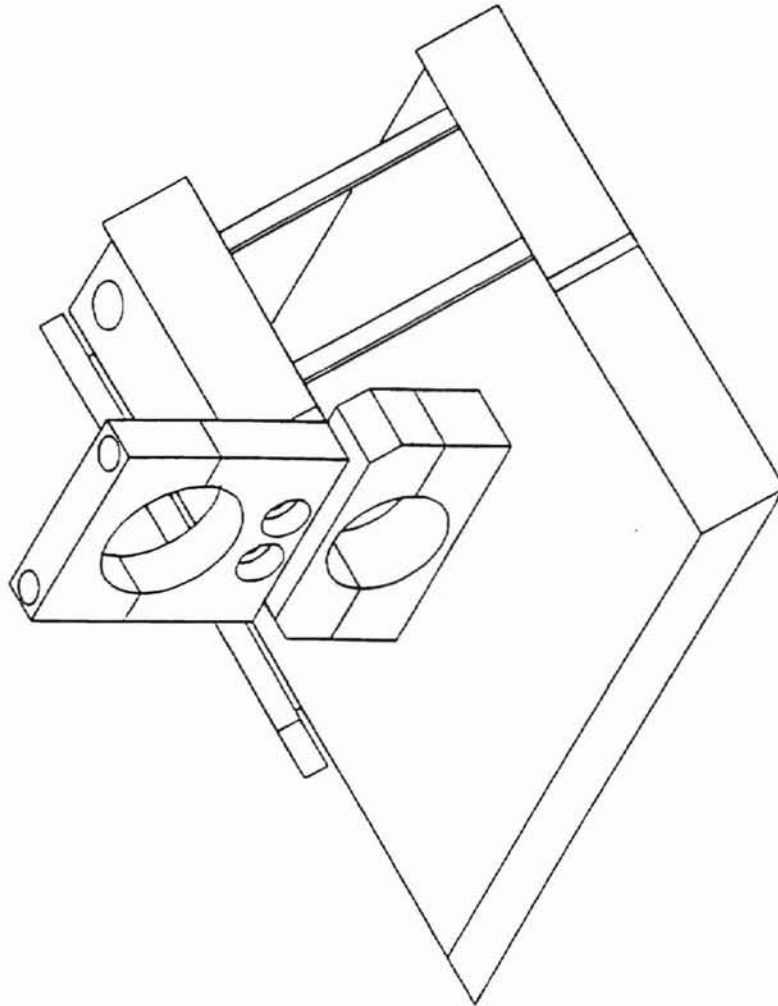


**Figure 41. Isometric View -- Motor Mount Added**

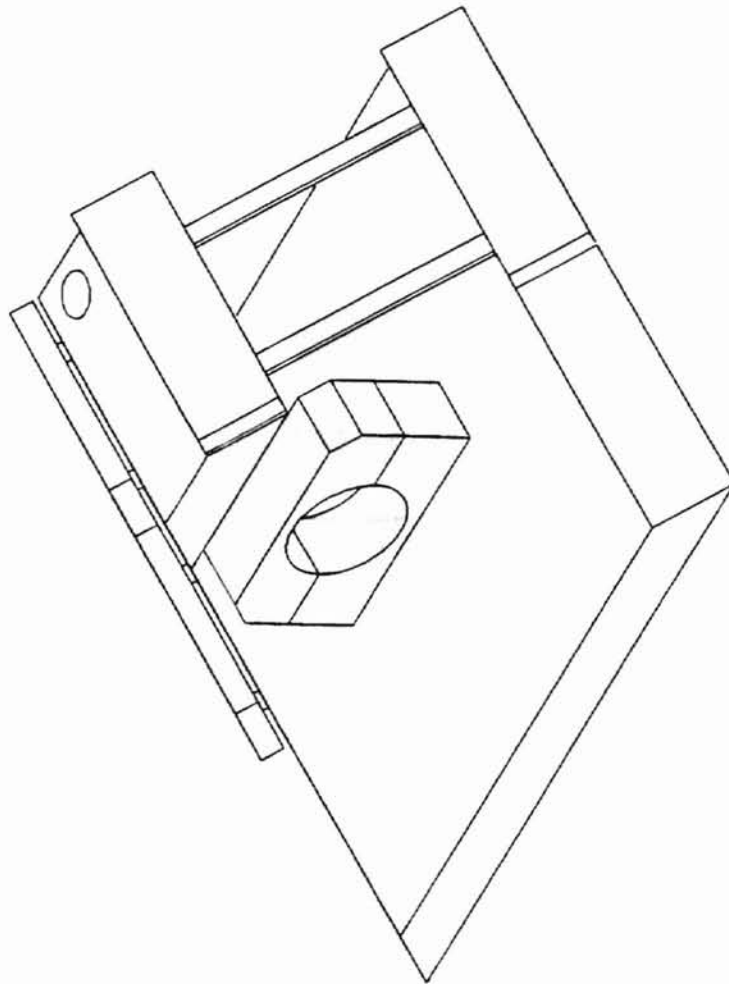


**Figure 42. Isometric View -- Base and Platform**

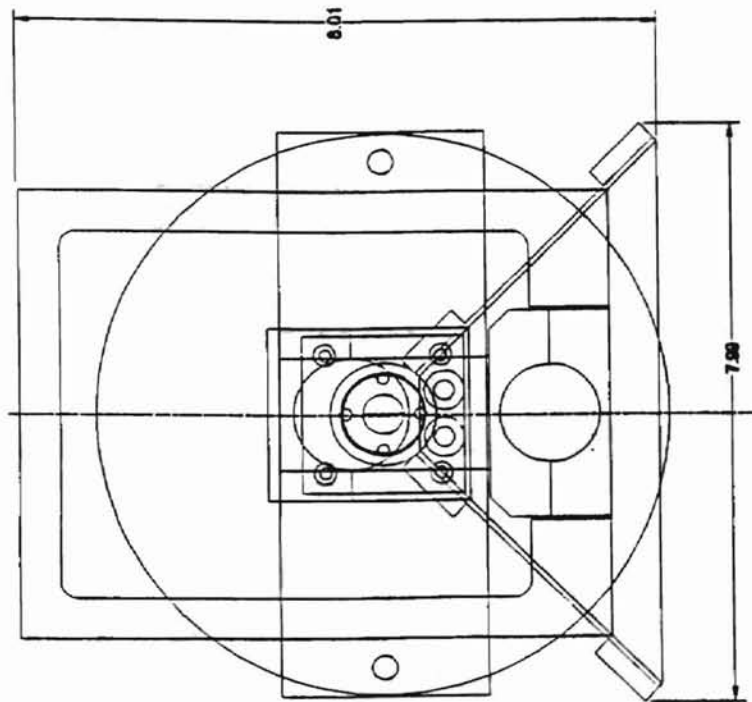


Figure 43. Front View

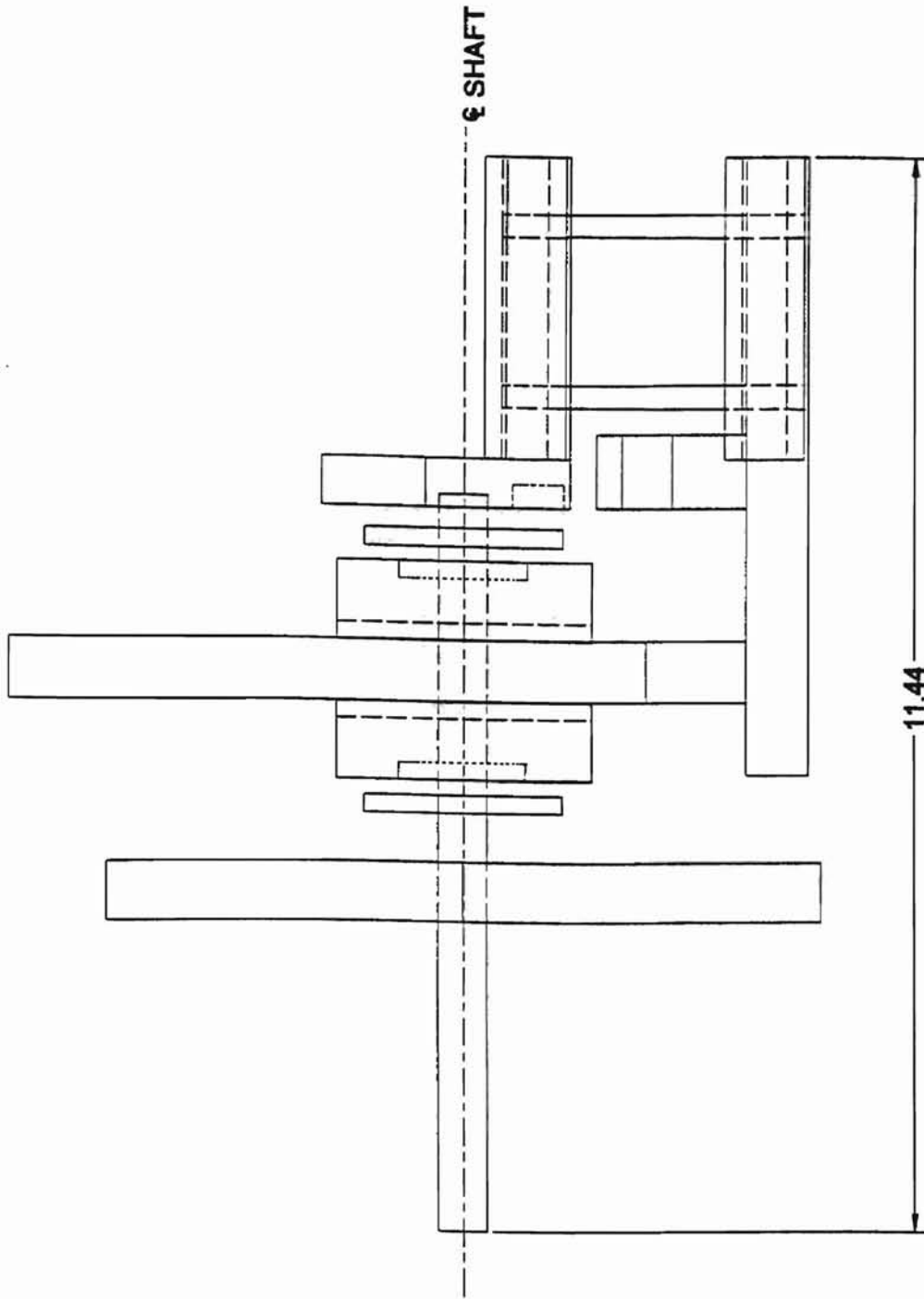


Figure 44. Side View

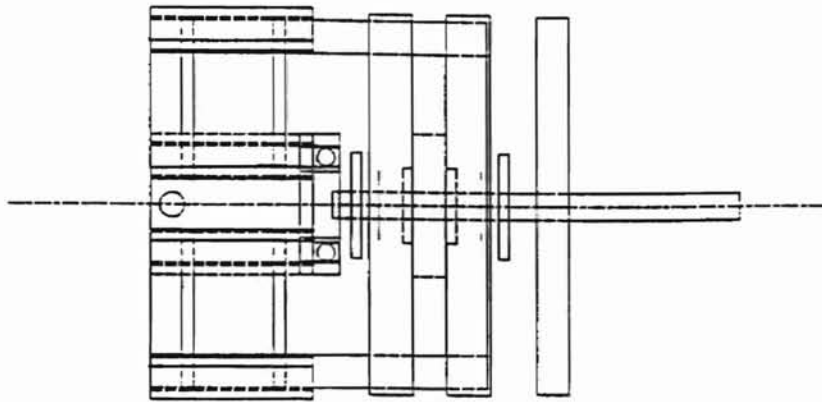


Figure 45. Top View

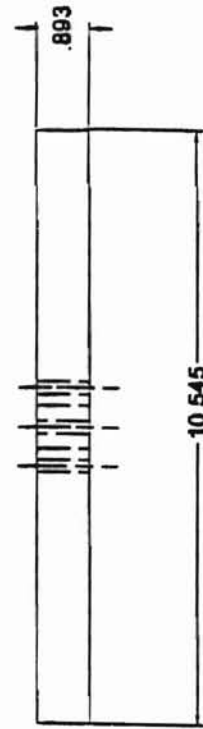
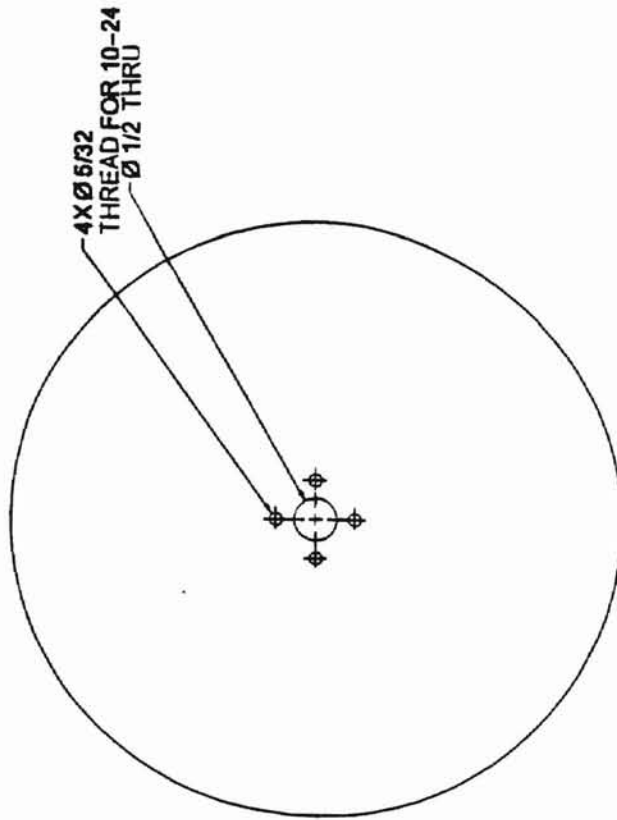
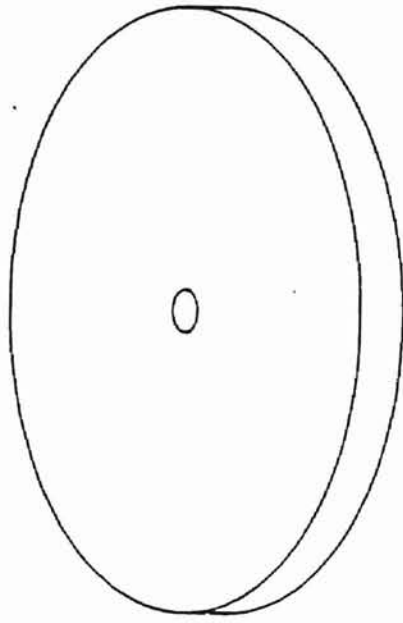


Figure 46. Inertial Disk

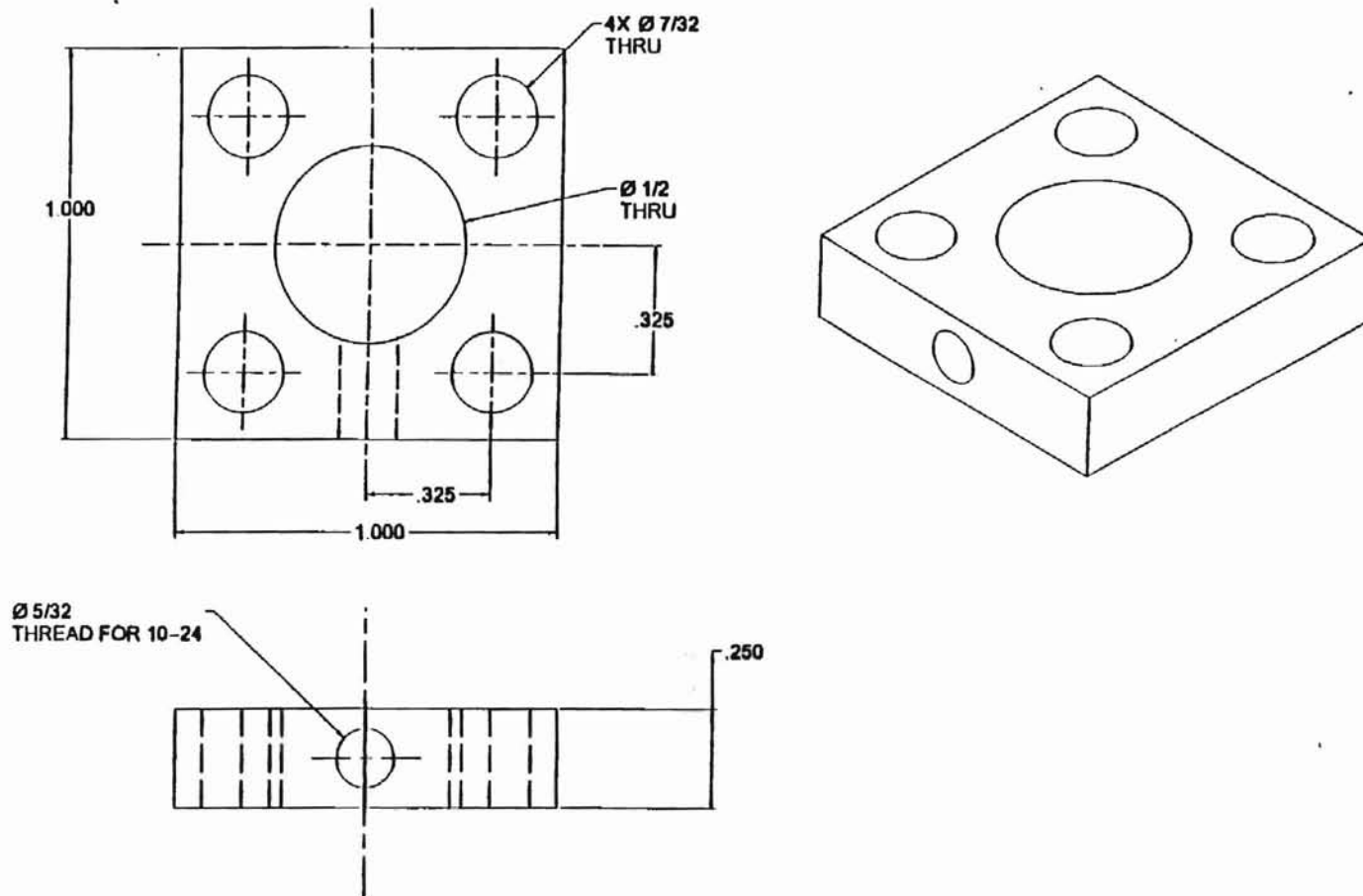


Figure 47. Inertial Disk Set Screw Plate

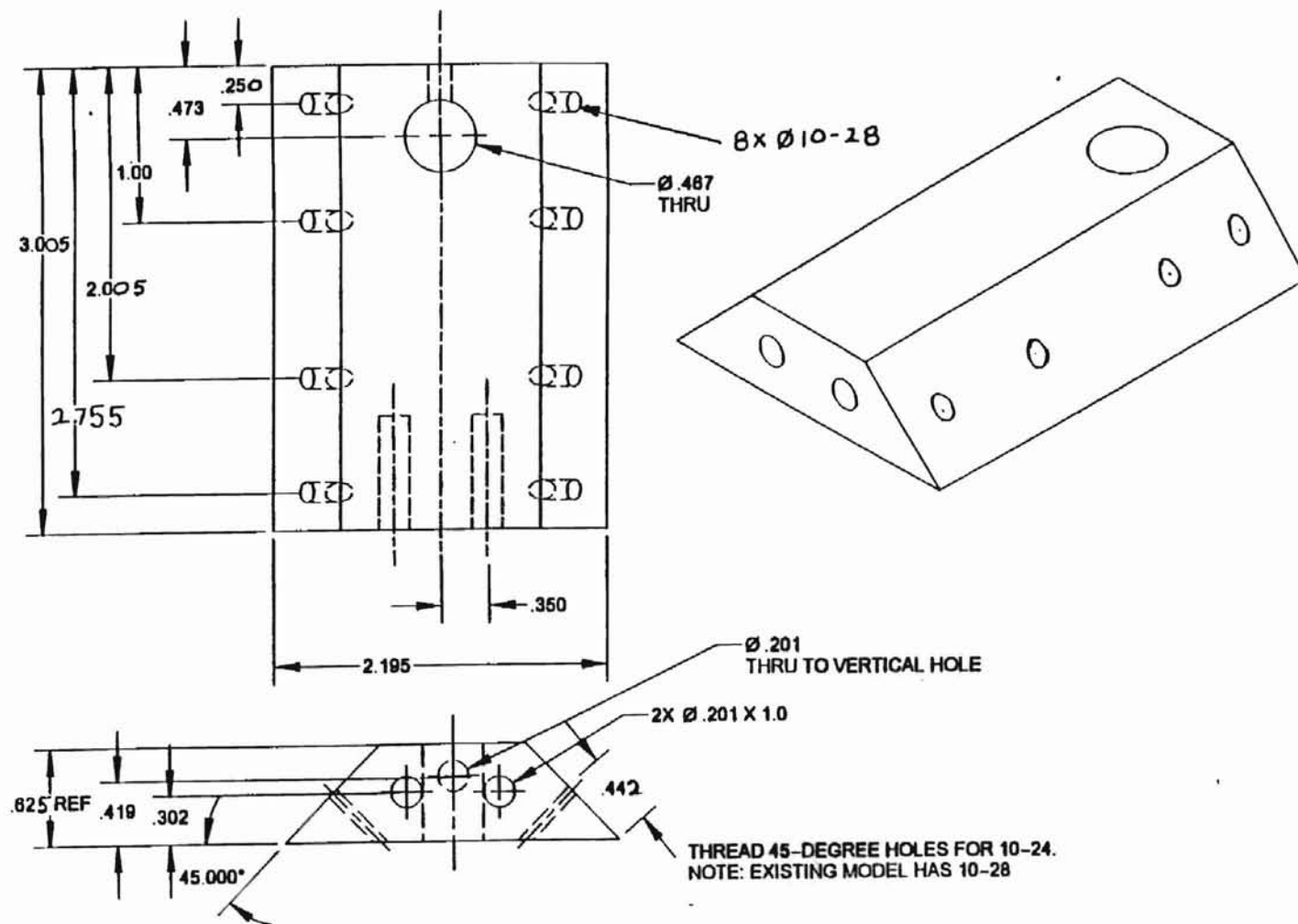


Figure 48. Motor Platform



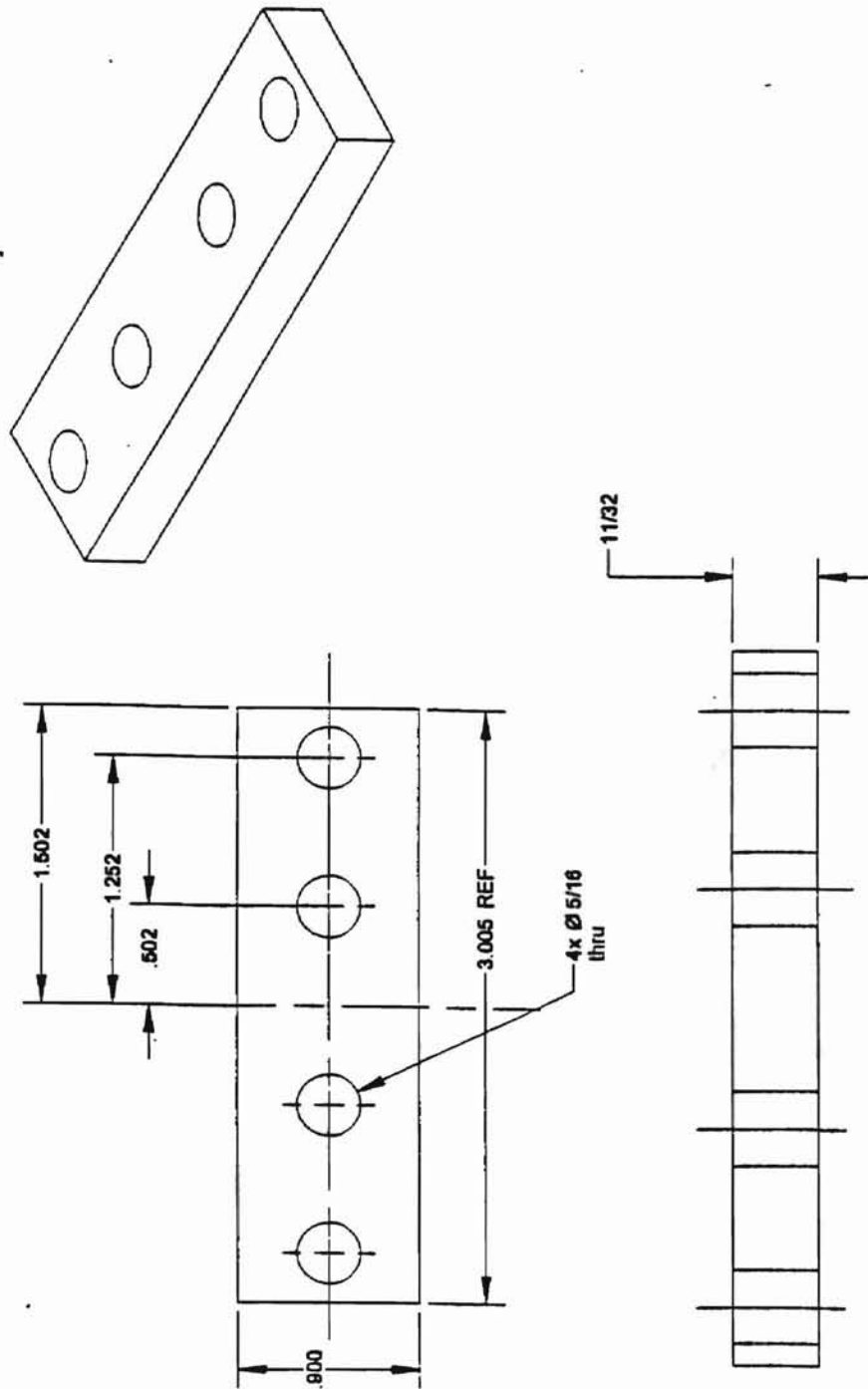


Figure 49. Leg Clamp

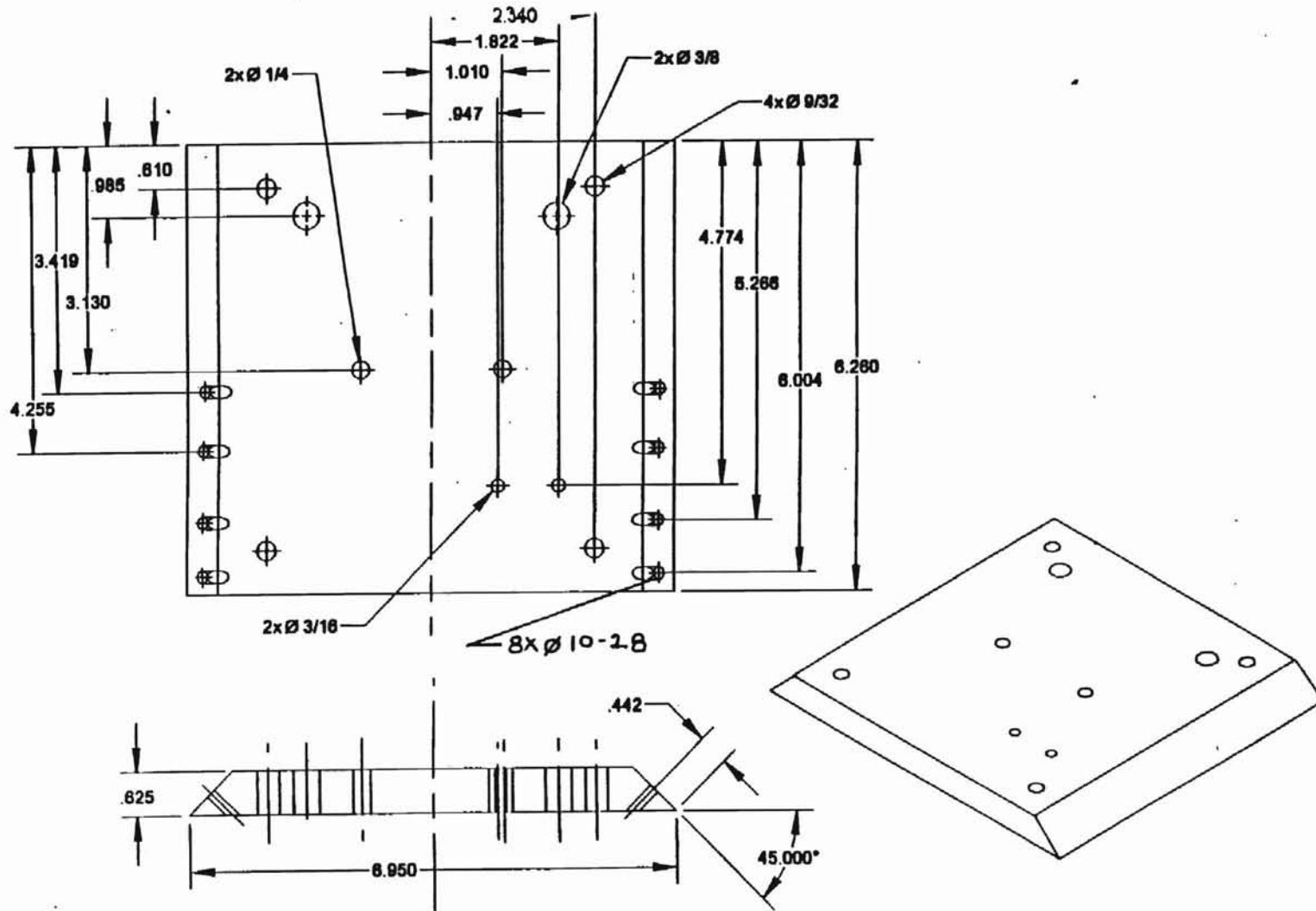


Figure 50. Base

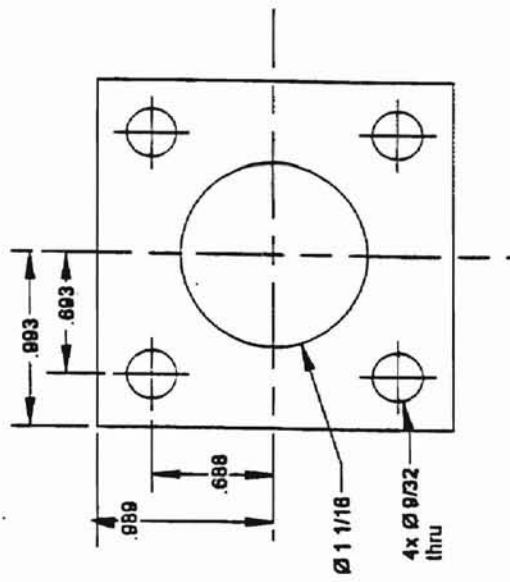
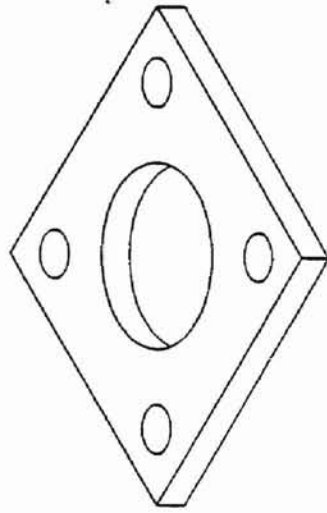


Figure 51. Shaft Bearing Retainer

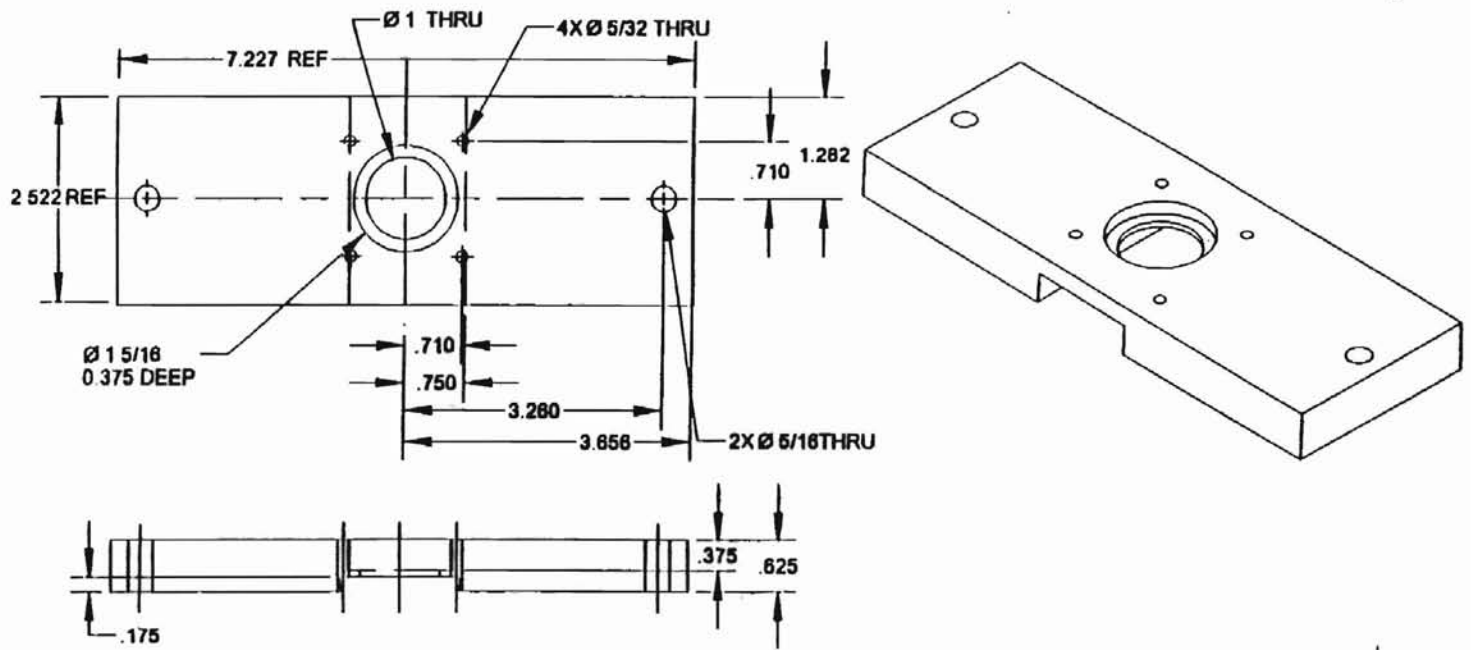


Figure 52. Shaft Bearing Housing

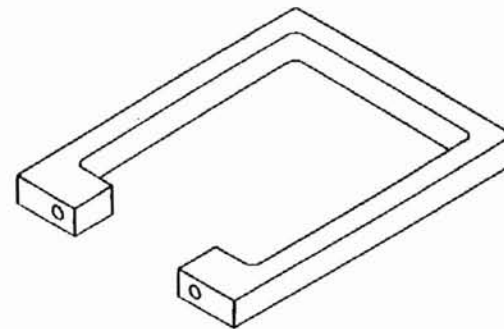
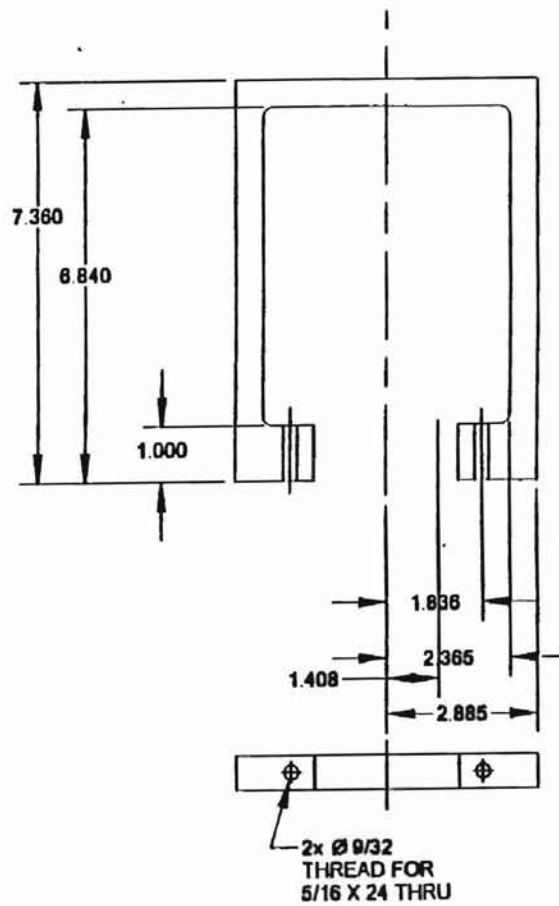
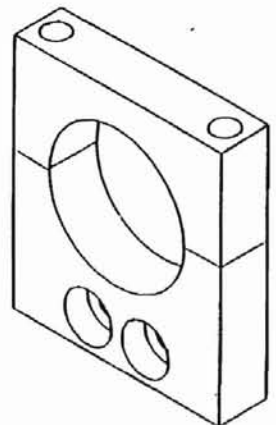
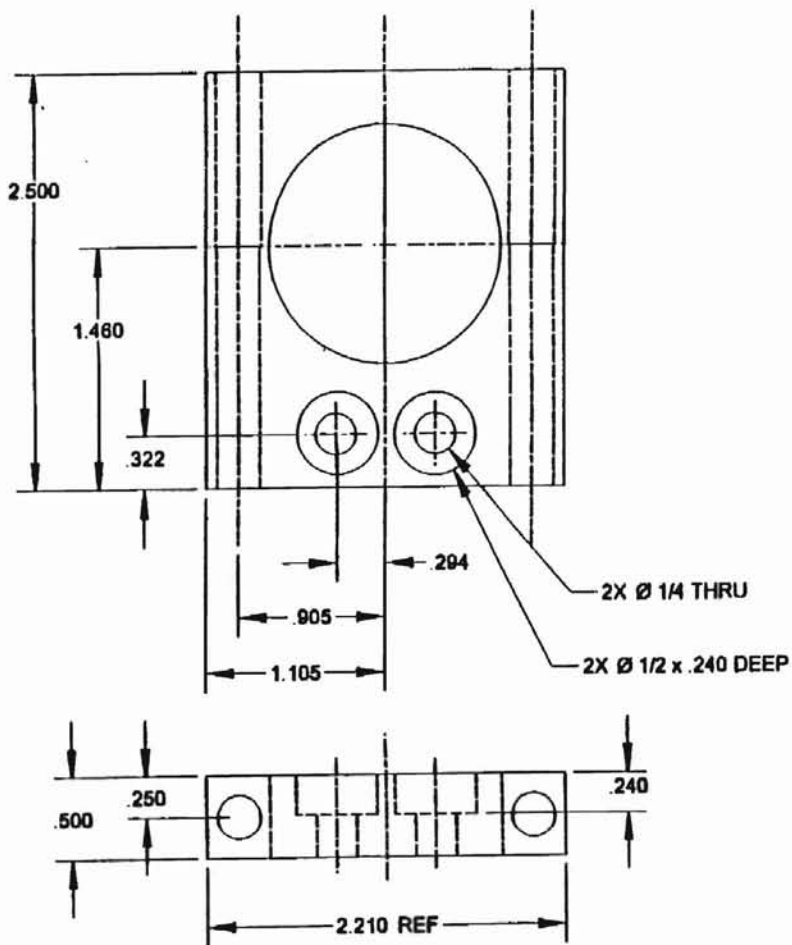
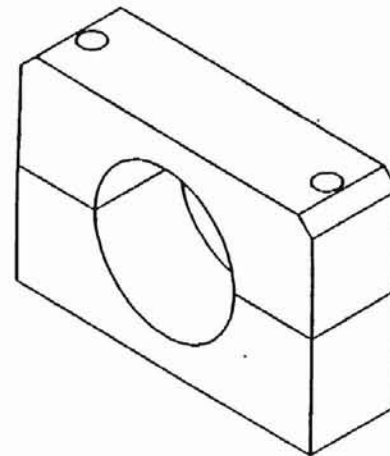
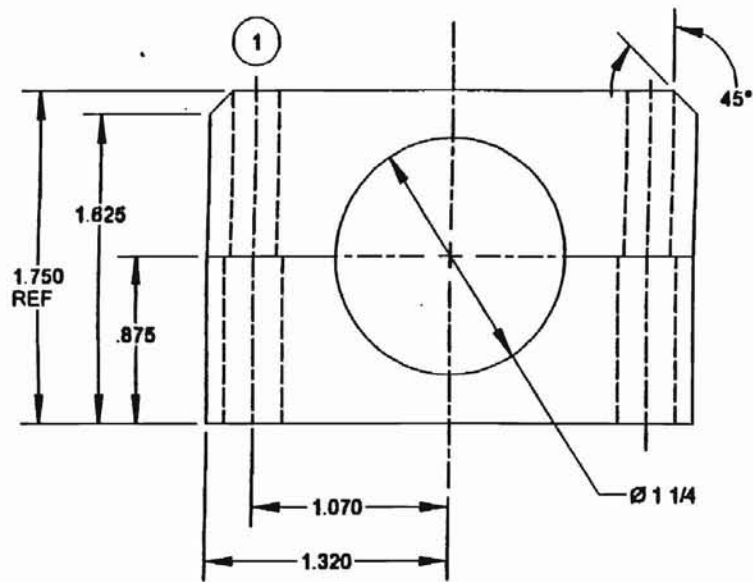


Figure 53. Shaft Support



NOTE: DRILL VERTICAL 5/16 HOLES, THEN CUT PART IN TWO, AS SHOWN. TAP BOTTOM PORTION AND DRILL TOP PORTION 3/8.

Figure 54. Motor Mount



1  
 DRILL VERTICAL HOLES DIA .2010 TO PREPARE FOR THREADING 1/4 X 20. CUT PART IN TWO AS SHOWN, THEN DRILL BOTTOM PORTION DIA .3125. FINALLY, TAP TOP PORTION OF PART.

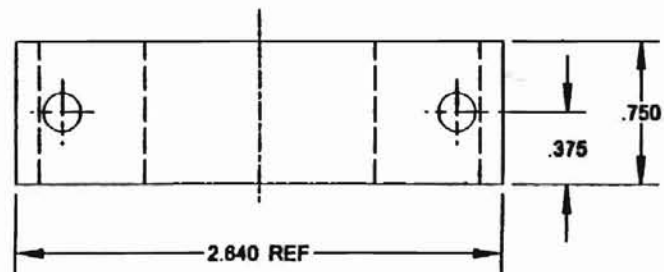


Figure 55. Tachometer Mount

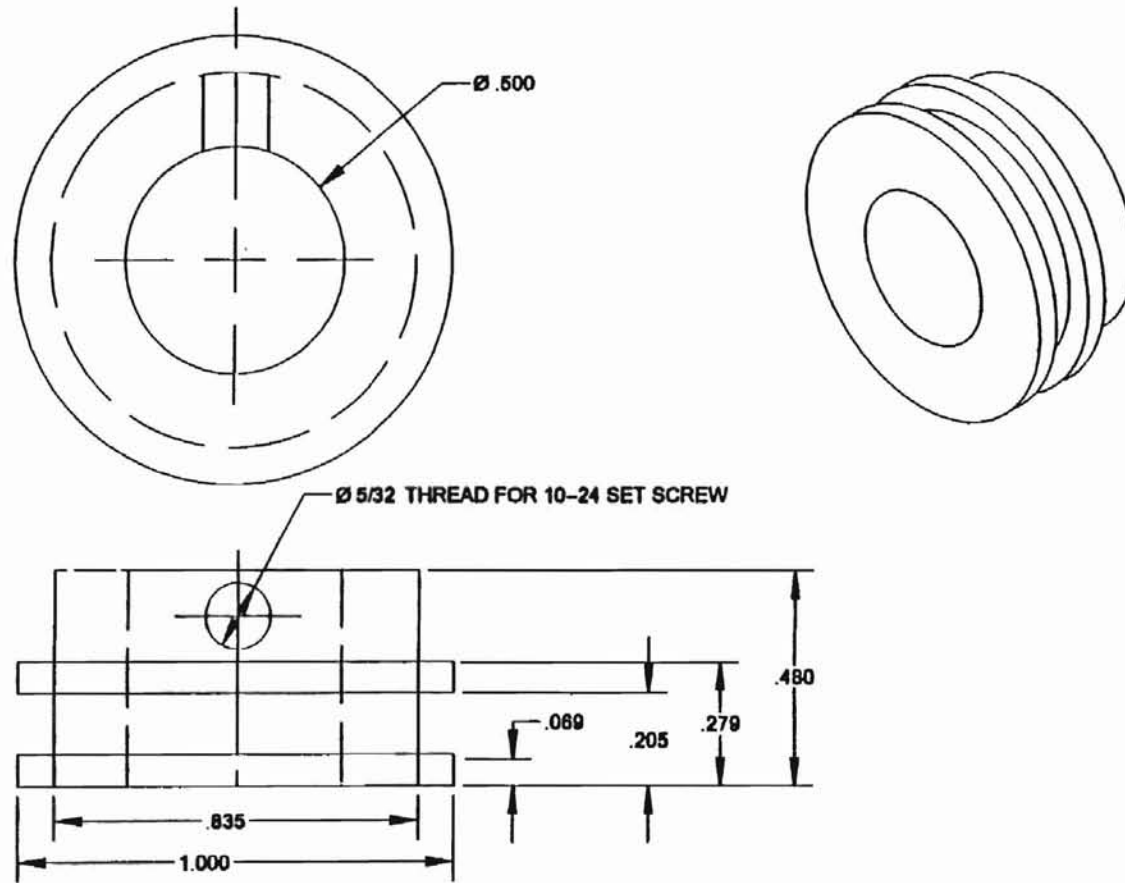


Figure 56. Shaft Pulley



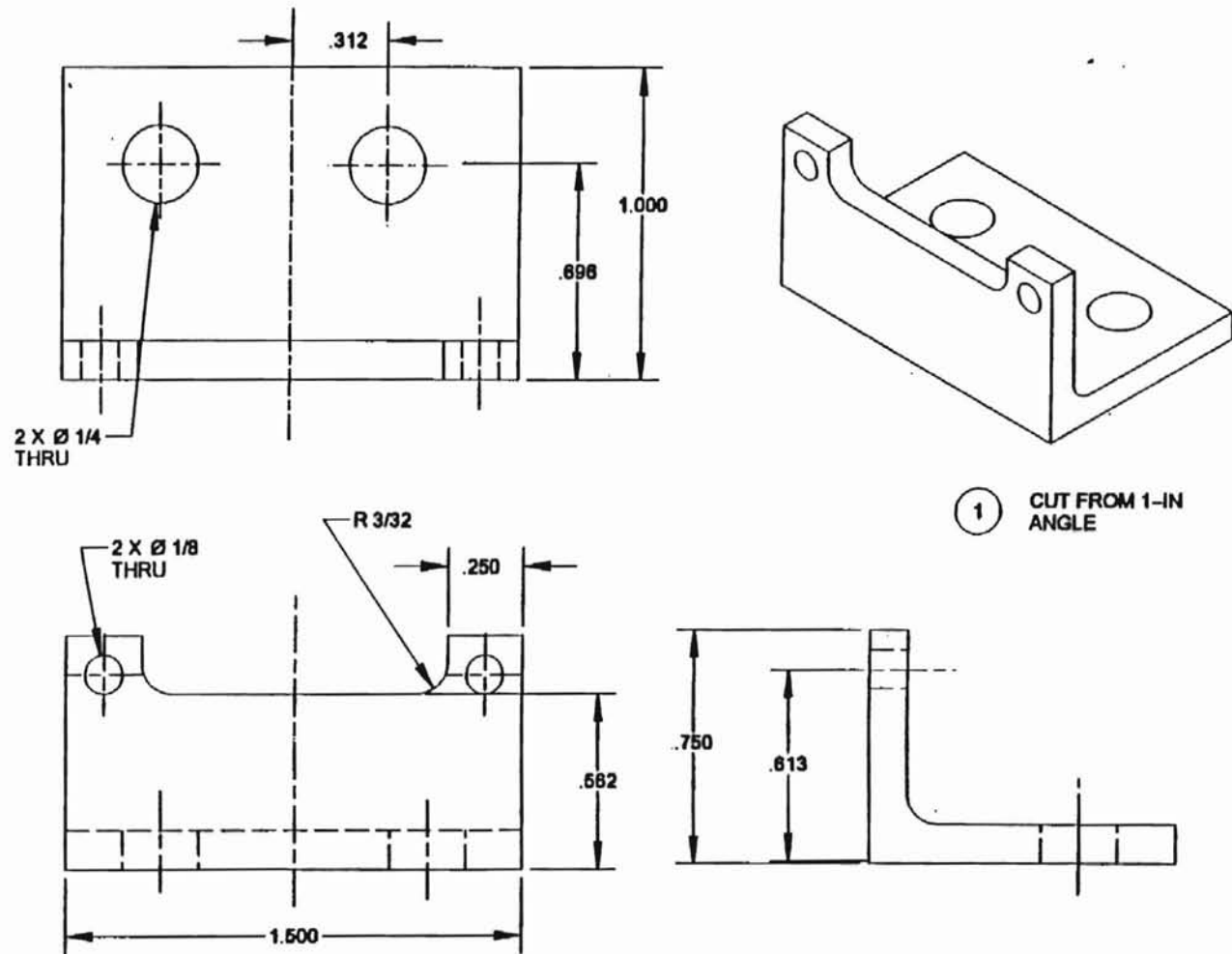


Figure 57. Electrical Connector Mount

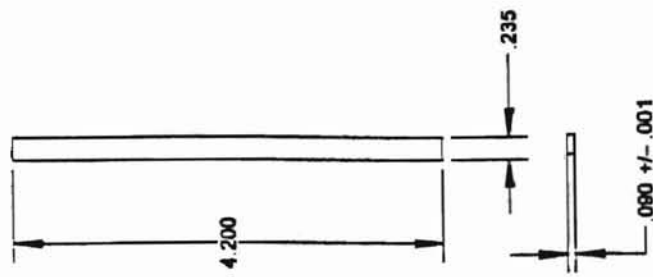


Figure 58. Support Leg

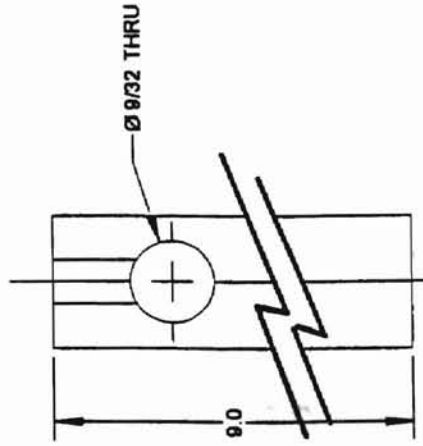
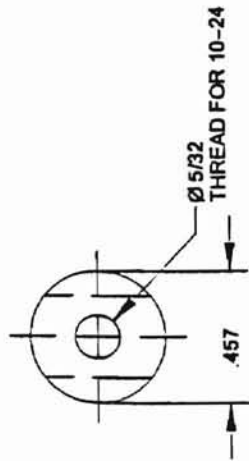
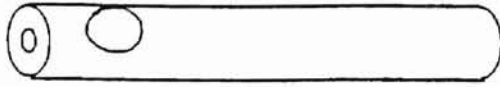
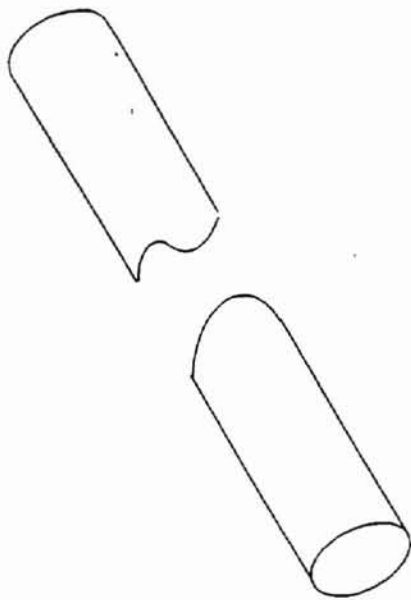
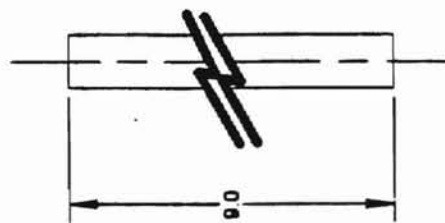
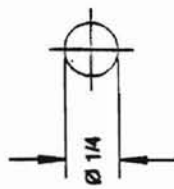
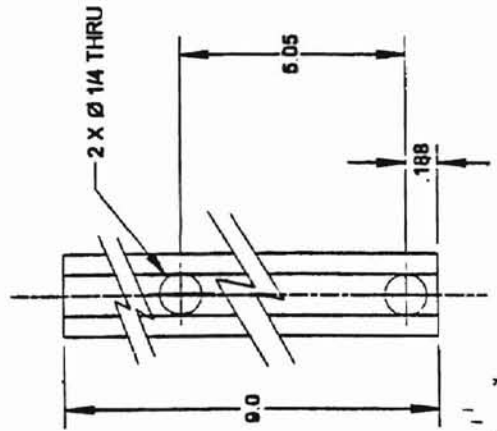
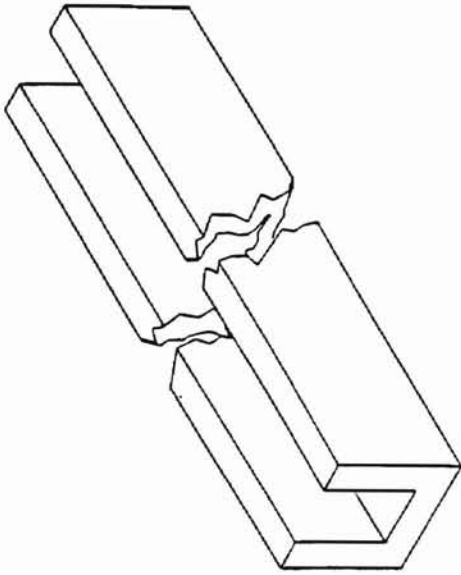
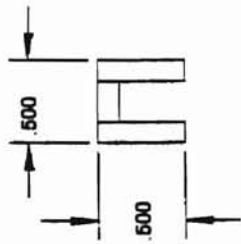


Figure 59. Calibration Bar Post



1 NOTCH PART ON ONE SIDE EVERY INCH.

Figure 60. Calibration Bar



① USE 1/2 X 1/2 ALUMINUM CHANNEL

Figure 61. Base Support

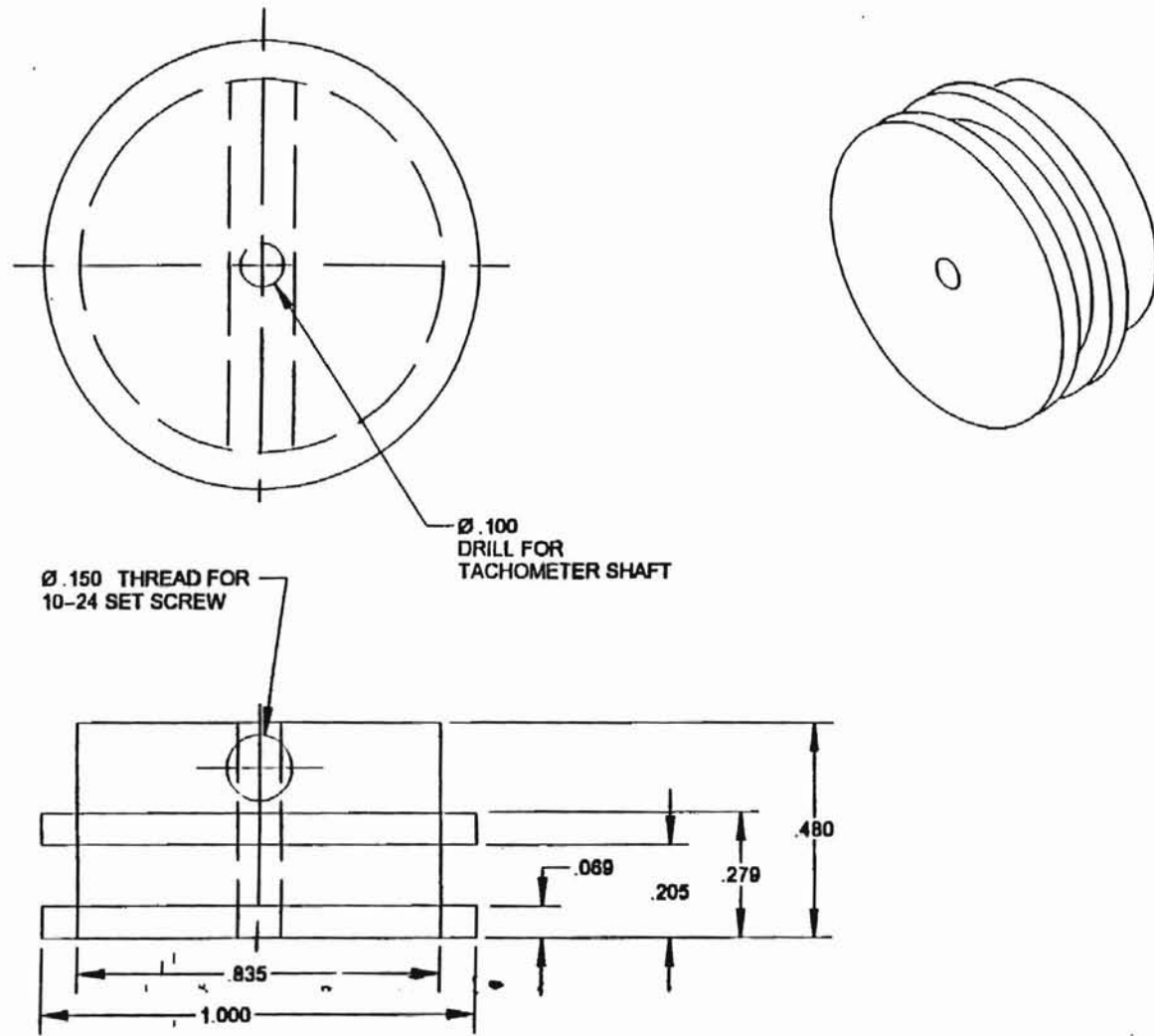
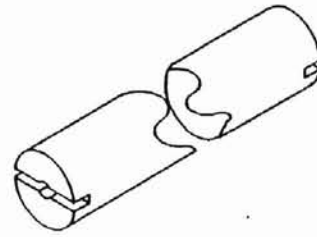
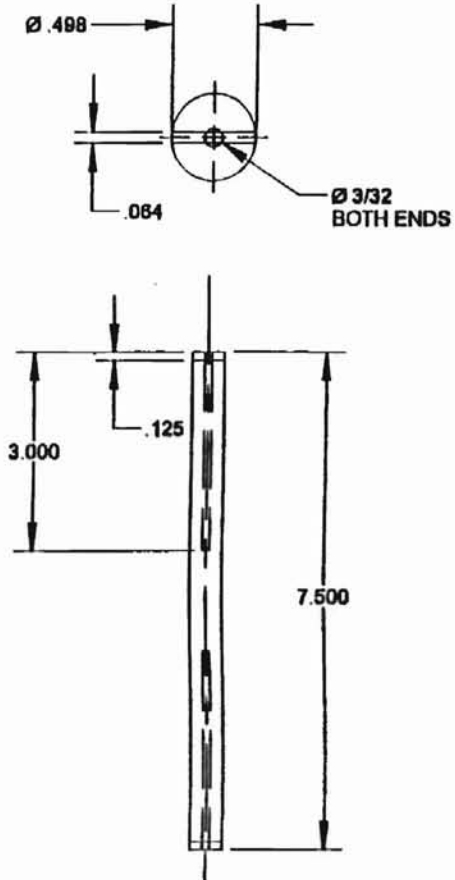


Figure 62. Tachometer Pulley



1 CUT PART FROM 1/2 IN ROUND STOCK STEEL. SAND TO A SNUG FIT IN MATING PARTS.

Figure 63. Steel Shaft

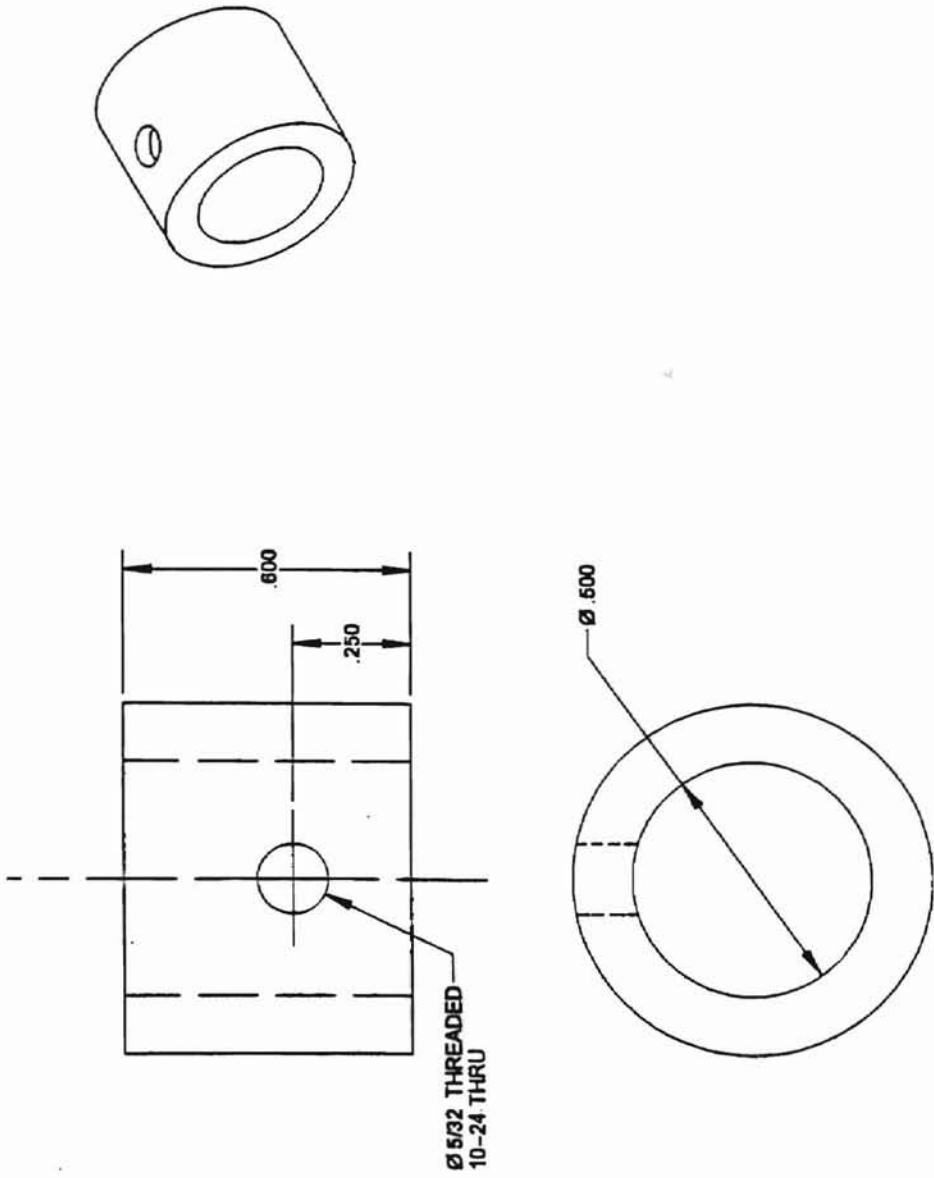


Figure 64. Collar



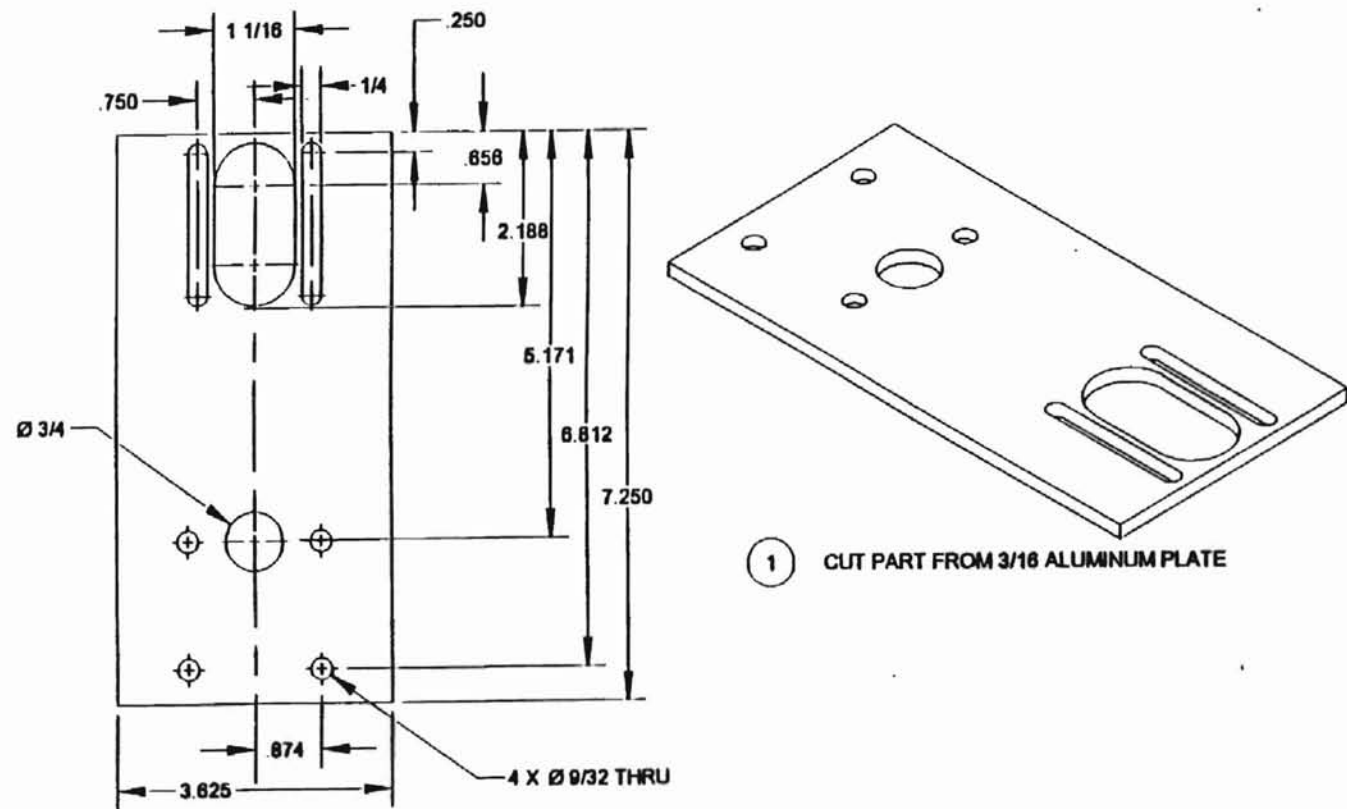


Figure 65. Drive Train Plate

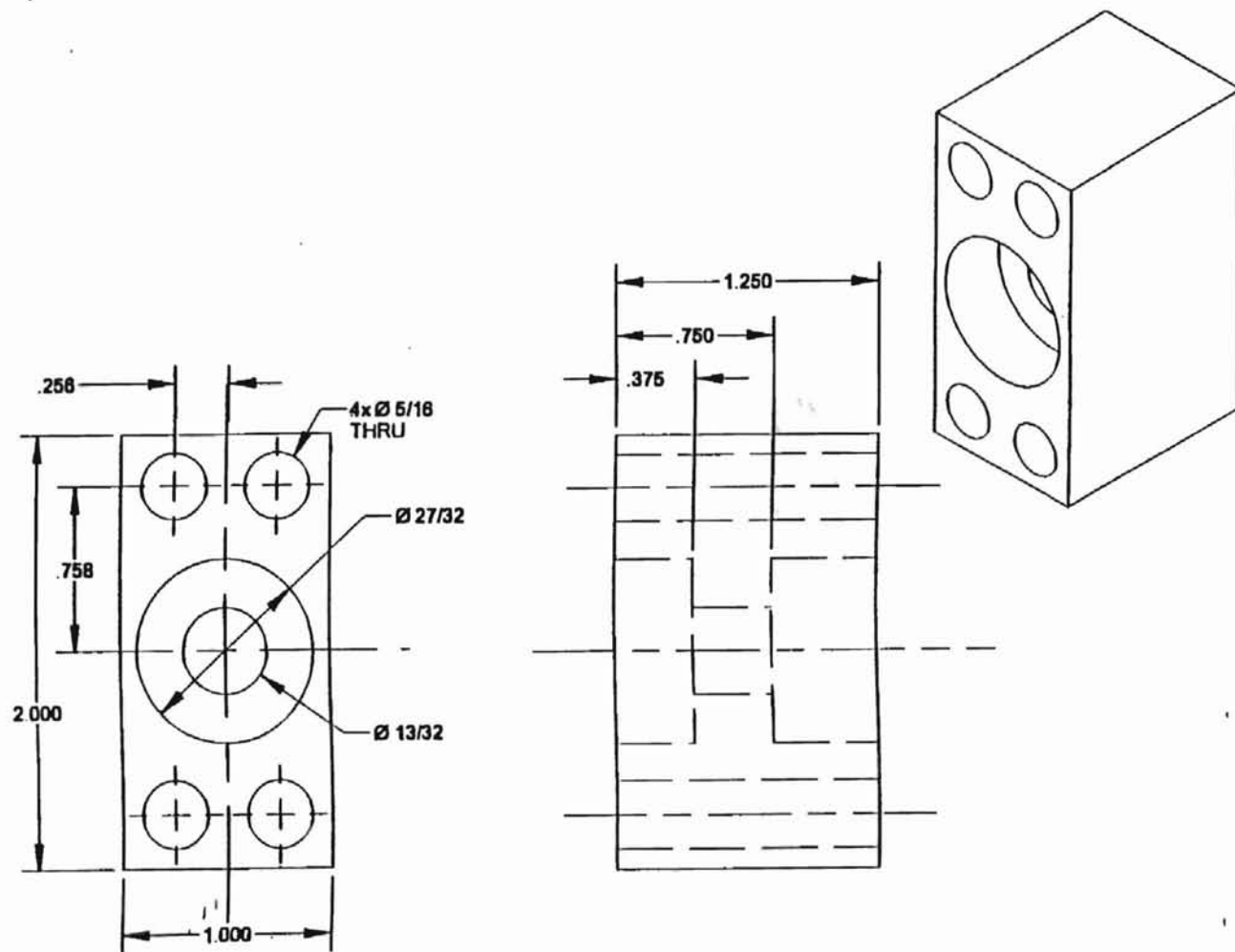


Figure 66. Bearing Block

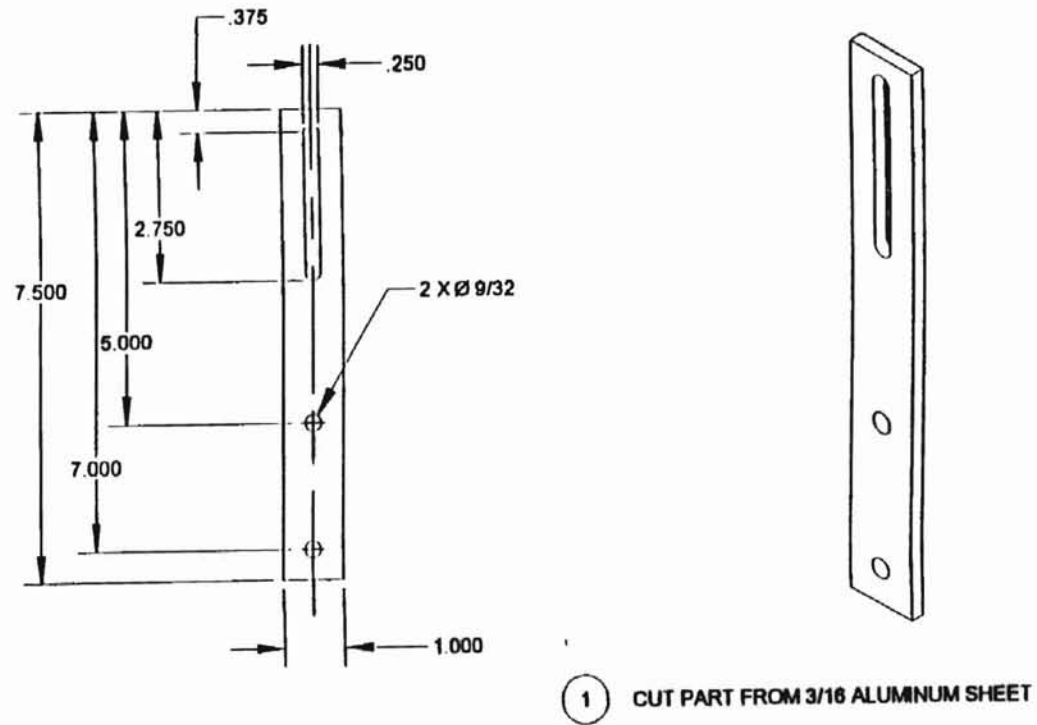
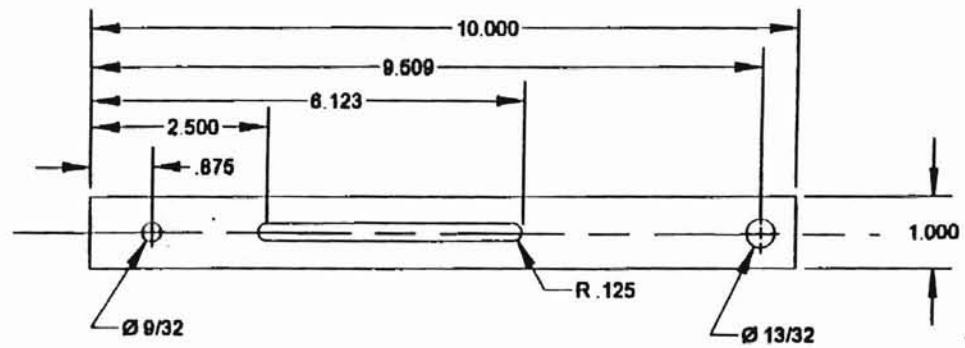


Figure 67. Vertical Idler Arm



① CUT PART FROM 3/16 ALUMINUM SHEET

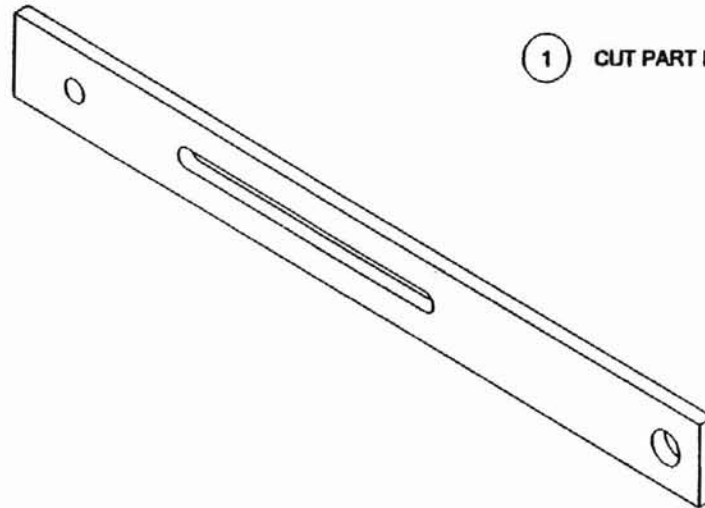


Figure 68. Horizontal Idler Arm

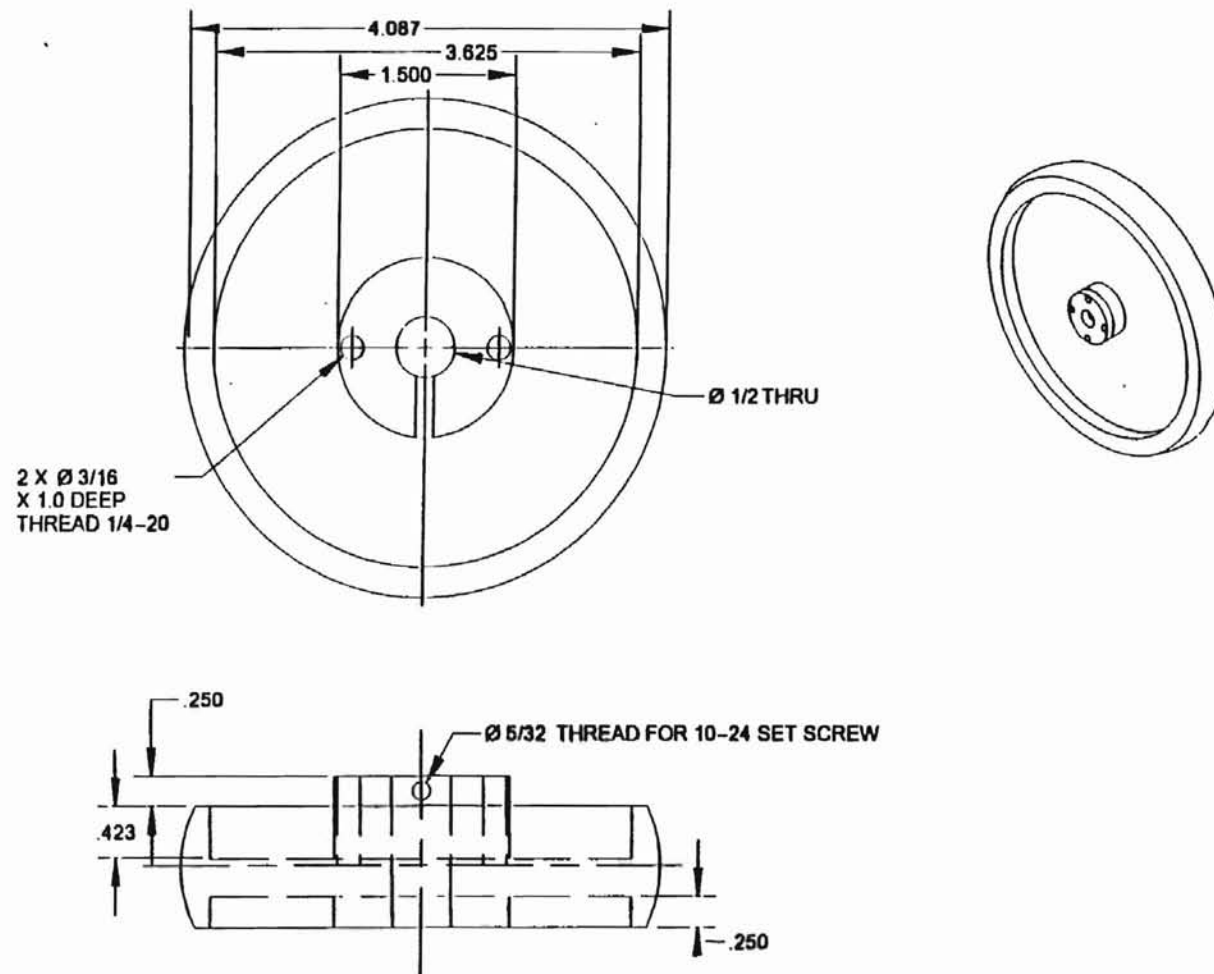


Figure 69. Drive Wheel

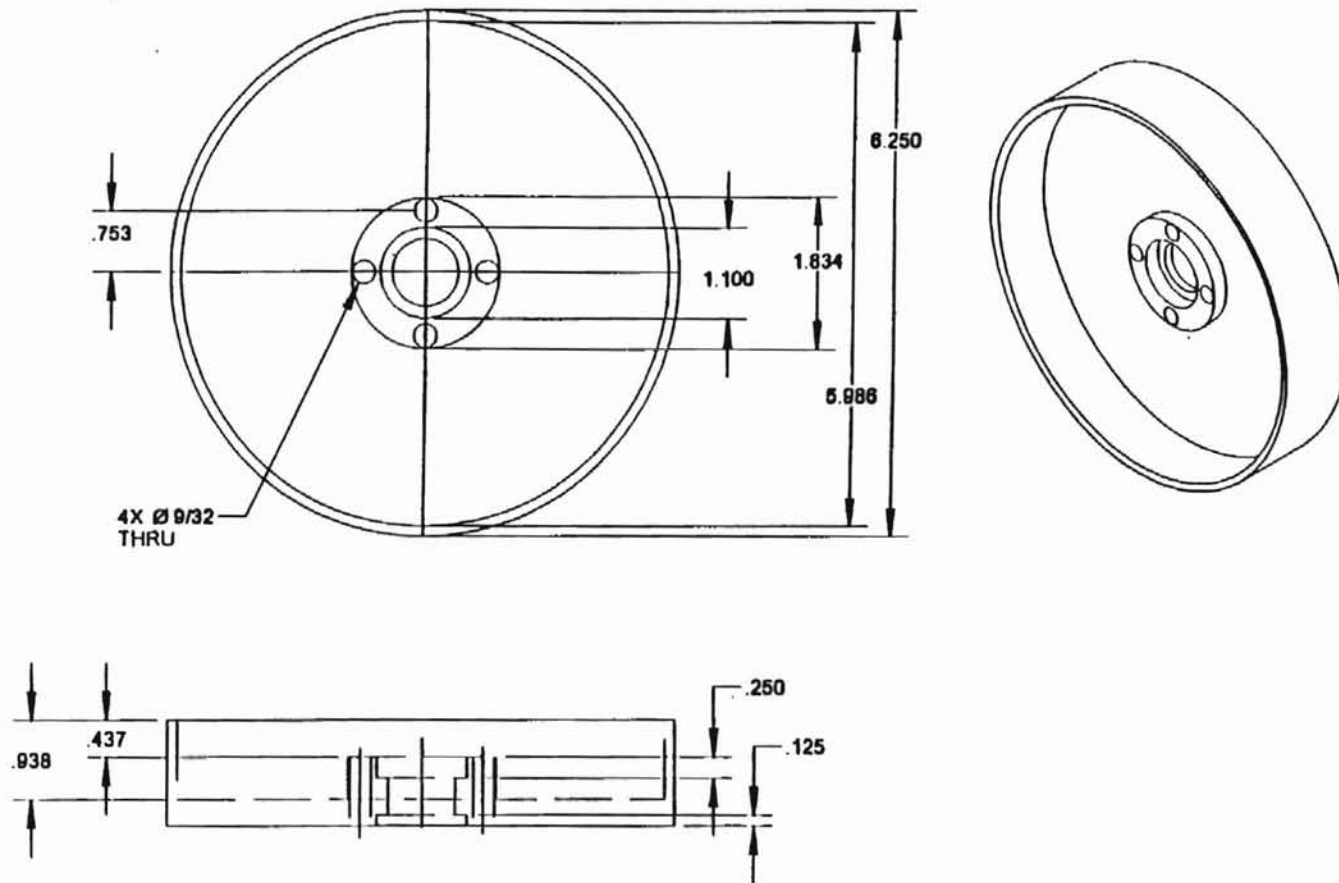


Figure 70. Idler Wheel

① CUT PART FROM 3/16 ALUMINUM SHEET

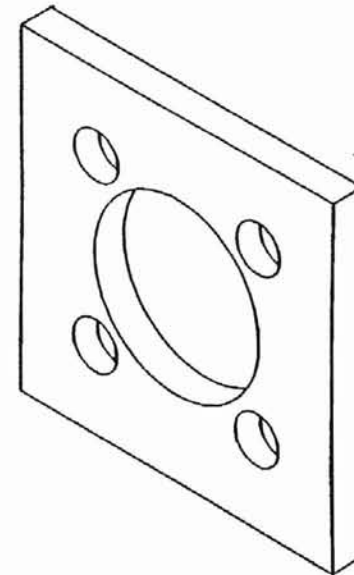
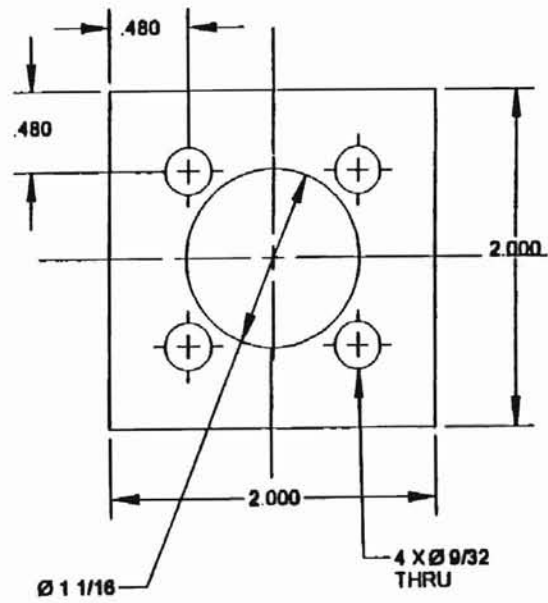


Figure 71. Outer Idler Bearing Retainer

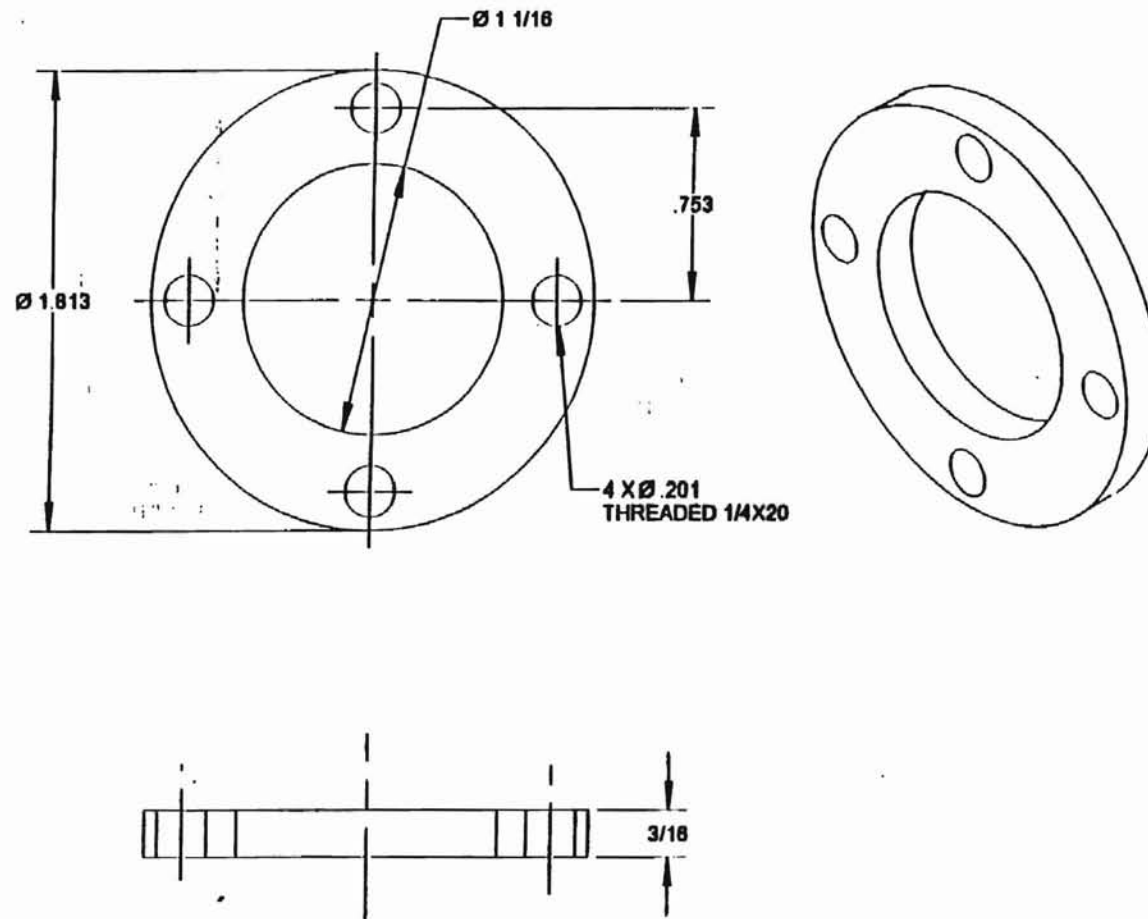
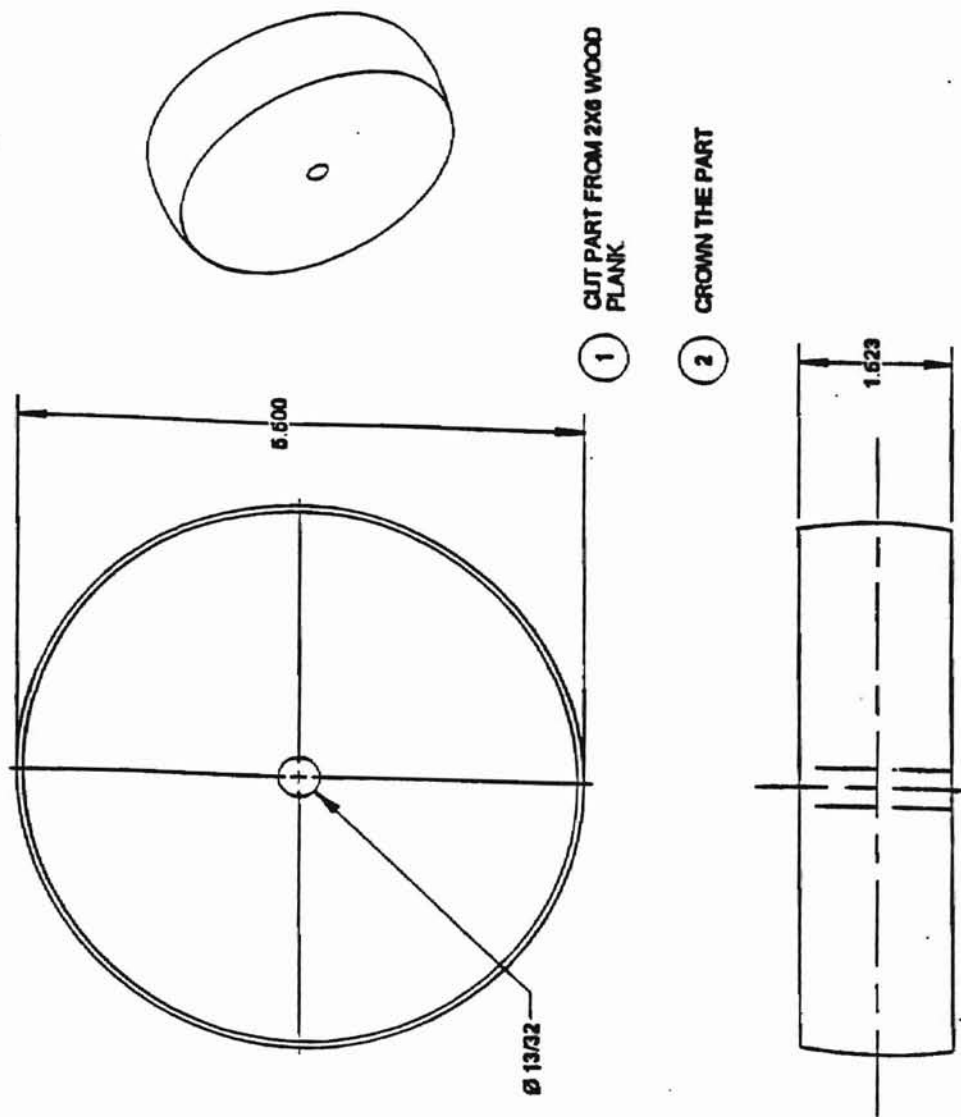


Figure 72. Inner Idler Bearing Retainer





**Figure 73. Driven Wheel**

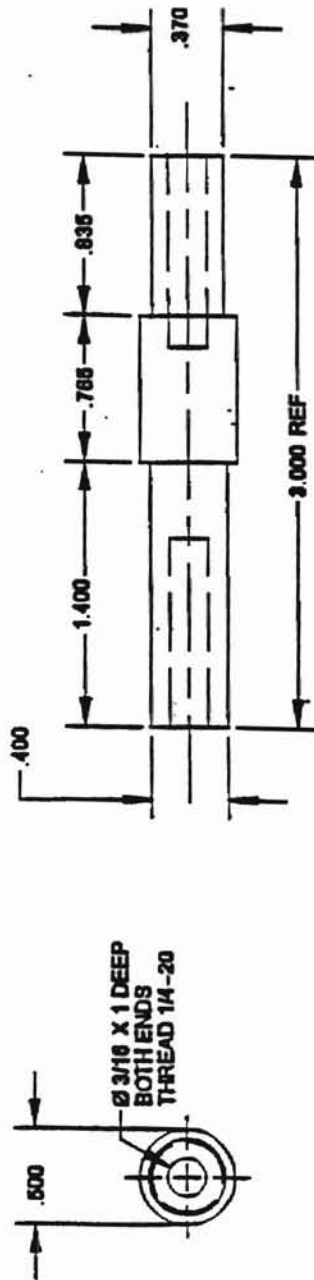
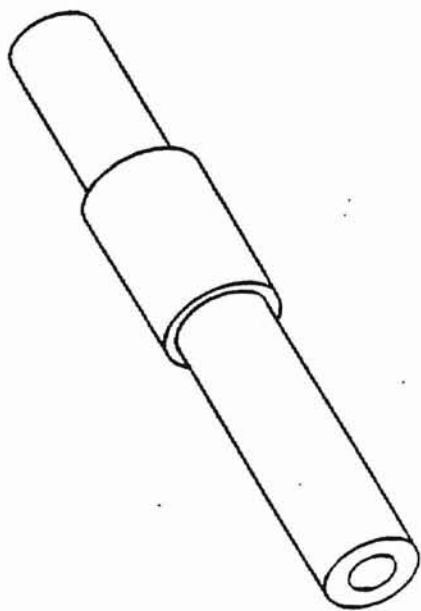


Figure 74. Driven Wheel Shaft

## **Appendix B – User's Manual and Helpful Suggestions**

### **1) To Set The Torque Table Dynamometer Platform Position**

Unbolt and remove the shaft housing assembly from the base of the dynamometer. Loosen the leg screws so that the motor platform may be shifted. Make sure that each leg is positioned in its platform clamp groove so that the top edge of the strain gage backing is just free from being pinched between the platform body and the leg to which the gage is mounted. Finger tighten the platform leg bolts so that the legs may be shifted for positioning the platform in an axial direction. Now, set the platform in place on the base so that it is supported by the legs. Measure the distances from the back of the dynamometer to the attachments of the legs in the base and in the platform. Though these distances are not critical, tolerances should be within 1/16 inches or so. The next step is to position the legs.

To position the legs in the planes of the 45-degree surfaces, choose one side to align first. From the back of the dynamometer, sight towards the front of the dynamometer along the inside of the legs. Place a ruler on the 45-degree surface of the base beyond the legs, near the very front of the dynamometer. Align the inside of the two legs with the edge of the ruler so that the legs truly lie in the plane made by the 45-degree surface. Tighten the base leg bolts when the alignment is made, and re-sight using the ruler. Perform this same operation for the other side of the dynamometer. The legs should now lie in the planes made by the 45-degree surfaces. Perform a final sighting using the ruler to verify this. The next step is to align the axis of rotation of the motor with the intersection of the planes of the 45-degree surfaces.

To align the axis of rotation of the motor with the intersection of the planes, first fasten a motor in the motor mount so that the axis of rotation of the motor shaft is both horizontal, and is located directly on the center line of the motor mount clamp. Make sure that the motor mount bolts are loose enough so that the motor mount may be shifted by bumping it. Next, using a ruler, align the center of the motor shaft with one of the 45-degree surfaces on the base. Remember that the centerline of the motor shaft must be aligned with the centerline of the legs, and not simply with the 45-degree surfaces of the base. It is helpful to scribe a clear ruler  $1/2$  the thickness of the legs from the edge. Then this scribe mark may be used to align the centerline of the motor shaft. Next, align the remaining side using the ruler, and tighten the motor mount screws. At this point, the motor has been positioned so that its axis of rotation coincides with the intersection of the planes made by the 45-degree surfaces of the base. The next step is to attach the shaft assembly onto the base so that the motor shaft fits into the larger torque transmitting shaft.

To position the shaft assembly, first loosen the two bolts which clamp the shaft bearing housings to the shaft housing stand, so that the shaft may be able to fit onto the motor shaft as the shaft housing stand is bolted back onto the base. Then, if the shaft is not in place in the bearings, place it in at this point. Its position may be roughly adjusted so that the motor shaft fits into the hole and the roll pins fit well into the roll pin slots in the shaft. A finer adjustment may be made later. Bolt the shaft housing stand firmly in place while the motor is running. If the motor audibly loads substantially while the stand is being bolted, loosen the stand bolts and re-position the

stand. It may be necessary to loosen the two bolts clamping the shaft bearing housings even more. Next, continue running the motor as the two shaft bearing housing bolts are tightened. If appreciable motor loading is evident, re-position the shaft bearing housings as the bolts are tightened. Remove the motor and check the position of the shaft by sliding a slender ruler between the motor shaft socket and the motor mount. It is fairly easy to check the alignment of the motor shaft socket with the 45-degree surfaces on the base in this way.

## **2) Connect the Computer, Power Supply, Dynamometer, and Circuit Box**

Connect the line from the power supply labeled "To Car" to the inport into the black circuit box. Connect the bundle of colored outlet lines from the circuit box to the acquisition board's port in the back of the computer. Connect the gray cable from the circuit box to the port on base of the dynamometer. Turn on the computer and go to the appropriate directory containing the computer program. Turn on the power supply and the circuit box.

## **3) Run the Program to Collect Motor Data**

Make sure that the tachometer drive belt is in place. Place a motor in the motor bracket by inserting the motor until the roll pin fits into the appropriate slot in the end of the shaft. Attach the clip leads from the circuit box to the motor leads. Preferably, run the motor by tilting the joystick as the motor bracket bolts are tightened by hand. If the motor audibly loads as it is run, or if variation of speed due to misalignment is judged to be significant, then adjustment needs to be made to the motor alignment in the bracket, or to the alignment of the steel shaft. Run the motor using the joystick.

noting how direction corresponds to joystick position. The direction of the motor can be reversed simply by changing the clip lead position.

Run the program. A series of brief instructions is displayed. Following this is a continuous real-time readout of torque voltages. The operator should press lightly on the calibration bar to observe a change in the voltage printed on the screen. If a change is not observed, make sure the power supply and the circuit box are on, and that all connections are good. Zero the reading as well as possible by adjusting the bridge balance. Roughly check the range by placing the 12-oz. weight at 8 inches on the calibration bar. Adjust the gain adjust on the circuit box until the voltage is below about 4.5 volts. Also, a voltmeter can now be used to check the accuracy of the computer's data acquisition board.

Next is the calibration mode. At each prompt the user should place the 12-ounce weight at any marked location on the calibration bar and enter this distance into the computer. Four data points are chosen in order to perform a least squares fit between the torque imposed upon the platform and the strain gage bridge circuit output. The slope of this line, in oz/inches per strain gage bridge output volt, the intercept, and the correlation coefficient are calculated and printed to the screen for the user to see. The program features a flag which alerts the user if the correlation coefficient is below 0.995. It had been experimentally determined that reporting a weight position which was off by one inch results in a coefficient below 0.995. After the flag is triggered, the user is prompted to re-calibrate the dynamometer. Following the calibration is another real-time screen readout of torque in ounce-inches, and speed in RPM. This

mode can be used to check the calibration and to observe the motor speed and direction. The calibration can be checked simply by placing the weight at some location on the calibration bar without the motor running. The error between the actual torque and the reported torque can be calculated.

The final feature of the program is the file data collection mode. Place the inertial disk on the steel shaft and tighten the set screw. Set the relay switch on the circuit box to "ENGAGED", and hold the joystick fully in one direction. Hold the disk firmly, and press "ENTER". About 1/2 seconds after the motor is activated, let go of the disk, and allow the motor to accelerate the disk freely. The torque and speed data are printed to the screen, and the user is prompted to enter a file name for the data. One file is output to Matlab for graphing, and another general output file is created containing torque and speed data. The Matlab files can be used to generate torque vs. speed and power vs. speed curves for the motor. These curves can then be used for design and diagnostic purposes. Additional files can be generated to determine the torque requirements of belts and bearings. Getting additional torque data is simple. For example, to get torque data for the dynamometer's shaft bearings, flip the RELAY switch to "DISENGAGED" and run the motor without the disk at constant speed. Press ENTER at the prompt to collect 25 torque readings. Name the file at the prompt. In Matlab this file can be opened and the mean torque reading can be found, along with the standard deviation of all the readings. In order to get belt friction, perform the same operation with the belt in place. Torque requirements of bearings at any load can be obtained by positioning the center of the idler wheel directly over that of the driven

wheel and running the constant-speed test. The idler wheel arm should be loaded with an appropriate weight to simulate one half the weight of the vehicle.

### **Suggestions for installing strain gages**

The following procedure has been proven to produce acceptable strain gage bonding to flat surfaces. Cleanliness of the surface is very important. It is also important that the strain gage not be handled or contaminated before application.

- 1) Wet sand the surface using alcohol and 320 grit sandpaper until the surface is smooth and free of scratches. Wipe off the surface, bathe it with alcohol, and clean it with a clean cotton ball.
- 2) Using the alcohol and a cotton ball, clean a small area on a work table. Tear apart the clear plastic cover sandwiching a strain gage, and position the gage on the clean work area with the taps facing up. Tear off a strip of scotch tape about 1 inch in length, and stick the tape lightly to the strain gage. Pick up the strain gage by peeling the tape off the table (if any portion of the tape stuck to the table). Make sure that the tape is not peeled back at a sharp angle, so that the gage is not bent at an angle.
- 3) Now, position the strain gage by sticking the tape so that the gage is in the desired location. If the position needs adjustment, simply peel the tape off the surface at a low angle. Once the gage is positioned properly, peel enough of one end of the strip of tape off the surface so that the entire underside of the gage is exposed, but no more. One end of the strain gage should be almost touching the surface. Place a small drop of super glue at this point. Squeeze the strain gage back down onto the surface so



that the glue is forced up the entire length of the gage. Press the gage against the surface for 20 seconds or so. Peel back the tape at a very sharp angle so that the strain gage is not subjected to a vertical force. At this point, you may examine the bond for bubbles or improper bonding. If the gage must be resealed, it is best to take the time to re-sand the surface.

4) You should now be ready to solder leads to the strain gage tabs. First, place a small drop of solder on the tabs. Next, tin the lead wires and then cut them to very short stubs, perhaps 1/16 inches. Bend the tips of the lead wires into a small radius of perhaps 1/8 inches, and tape the lead wire to the surface so that the tinned tips contact the beads of solder on the tabs. Then, simply touch a solder iron to the lead wire tips to connect the tabs. At this point it is a good idea to test the gage and your connections with an ohm meter.

It is the author's experience that while the above procedure is not exactly that recommended by the vendor, it produces very good, long lasting bonds between the gages and the aluminum legs.

## **Appendix C -- Data Acquisition Computer Code**

```

/*****
/*****          DC MOTOR ANALYSIS          *****/
/*****
/*****
/*****

```

```

#include <math.h>
#include <stdlib.h>
#include <stdio.h>
#include <graphics.h>
#include <conio.h>
#include <dos.h>
#include "nr.h"
#include "nrutil.h"

```

/\*Function Declarations\*/

```

float setup(float *offset);
float power_curve(float torque_cal_factor,float offset);
float torque_calibration(int number_of_points, float *correlation_coeff,float *offset);
float read_AD_motor_on(int channel);
float create_outfile(float *rpm, float *torque, float *power_out, int i);

```

```

#define BASE      0x300    /* ADC16 Board Base Address */
#define DATREG    BASE    /* Data Register Address */
#define LDATREG   BASE+1  /* Data Register Address */
#define MUXGREG   BASE+2  /* MUX/Gain Address */
#define STATREG   BASE+3  /* Status Register Address */
#define CMDMSK    0x80
#define MAXCH     8       /* Maximum number of channels */
#define NUMCH     2       /* Number of channels in use */
#define NP        9
#define STRING    80
#define BIG       1e31
#define TRUE      1
#define NMAX      30
#define NUM_AVERAGING_RUNS 10 /* Number of AD conversions to */
/* get a good voltage avg reading */
#define NUM_READINGS 4 /* number of torque calibration points */
#define WEIGHT      12.0 /* weight of calibrating weight in oz */
#define TACH_FACTOR 53.78 /* RPM/volts */
#define TACH_INTERCEPT 0.0 /* Add this to the tachometer value*/
#define VOLTAGE_FACTOR 6.0 /* voltage division in circuit */
#define WATTS_TO_OZ 141.6115 /*conversion from watts to oz-in/s */
#define PI          3.141592654
#define BOARD_FACTOR 1.00 /* A board calibration factor*/
#define STOP_RPM    230.0 /* Cutoff rpm for power curve */
#define CLOSE_RELAY 0X30
#define OPEN_RELAY  0x00
#define AMP_DELAY   1 /* delay time (*20 mS) for amp to settle*/
#define DATA_ARRAY_SIZE 50

```

```

#define NUM_DATA_POINTS      25
#define TIME_STEP            0.125 /* time step related to board speed*/
#define ORDER_POWER_FIT     3
#define ORDER_SPEED_FIT     3
#define ORDER_TORQUE_FIT    2

#define TACH_CHAN            0
#define TORQUE_CHAN          1
#define VOLTS_CHAN           2
#define CURRENT_CHAN         3

main()
{
    float torque_cal_factor.offset;
    char junk;

    torque_cal_factor = setup(&offset);

    power_curve(torque_cal_factor,offset);

    printf("\n\n Hit any key and enter to exit now.\n");
    scanf("\n%c%c",&junk);
}

float setup(float *offset)
{
    int          i, k, again=TRUE, restart=TRUE, same_factor,
                ok_cal, number_of_points=4,/*user input later*/
                message_l_flag=0, do_cal, channel, input_flag;
    float        reading, torque_factor, torque_reading, tach_reading,
                current_reading, power, voltage_reading, correlation_coeff;
    char         junk;

    clrscr();
    printf("\n\n Welcome to the dynamometer program. To start out,");
    printf("\n please make sure the RELAY switch is DISENGAGED, and that\n");
    printf(" the system power and the bridge power are on. Now you must \n");
    printf(" first adjust the bridge balance and then the gain.\n");
    printf("\n To balance the bridge, after momentarily pressing some key and ENTER,\n");
    printf(" adjust the dials to get a voltage reading as");
    printf("\n close to zero as possible. Then, adjust the gain by\n");
    printf(" placing the weight at 8 inches, and dialing the GAIN ADJUST\n");
    printf("until about +/- 4.5 volts is displayed. Also, now you could use a DMM\n");
    printf("to see if the computer's voltage reading is accurate.\n");
    printf("\n Now, hit some key and press enter to continue.\n");
    scanf("%c",&junk);
    clrscr();
    do

```

```

{
    gotoxy(1.5); /*This is necessary to keep the screen from scrolling*/
    printf("\n \t% Voltage (V)\n");
    reading = 0.0;
    for(i=0; i<NUM_AVERAGING_RUNS;i++)
    {
        reading += read_AD_motor_on(TORQUE_CHAN);
    }
    reading = reading/NUM_AVERAGING_RUNS;
    printf("\t %5.3f",reading);
    printf("\n\n Hit the space bar to stop ... \n");
} while(!kbhit());

while(restart == TRUE)
{
    if(message_1_flag)
    {
        printf("\n Would you like to re-calibrate the torque? (1=yes,
0=no)\n");
        printf(" The present torque factor is %5.3f\n",torque_factor);
    }
    else
    {
        printf("\n Would you like to calibrate the torque? (1=yes, 0=no)\n");
    }
    message_1_flag++;
    scanf("%d",&ok_cal);

/*
    input_flag = scanf("%d",&ok_cal);
    printf("\n input flag = %d\n",input_flag);
    while(input_flag &&(ok_cal > '49')||(ok_cal < '48'))
    {
        printf("\n Incorrect entry. Please enter either a 1 or a 0.\n");
        scanf("%d",&ok_cal);
        if((ok_cal == '49')||(ok_cal == '48'))
            input_flag = 1;
        printf("\n input flag = %d\n",input_flag);
    }
*/

    if(ok_cal)
    {
        do_cal = 1;
        while(do_cal)
        {

            torque_factor=torque_calibration(number_of_points,&correlation_coeff,offset);
            printf("\n correlation coefficient = %5.5f, offset =
%5.2f\n",correlation_coeff,*offset);
            if(correlation_coeff < 0.995)

```

```

1");
ENTER.\n");
        {
            printf("\n ALERT!!! Your data is not very linear. Press
            printf("\nto re-calibrate, or 0 to continue, then
            scanf("%d",&do_cal);
            scanf("%c",&junk);
        }
        else
            do_cal = 0;
    }
    printf("\n The torque factor is %f oz-in/Volt.\n",torque_factor);
    printf("\n Hit some key and press enter to continue.\n");
    scanf("%c%c",&junk);
}
else
{
    printf("\n Do you want to input a calibration factor,(0)\n");
    printf(" or use the same one you may have been using? (1)\n");
    scanf("%d",&same_factor);
    if(!same_factor)
    {
        printf("\nEnter your calibration factor\n");
        scanf("%f",&torque_factor);
    }
    else
        printf("\n You will use the same factor of %f\n",torque_factor);
    same_factor = 0;          /* reset the test variable */
}

```

```

/**** This portion of the program provides real-time readout from the ADC16 board *****/
while(CMDMSK & inportb(STATREG));    /* While Board isn't Busy */
again=TRUE;
while(again==TRUE)
{
    clrscr();
    do
    {
        gotoxy(1,5);    /*This is necessary to keep the screen from
scrolling*/
        printf("\n%8s %12s \n", "Speed (RPM)", "Torque (oz-in)");
        for(channel=0; channel<NUMCH; channel++)    /* While not
Done    */
        {
            reading = read_AD_motor_on(channel);
            switch(channel)
            {

```

```

        case 0:
            tach_reading =
reading*TACH_FACTOR + TACH_INTERCEPT;
            printf("\n %4.1f",tach_reading);
            break;
        case 1:
            torque_reading = reading*torque_factor
            power =
2.0*PI*torque_reading*tach_reading/60.0;
            printf(" %5.1f",torque_reading);
            break;
        case 2:
            voltage_reading =
reading*VOLTAGE_FACTOR;
            printf("
            %5.1f",voltage_reading);
            break;
        case 3:
            current_reading = reading;
            printf(" %5.3f",current_reading);
            break;
    }
}
/*
**** This concludes one A/D conversion for each channel ****/

        printf("\n\n Hit the space bar to stop ... \n");
        } while(!kbhit());
        printf("\n\nDo you want to try another motor now using the same \n");
        printf("calibration factors? (1 for yes/0 for no) : ");
        scanf("%d",&again);
    }
    printf("\n\nDo You Want To Restart (with the option to re-calibrate)? ");
    printf("\nPlease enter 1 for yes, or 0 for no. ---> ");
    scanf("%d",&restart);
}
return(torque_factor);
}

float torque_calibration(int number_of_points, float *correlation_coeff, float *offset)
{
    int radius[NUM_READINGS], i, j, k;
    float sum_xy, sum_x, sum_y, sum_xsq, sum_x_sq, denom,
        numerator,s_sq,torque_avg,sum_torque,intercept,
        torque_array[NUM_READINGS],sum;
    float voltage[NUM_READINGS], average_array[NUM_AVERAGING_RUNS],slope,v;
    char junk;

```

```

while(CMDMSK & inportb(STATREG));    /* While Board isn't Busy */

/*
*/
printf("\n number of points = %d\n",number_of_points);

printf("\nPlease calibrate the torque measurement. At each prompt, place the\n");
printf(" calibration weight at the desired radius on the calibration bar,\n");
printf(" enter this value, and then press enter. Remember to check for hysteresis.\n\n\n");
for(i=0;i<NUM_READINGS;i++)
{
    printf("\n Place the weight where you want it,");
    printf("\n          enter this value (inches) and press enter.\n");
    scanf("%d",&radius[i]);
        /* Now take a whole bunch of voltage readings */
    for (j=0;j<NUM_AVERAGING_RUNS;j++)
    {
        average_array[j] = read_AD_motor_on(TORQUE_CHAN);
    }
    sum = 0;
    for (j=0;j<NUM_AVERAGING_RUNS;j++)
    {
        sum += average_array[j];
    }
    voltage[i] = sum/NUM_AVERAGING_RUNS; /* Now get a good average of
voltage readings. */
    printf("    Voltage = %6.4f at radius = %d (inches).\n\n",voltage[i],radius[i]);
}

        /* Now, find the voltage-torque calibration factor */
sum_xy=0; sum_x=0; sum_y=0; sum_xsq=0; sum_x_sq=0;
for(i=0;i<NUM_READINGS;i++)
{
    sum_xy += voltage[i] * (radius[i] * WEIGHT);
    sum_x += voltage[i];
    sum_y += (radius[i] * WEIGHT);
    sum_xsq += (voltage[i]*voltage[i]);
}
sum_x_sq = sum_x * sum_x;
slope = (NUM_READINGS*sum_xy - sum_x * sum_y)/(NUM_READINGS*sum_xsq -
sum_x_sq);

        /* Now, find the correlation coefficient */
intercept=(sum_y*sum_xsq-sum_x*sum_xy)/(NUM_READINGS*sum_xsq-sum_x_sq);
sum_torque = 0;
for (i=0; i<NUM_READINGS; i++)
{
    torque_array[i]=intercept+slope*voltage[i];
    sum_torque += torque_array[i];
/*
*/
    printf("\ntorque %d = %f, sum=%f",i,torque_array[i],sum_torque);
}
}

```



```

torque_avg = sum_torque/NUM_READINGS;
numerator = 0;
s_sq = 0;
for (i=0; i<NUM_READINGS; i++)
{
    numerator += ((torque_array[i]-torque_avg)*(torque_array[i]-torque_avg));
    s_sq += (((radius[i]*WEIGHT)-torque_array[i])*((radius[i]*WEIGHT)-
torque_array[i]));
}
denom = s_sq + numerator;
*correlation_coeff = numerator/denom;
*offset = intercept;
printf("\n corr coeff= %5.5f, intcpt = %4.2f, slope=%4.3f, offset =
%4.2f.\n", *correlation_coeff,intercept,slope,*offset);
return(slope);
}
float power_curve(float torque_cal_factor,float offset)
{
    float speed, torque_reading, rpm[DATA_ARRAY_SIZE],
torque[DATA_ARRAY_SIZE],
    power_out[DATA_ARRAY_SIZE], power_in[DATA_ARRAY_SIZE],
    current[DATA_ARRAY_SIZE],volts[DATA_ARRAY_SIZE];
    int i, j, k, mark, keep_testing=1, loop_flag=0;
    char trash;

    /* may need scanf %c here while debugging to throw away previous CR*/
    scanf("%c",&trash);

    outportb(STATREG,OPEN_RELAY); /* make sure the relay is open */
    printf("\n Flip the RELAY switch to ENGAGED, hold the joystick at\n");
    printf(" full throttle either direction, then press ENTER to start the dynamic test.\n");
    scanf("%c",&trash); /* Throw away the carriage return. */
    printf("%c","\007");
    while(keep_testing)
    {
        if(loop_flag)
        {
            scanf("%c",&trash);
            printf("\n Hold the joystick at full tilt as before and press ENTER.\n");
            scanf("%c",&trash);
        }
        loop_flag++;
        printf("%c","\007");
        clrscr();
        /* delay(5000);
        */
        outportb(STATREG,CLOSE_RELAY); /* Close the relay to run the motor */
        /* delay(10);
        */

```

```

i=0; speed = 0.0;
while (i<NUM_DATA_POINTS)
{
    torque[i]=((read_AD_motor_on(TORQUE_CHAN))*torque_cal_factor +
offset);
    rpm[i]=((read_AD_motor_on(TACH_CHAN))*TACH_FACTOR +
TACH_INTERCEPT);
    i++;
}

outportb(STATREG,OPEN_RELAY); /* Open the motor relay to stop the motor */
/* Print the data */
printf("\nRPM\tTorque\n");

for (j=0; j<i; j++)
{
    printf("\n %5.1f\t%4.1f",rpm[j],torque[j]);
}

create_outfile(&rpm,&torque,&power_out,i);
printf("\nWould you like to run another dynamic test?\n");
printf(" Press 1 for yes, 0 for no.\n");
scanf("%d",&keep_testing);
}
}

float create_outfile(float *rpm, float *torque, float *power_out, int i)
{
    int j,k;
    char outfilename[80], prefix[80], trash;
    FILE *out;

    strcpy(outfilename,"c:\\matlab\\");

    printf("\n Enter the output file name.\n");
    scanf("%s",prefix);
    scanf("%c",&trash); /* Get rid of the carriage return */
    strcat(outfilename,prefix);
    strcat(outfilename,".m");
    out = fopen(outfilename,"w");

    fprintf(out,"\n rpm = [");
    /* begin the first matlab array*/
    for (k=0; k<i; k++) /*make horizontal rows of data for matlab*/
    {
        fprintf(out,"%5.3f\t",fabs(rpm[k]));
    }
    fprintf(out,");\n");
}

```

```

/* End the matlab array and
advance to a new line */

fprintf(out, "\n torque = [");
for (k=0; k<i; k++)
{
    fprintf(out, "%5.1f\t", fabs(torque[k]));
}
fprintf(out, "];\n");

/* now build the rest of the M file*/
fprintf(out, "\n num_data_points = %d;", i);
fprintf(out, "\n rpm_t = 0.0625:0.125:(num_data_points-1)*0.125+0.0625;");
fprintf(out, "\n torque_t = 0:0.125:(num_data_points-1)*0.125;");
fprintf(out, "\n time = 0:(num_data_points-1)*0.125/269:(num_data_points-1)*0.125;");
fprintf(out, "\n\n rpm_c1 = spline(rpm_t,rpm,torque_t);");
fprintf(out, "\n end_rpm_c1 = rpm_c1(num_data_points);");
fprintf(out, "\n x_axis = 0:end_rpm_c1/269:end_rpm_c1;");
fprintf(out, "\n polyrpm = polyfit(torque_t,rpm_c1,3);");
fprintf(out, "\n val_polyrpm = polyval(polyrpm,time);");
fprintf(out, "\n % then plot torque and speed as functions of time");
fprintf(out, "\n plot(torque_t,torque,'o',rpm_t,rpm_c1/2,'+');");
fprintf(out, "\n xlabel('Time (S)');ylabel('Torque (oz-in) and Speed (RPM)/2');grid;");
fprintf(out, "\n figure \n % then plot torque as a function of speed ");
fprintf(out, "\n\n polytorque_c = polyfit(rpm_c1,torque,%d)", ORDER_TORQUE_FIT);
fprintf(out, "\n val_polytorque_c = polyval(polytorque_c,x_axis);");
fprintf(out, "\n\n plot(x_axis,val_polytorque_c,'-',rpm_c1,torque,'+');");
fprintf(out, "\n title('Motor Torque vs. Motor Speed');");
fprintf(out, "\n xlabel('Motor Speed (RPM)');");
fprintf(out, "\n ylabel('Motor Torque (oz-in)');\n grid;");
fprintf(out, "\n\n figure \n % then plot the power speed curve");
fprintf(out, "\n\n power_c = 2*pi/60 .* torque .* rpm_c1;");
fprintf(out, "\n polypower_c = polyfit(rpm_c1,power_c,%d)", ORDER_POWER_FIT);
fprintf(out, "\n val_polypower_c = polyval(polypower_c,x_axis);");
fprintf(out, "\n\n plot(x_axis,val_polypower_c,'-',rpm_c1,power_c,'o');");
fprintf(out, "\n title('Motor Power Output vs. Motor Speed');");
fprintf(out, "\n xlabel('Motor Speed (RPM)');");
fprintf(out, "\n ylabel('Motor Power Output (oz-in/sec)');");
fprintf(out, "\n grid;");

/* following is for building a vehicle simulation in matlab */

/*
fprintf(out, "\n figure");
fprintf(out, "\n % Last, graph speed-time and distance-time data.");
fprintf(out, "\n % It is necessary to manually enter the coefficients for the");
fprintf(out, "\n % Matlab file 'mysim.m'.");
fprintf(out, "\n t0 = 0; tf = 1.5; \n x0 = [0 0]");
fprintf(out, "\n [t,x] = ode23('mysim',t0,tf,x0);");
fprintf(out, "\n plot(t,x);");
fprintf(out, "\n title('Calculated Vehicle Speed and Distance Traversed vs. Time');");
fprintf(out, "\n xlabel('Time (Seconds)');");

```

```

fprintf(out, "\n ylabel('Speed (in/s), and Distance (in)');\n grid;");
fprintf(out, "\n grid;");
fprintf(out, "\n all = [t,x]");
*/

fclose(out);          /* close the file */
/* Now, open a general data file */
strcat(prefix, ".dat");
out = fopen(prefix, "w");
fprintf(out, "\n Time (S)\t Torque (oz-in)\t Speed (RPM)\n\n");
for(j=0; j<i; j++)
{
    fprintf(out, "%5.3f\t %5.1f\t %5.0f\n", j*TIME_STEP, torque[j], rpm[j]);
}
fclose(out);
}

float read_AD_motor_on(int channel)
{
    int polarity;
    unsigned char zero=0, low_byte, high_byte, overrange;
    float return_value;

    outportb(MUXGREG, channel*8);    /* Write Channel Number */
    delay(AMP_DELAY);              /* Let amplifier settle */
    outportb(DATREG, zero);        /* Start A/D Conversion by writing to BASE*/
    while(CMDMSK & inportb(STATREG)); /*Wait for not busy signal*/

    /* outportb(STATREG, 0x50); */ /*Set overrange read bit to 'on'*/
    /* overrange = inportb(LDATREG);
    if (CMDMSK & inportb(DATREG))
        printf("\n Over range on Channel %d\n\n", channel);
    outportb(STATREG, 0x10);
    */
    /* Reset overrange read bit to 'off',
    ** but keep relay closed */

    /* Now check the polarity */
    if (CMDMSK & inportb(DATREG))
        polarity = 1;
    else
        (polarity = 0);

    low_byte = inportb(LDATREG);
    high_byte = inportb(DATREG);
    high_byte = (high_byte & 0x7f);

    return_value = ((256 * high_byte) + low_byte)*5.0/(32767*BOARD_FACTOR);

    if (polarity == 0)

```

```
        return_value = (-1.0)*return_value;
/*      printf("\n %5.1f", return_value);
*/
    return(return_value);
}
```

## Appendix D -- Matlab Code

Calib1.m

```
x=0:.1:25;
lbs = [0.0 1.8 4.3 6.5 8.8];
y=[5.2 7.4 10.4 15.1 16.4 ];

polyf = polyfit(lbs,y,1)
vals = polyval(polyf,x);
torque = spline(x,vals,(33.4+7+14/16)/2)

plot(x,vals,'--',lbs,y,'+',(33.4+7+14/16)/2,torque,'o');
title('Torque Required vs. Added Vehicle Load');
xlabel('Added Vehicle Load (Lbs.)');
ylabel('Required Torque (oz-in)');
grid;
```

## T161.M

```

rpm = [
3.208 129.620      16.633 34.288 54.346 74.610 95.042 11
181.997      189.924      144.604      158.582      172.216
];

torque = [
3.9 48.8 44.7 39.2 31.7 31.0 26.3 17.9 5
9.7 ];
% rpm = [0.153 5.989 1.099 0.015 0.023 0.008 0.031 0.
000 0.015 0.000 2.113 16.633 34.288 54.346 74.610 95
.042 113.208      129.620      144.604      158.582
172.216      181.997      189.924      196.715      20
2.101 ];

% torque = [ 0.1 42.1 59.8 90.0 104.0 104.4 10
4.0 102.9 102.0 102.4 95.5 53.9 51.9 53.8 5
6.0 55.9 53.9 48.8 44.7 39.2 31.7 31.0 2
6.3 17.9 19.7 ];

num_data_points = 14;
rpm_t = 0.0625:0.125:(num_data_points-1)*0.125+0.0625;
torque_t = 0:0.125:(num_data_points-1)*0.125;
time = 0:(num_data_points-1)*0.125/269:(num_data_points-1)*0.125;

rpm_c1 = spline(rpm_t,rpm,torque_t);
end_rpm_c1 = rpm_c1(num_data_points);
x_axis = 0:end_rpm_c1/269:end_rpm_c1;
polyrpm = polyfit(torque_t,rpm_c1,3);
val_polyrpm = polyval(polyrpm,time);
torquefit_to_time = polyfit(torque_t,torque,3);
val_torquefit = polyval(torquefit_to_time,time);
% then plot torque and speed as functions of time

shifted_spline = spline(torque_t,rpm,time); % This is the erro
neous spline
sec_time = 0:.0625:1.625;
set(gca,'XTick',[sec_time]);
set(gca,'XTickLabels',[]);hold on;

plot(time,val_torquefit,'-.',torque_t,torque,'o',time,val_polyrpm
/2,'--',rpm_t,rpm/2,'*');
xlabel('Time in 1/16th Second Increments');ylabel('Torque (oz-in)
and Speed (RPM)/2');
title('Torque and Speed Sampled at 16 Hz');grid;
figure

sec_time = 0:.0625:1.625;
set(gca,'XTick',[sec_time]);
set(gca,'XTickLabels',[]);hold on;

```



## T161.M

```

plot(time, val_torquefit, '-.', torque_t, torque, 'o', time, val_polyrpm
/2, '-.', ...
      rpm_t, rpm/2, '*', time, shifted_spline/2, '--', torque_
t, rpm/2, '*');
xlabel('Time in 1/16th Second Increments'); ylabel('Torque (oz-in)
and Speed (RPM)/2');
title('Torque, Actual Speed, and Time-Shifted Speed'); grid;
figure

sec_time = 0:.0625:1.625;
set(gca, 'XTick', [sec_time]);
set(gca, 'XTickLabels', []); hold on;

plot(time, val_torquefit, '-.', torque_t, torque, 'o', time, val_polyrpm
/2, '-.', torque_t, rpm_c1/2, '+', ...
      rpm_t, rpm/2, '*', time, shifted_spline/2, '--', torque_
t, rpm/2, '*');
xlabel('Time in 1/16th Second Increments'); ylabel('Torque (oz-in)
and Speed (RPM)/2');
title('Torque, Time-Shifted Speed, and Interpolated Speed Points'
); grid;
figure

sec_time = 0:.0625:1.625;
set(gca, 'XTick', [sec_time]);
set(gca, 'XTickLabels', []); hold on;

plot(time, val_torquefit, '-.', torque_t, torque, 'o', time, val_polyrpm
/2, '--', rpm_t, rpm/2, '*', torque_t, rpm_c1/2, '+');
xlabel('Time in 1/16th Second Increments'); ylabel('Torque (oz-in)
and Speed (RPM)/2');
title('Torque, Measured Speed, and Interpolated Speed'); grid;

figure % then plot torque as a function of speed

polytorque_c = polyfit(rpm_c1, torque, 2);
val_polytorque_c = polyval(polytorque_c, x_axis);

wrong_polytorque = polyfit(rpm, torque, 2);
val_wrong_polytorque = polyval(wrong_polytorque, x_axis);

plot(x_axis, val_polytorque_c, '--', rpm_c1, torque, '+', x_axis, val_wr
ong_polytorque, ':', rpm, torque, '*');
title('Motor Torque vs. Motor Speed');
xlabel('Motor Speed (RPM)');
ylabel('Motor Torque (oz-in)');
grid;

figure % then plot the power speed curve

power_c = 2*pi/60 .* torque .* rpm_c1;

```

## T161.M

```
polypower_c = polyfit(rpm_c1,power_c,3);
val_polypower_c = polyval(polypower_c,x_axis);

wrong_power = 2*pi/60 .* torque .* rpm;
wrong_polypower = polyfit(rpm,wrong_power,3);
val_wrong_polypower = polyval(wrong_polypower,x_axis);

plot(x_axis,val_polypower_c,'--',rpm_c1,power_c,'+',...
      x_axis,val_wrong_polypower,':',rpm,wrong_power,'*'
);
title('Motor Power Output vs. Motor Speed');
xlabel('Motor Speed (RPM)');
ylabel('Motor Power Output (oz-in/sec)');
grid;
```

MYSIM17.M

```

function xdot=mysim17(t,x)
%polytorque_c = [-0.0006 -0.1132 71.28]; %torque speed for t171.m
%polytorque_c = [-0.0009 -0.0174 65.038]; % torque speed for t172
.m
polytorque_c = [-0.0004 -0.1682 73.54]; %torque speed for t173.m

%offset = 0.8; % this is the torque loss with no belt due
to shaft bearing or offset
%offset = 11.9-0.8; % this is the torque loss due to a
belt, no load
offset = 27.3 - 0.8; % this is the torque loss due to t
he driven wheel being loaded
%offset = 18.7 - 0.8; % this is the torque loss due to t
he drive being loaded

wc=7 + 2/16;
ww=2/16;
dw=2.5;
coef_static_frict = 0.8;
coef_sliding_frict = 0.5;
% set up a conditional statement so that if T/(dw/2) > coef_static
frict x N, then
% the car is powered by the force of the sliding wheel, T/(dw/2) -
coef_sliding_frict x N.
a = 386.4;
const=60/(pi*dw);
lb_to_oz = 16;
xdot = zeros(2,1);
xdot = [2*a*(polytorque_c(1)*const^2.*x(1).^2 + polytorque_c(2)*co
nst.*x(1)+polytorque_c(3) - offset)...
/(dw*(wc+1.5*ww)*lb_to_oz) ; x(1)];

```

WHEELDI1.M

```
dia = 1:1:15;
time = [4.17 1.94 1.39 1.18 1.12 1.12 1.14 1.18 1.22 1.27 1.31 1.3
6 1.40 1.45 1.50];
xaxis = 0:.1:15;

p=polyfit(dia,time,8);          % (X,Y,N)
vals=polyval(p,xaxis);        % Evaluate p for times at each of 150
    points (diameters) on the x axis
low = min(vals);
low_val = polyval(p,4)

plot(dia,time,'+',xaxis,vals,'--')
xlabel('Wheel Diameter (Inches)');
ylabel('Calculated Time To Traverse 48 Inches');
title('The Effect of Wheel Diameter on Simulated Vehicle Speed');
grid;

%all = [vals]
```

TESTWO3B.M

```
% graph speed-time and distance-time data.
% It is necessary to manually enter the coefficients for the
% Matlab file 'mysim17.m'.
t0 = 0; tf = 1.5;
x0 = [0 0]';
[t,x] = ode23('mysim17',t0,tf,x0);
plot(t,x);
title('Calculated Vehicle Speed and Distance Traversed vs. Time')
;
xlabel('Time (Seconds)');
ylabel('Speed (in/s), and Distance (in)');
grid;
all = [t,x]
expl=['      Time (s)      Vel (in/s)      Dist (in)']
```

Actwt1.m

```
x=0:.1:45;
lbs = [7.9 9.9 14.9 41.3];
y=[1.71 1.81 1.83 2.46];

polyf = polyfit(lbs,y,1)
vals = polyval(polyf,x);

plot(x,vals,'--',lbs,y,'+');
title('Measured Vehicle Time vs. Vehicle Load');
xlabel('Vehicle Load (Lbs.)');
ylabel('Measured Vehicle Time (S)');
grid;
```

## Appendix E – Black Box Circuit Diagram and Filtering

Figure 75 shows the general layout for the black box circuitry. Perhaps one of the greatest challenges encountered in the project involved processing the output signal from the wheatstone bridge circuit. A variable potentiometer was used to set the gain as the signal was amplified through the non-inverting amplifying circuit. Experimentation was made with filtering after amplification using many different capacitors. Currently, no filtering after amplification is in place. However, a 100  $\mu\text{F}$  capacitor placed between locations 1 and 3 in the Wheatstone Bridge shown in Figure 75 provides filtering prior to amplification. The experiments consisted of observing torque output on an oscilloscope with various capacitors in place. Judgements were made in regard to the degree of filtering of each capacitor, and the location of filtering.

Note in Figure 75 that location 1 of the Wheatstone Bridge circuit is the strain gage input. Location 2 is the bridge output which is fed to the non-inverting amplifying circuit. Location 3 is the 18 VDC power supply ground, which is separate from the Main Power Supply ground. Location 4 is connected to the Main Power Supply ground.

Figure 76 is a wiring schematic of the torque table, the black box, and the computer data acquisition cord. The main power supply was purchased as a unit, and its circuitry is not detailed. Additionally, not shown are the wall transformer circuitry, the motor power supply circuitry, and the data acquisition board circuitry.

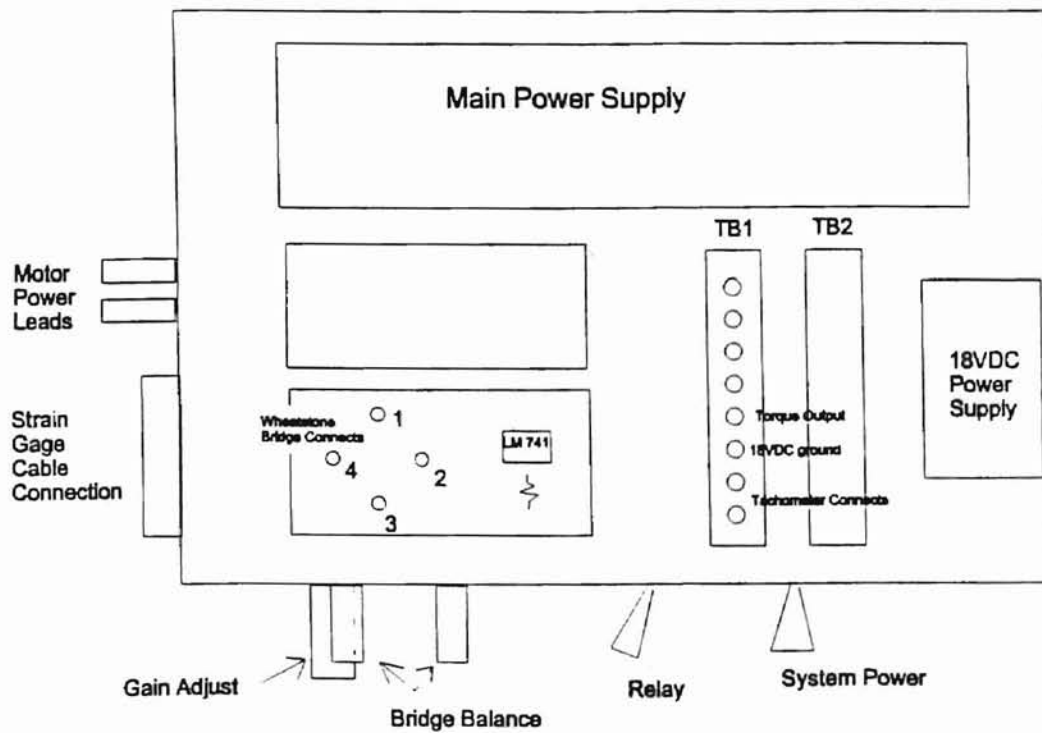


**Figure 75. Black Box Layout**



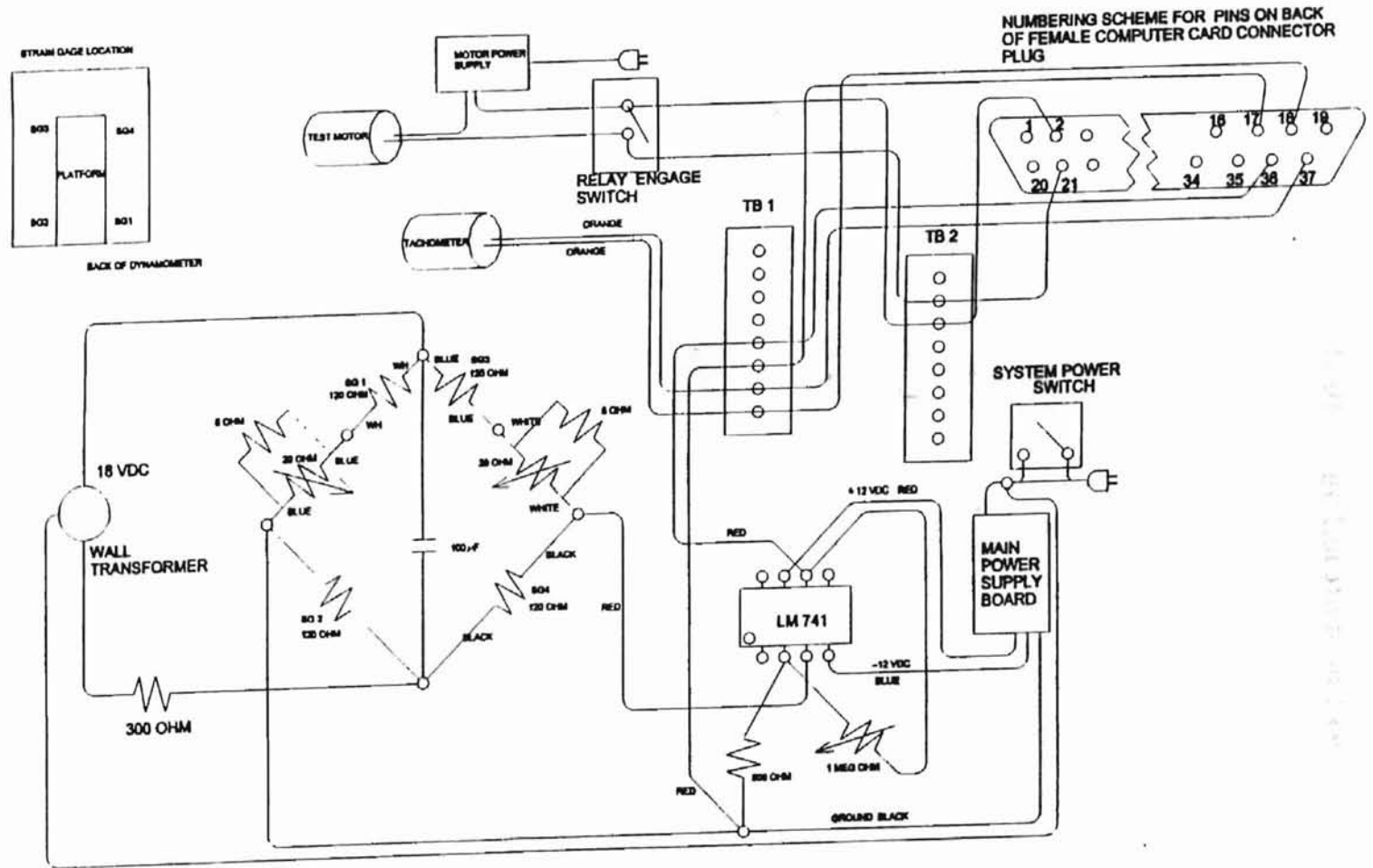
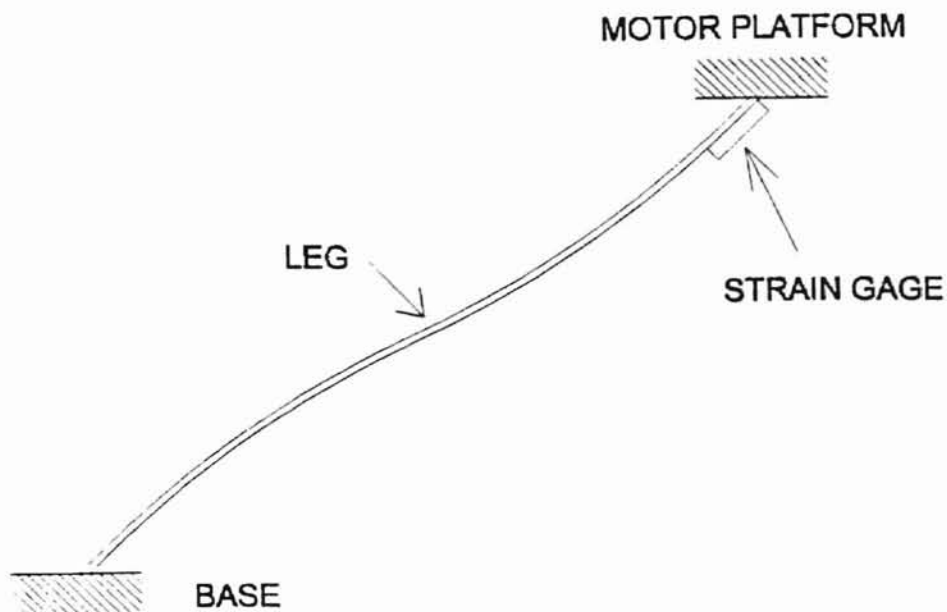


Figure 76. System Wiring Schematic

## Appendix F – Strain Gage Location on Leg

Figure 77 shows how the strain gages are located immediately adjacent to the joint made by the leg and the motor platform. This location is the most attractive because stress at this point is greatest. Furthermore, reasonably uniform placement of the gage on each leg was obtained simply by attaching the gage on the leg in the general position which would allow the gage to be located as shown. Fine measurements can be made by adjusting the legs within their clamps so that the backing material just touches the bottom of the motor platform. In this way it was not necessary to maintain fine tolerances as gages were glued onto the legs.

Please note that the platform and base are modelled as simple surfaces, and that the clamping mechanism is not shown for simplicity.



**Figure 77. Strain Gage Location With Respect to the Motor Platform and the Base**

## VITA

John Charles Bethea

Candidate for the Degree of

Master of Science

Thesis: A TORQUE TABLE DYNAMOMETER FOR QUALIFYING DC  
ELECTRIC MOTORS AND DETERMINING THE POWER  
REQUIREMENTS OF POWER TRAIN COMPONENTS

Major Field: Mechanical Engineering

Biographical:

Personal Data: Born in Kediri, Indonesia, on April 26, 1963, the son of Ralph C. and Lizette M. Bethea.

Education: Graduated from Jenks High School, Jenks, Oklahoma in May 1981; received Bachelor of Arts degree in English Literature from Oklahoma Baptist University, Shawnee, Oklahoma, in May 1985. Received Associate Degrees in Physics and Mathematics from Rogers State College, Claremore, Oklahoma, in May, 1992. Received Bachelor of Science degree in Mechanical Engineering from Oklahoma State University, Stillwater, Oklahoma, in December 1995. Completed the requirements for the Master of Science degree in Mechanical Engineering at Oklahoma State University in July, 1997.

Professional Memberships: American Society of Mechanical Engineers, Oklahoma Society of Professional Engineers.